INFORMATION TO USERS

RICE UNIVERSITY

Advanced Techniques for Next-Generation Wireless Systems

by
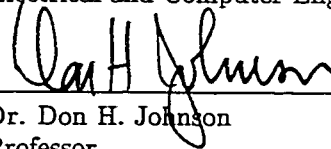
Andrew Sendonaris

A THESIS SUBMITTED
IN PARTIAL FULFILLMENT OF THE
REQUIREMENTS FOR THE DEGREE

Doctor of Philosophy

APPROVED, THESIS COMMITTEE:
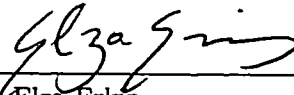
Dr. Behnaam Aazhang, Chair
Professor
Electrical and Computer Engineering
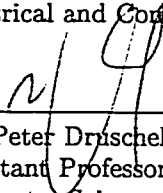
Dr. Don H. Johnson
Professor
Electrical and Computer Engineering

Dr. Joseph R. Cavallaro
Associate Professor
Electrical and Computer Engineering

Dr. Elza Erkip
Faculty Fellow
Electrical and Computer Engineering

Dr. Peter Druschel
Assistant Professor
Computer Science

Houston, Texas

May, 1999

UMI Number: 9928597

UMI

Advanced Techniques for Next-Generation Wireless Systems

Andrew Sendonaris

Abstract

In order to meet the demands of next-generation wireless systems, which will be required to support multirate multimedia at high data rates, it is necessary to employ advanced algorithms and techniques that enable the system to guarantee the quality of service desired by the various media classes. In this work, we present a few novel methods for improving wireless system performance and achieving next-generation goals. Our proposed methods include finding signal sets that are designed for fading channels and support multirate, exploiting knowledge of the fading statistics during the data detection process, exploiting the existence of Doppler in the received signal, and allowing mobile users to cooperate in order to send their information to the base station. We evaluate the performance of our proposed ideas and sh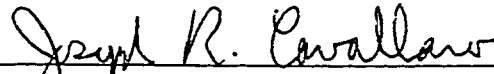ow that they provide gains with respect to conventional systems. The benefits include multirate support, higher data rates, and more stable data rates. It should be mentioned that, while we focus mainly on a CDMA framework for analyzing our ideas, many of these ideas may also be applied to other wireless system environments.

To Asta and Elina

Acknowledgments

First, I would like to thank my advisor Dr. Behnaam Aazhang for his continued guidance and support. Also, throughout my doctoral work, the help of Drs. Don Johnson, Joseph Cavallaro and Elza Erkip has been invaluable. Finally, I would also like to thank Dr. Peter Druschel for serving on my thesis committee, as well as all my fellow graduate students for helping me on several occasions.

The work in Chapter 4 was done in collaboration with Dr. Akbar M. Sayeed, currently at the Department of Electrical and Computer Engineering, University of Wisconsin–Madison. The work in Chapter 5 was done in collaboration with Dr. Elza Erkip, currently at the Electrical and Computer Engineering Department, Rice University.

Contents

Illustrations

Chapter 1

Introduction

Future wireless communications will bear little resemblance to present mostly-voice cellular systems. In order to meet the demands of multirate multimedia communications, next-generation wireless systems must employ advanced algorithms and techniques that enable the system to guarantee the quality of service desired by the various media classes. This implies that simply increasing the data rate will not be sufficient: other requirements, such as delay, outage probability and throughput variability, also need to be addressed and improved upon. In order to achieve the above goals, we must overcome various impairments of the mobile radio channel, such as the low power (RF and computational) available at the mobile transmitters, the multiple-access nature of the channel, and the inherent asynchronicity of the multiple users.

However, the nemesis of wireless systems, the biggest obstacle and challenge in achieving the desired goals, is multipath fading. Due to fading, within the duration of any given call, mobile users go through severe variations in signal attenuation. These variations cause not only a significant decrease in the average data rate that can be transmitted, they also cause the instantaneous achievable data rate to fluctuate. A decrease in the average data rate affects every type of wireless service, but the existence of severe fluctuations in the instantaneous achievable data rate adversely affects mostly real-time services such as audio and video. Therefore, while all wireless systems need to counteract the decrease in average data rate, next-generation

systems, which are expected to support multimedia, must also minimize the variability of the instantaneous channel throughput, at least for services with real-time constraints.

The techniques currently being investigated in the literature for meeting next-generation goals include advanced signal processing, tailoring system components such as coding, modulation and detection specifically for the wireless environment, departing from classic dichotomies such as between source and channel coding, and using various forms of diversity, that is, effectively transmitting or processing (semi)independently-fading copies of the signal. Some of these techniques, such the use of advanced signal processing, are not wireless-system specific: they are general performance enhancers. On the other hand, some techniques, such as the use of diversity, are able to improve wireless system performance by directly combating the effects of fading. In this work, we delve into most of the above general areas and present novel methods for improving wireless system performance and achieving next-generation goals.

Despite introducing multiple-access interference, CDMA (Code Division Multiple Access) is well-suited for combating the impairments of the wireless channel, more so than other multiple-access schemes such as TDMA (Time Division Multiple Access) and FDMA (Frequency Division Multiple Access). The advantages of CDMA have been well-documented and discussed and, therefore, will not be elaborated on in this work. We only point to the establishment of the IS-95 standard [1] in the U.S. and, more importantly, to the acceptance of CDMA as the enabling technology for the next generation of wireless systems in the U.S. and Europe (CDMA2000 and WCDMA, respectively). Therefore, in this work we focus mainly on a CDMA framework for analyzing our ideas, even though many of these ideas may also be applied to other wireless system environments.

The first subject that we explore falls under the general area of tailoring system components such as coding, modulation and detection specifically for the wireless environment. In particular, Chapter 2 addresses the issue of modulation and choice of a signal set. That is, given a sufficiently rapidly varying channel, one should design signals that are robust to channel distortion, in the sense that the information-bearing aspect of the transmitted signals is unaltered after passing through the channel. To this end, a class of $\mathcal{M}$-ary CDMA systems is described, and two systems from this class are analyzed in terms of their resulting channel throughput. Results indicate that $\mathcal{M}$-ary CDMA systems are able to provide reliable transmission at high data rates. In addition, this framework enables a multirate implementation, that is, one in which users have different data rates, an essential feature for any system that has to support multimedia.

Even though the statistics of the channel variations in a wireless system may be known, most multiuser detectors do not incorporate this knowledge into the detection process. Any such knowledge is most often used for tracking the channel variations. The minimum P_e (probability of bit error) receiver, however, is a MAP (Maximum a-posteriori probability) receiver, that is, a receiver that directly incorporates the density of the channel variations into the bit decisions. This idea falls under the general area of tailoring systems specifically for the wireless environment, in particular the detection process, and also under the general area of departing from classic dichotomies, in particular from the conventional separation of channel estimation and data detection. In Chapter 3 we derive the general form of an optimal one-shot multiuser detector given any density for the users' amplitudes. It is shown that well-known multiuser receivers such as the maximum likelihood detector, the decorrelating detector and even the MMSE detector are special cases of the above receiver, each optimal given a particular assumption about the density of the users'

amplitudes. When it is assumed that the amplitudes obey a Rayleigh distribution, we obtain the optimal one-shot multiuser detector for flat Rayleigh fading channels. Results show that, as expected, the resulting receiver has superior performance.

In Chapter 4, we address the issue of multiuser detection in channels that fade sufficiently fast so that the transmitted signals experience Doppler shifts. Perhaps contrary to intuition, and contrary to the approach taken by most researchers, it turns out that these Doppler shifts, instead of being a nuisance and a cause for performance degradation, may be exploited in order to increase system performance. This can be seen by looking at a canonical representation of the wide-sense stationary uncorrelated scatterer channel model, which indicates that fast fading results in time and frequency shifted copies of the transmitted signal. As a result, conventional multiuser-RAKE receivers, which are designed to exploit only time-shifted copies of the signal are not sufficient. We therefore propose a new framework for multiuser detection which is essentially a time-frequency generalization of the multiuser-RAKE receiver, and is able to exploit joint multipath-Doppler diversity. This work falls under the general area of advanced signal processing, due to the time-frequency processing performed at the receiver, and also under the general area of the use of diversity, due to the exploitation of Doppler diversity. Analytical and simulated results based on realistic fast fading assumptions demonstrate that the proposed multiuser detectors promise substantially improved performance compared to existing systems due to the inherently higher level of diversity afforded by multipath-Doppler processing.

Finally, in Chapter 5 we turn our attention to the use of spatial diversity at the mobile. Spatial diversity is a commonly-used form of diversity and relies on the principle that signals transmitted from geographically separated transmitters, and/or to geographically separated receivers, experience fading that is independent.

Therefore, independently of whether other forms of diversity are being employed, having multiple transmit antennas is desirable. Unfortunately, it is infeasible in the uplink of a cellular system, due to the size of the mobile unit. In order to overcome this limitation, yet still emulate transmit antenna diversity, we propose a new form of spatial diversity, whereby diversity gains are achieved via the cooperation of in-cell users. That is, in each cell, each user has a "partner". Each of the two partners is responsible for transmitting not only their own information, but also the information of their partner, which they receive and detect. Results show that, even though the inter-user channel is noisy, cooperation leads not only to an increase in capacity but also to a more robust system, where users' achievable rates are less susceptible to channel variations, thus leading to a higher quality of service.

Some concluding remarks pertaining to all the subjects presented herein can be found in Chapter 6.

Chapter 2

Total Channel Throughput of $\mathcal{M}$-ary CDMA Systems over Fading Channels

2.1 INTRODUCTION

We first turn our attention to the issue of finding new methods for increasing the data rate of wireless mobile users. A high data rate system requires a large transmission bandwidth, which normally implies frequency selective fading. This results in waveform distortion of the transmitted signals, and thus the use of channel equalizers is imperative.

However, even if the transmission bandwidth is large, the communication system may be designed so that the transmitted signals suffer only from flat fading (frequency non-selective fading), which does not distort the signal waveform. This may be accomplished, for example, using Multicarrier Modulation [2–5] or a RAKE receiver [2] that can estimate the delays and relative amplitudes of the multipath components.

Given the fact that we want to achieve high data rates and that the transmitted signals are randomly scaled before arriving at the receiver, our idea is to modulate multiple bits per symbol period on the *waveform* of the transmitted signals. The intuition behind our approach is that, given a sufficiently rapidly varying channel, one should design signals that are robust to channel distortion, in the sense that the information-bearing aspect of the transmitted signals is unaltered after passing through the channel.

2.2 $\mathcal{M}$-ARY CDMA SYSTEMS

There are many possible ways to implement the above idea. Our approach however, is to use CDMA spreading codes. That is, to obtain a system with increased data rate, we assign each user M distinct CDMA random spreading codes.

Given that a user has M codes, there are several transmission alternatives. In each symbol period, the user selects m codes $(1 \leq m \leq M)$, and transmits them after multiplying each one by plus or minus 1. As a result, the number of possible symbols that can be transmitted in one symbol period is given by

$$\mathcal{M} = \begin{pmatrix} M \\ m \end{pmatrix} 2^m \tag{2.1}$$

where $\begin{pmatrix} M \\ m \end{pmatrix}$ denotes M-choose-m. Therefore, the resulting system is referred to as $\mathcal{M}$-ary CDMA. For a fixed M, m parameterizes a large class of possible systems with data rates equal to $\log_2(\mathcal{M}(m))$. As m changes from 1 to M, the data rate varies from $\log_2(M) + 1$ to M, in a way similar to the one depicted in Figure 2.1.
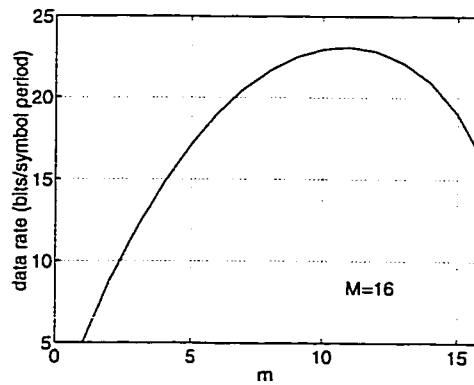
Figure 2.1 : Raw data rate vs m (for $M = 16$)

Given that all values of m result in systems with the same symbol period and

bandwidth, we need a performance measure that enables the comparison of these systems. The measure that we use is throughput, which has units of bits per symbol period. Throughput incorporates the raw data rate and the average probability of bit error (P_e or *BER*) of a system into one measure that represents the best data rate that can be achieved through coding, while achieving an arbitrarily low P_e. Therefore, throughput is the "reliable transmission" data rate. Calculating the throughput of a system consists of finding a discrete-time channel model for that system and calculating its capacity [6] in units of bits per channel use.

It should be mentioned that [7] proposes a system similar to $\mathcal{M}$-ary CDMA. However, in this work we carry out a different study. We use random codes, analyze the performance over a Rayleigh fading channel and determine the *throughput* of $\mathcal{M}$-ary CDMA, not the probability of bit error, which is not sufficient when considering systems with different raw data rates.

2.3 THROUGHPUT CALCULATIONS

For the purposes of this work, we will explore two possibilities: $m = 1$ and $m = M$. It should be noted that we assume that each user has the same power under both values of m. In this section we derive analytical expressions for the throughputs of these systems, which are then used in Section 2.5 for comparisons over several receivers.

First we analyze the case $m = 1$. In each symbol period, each user selects only one of his/her M available codes, and transmits it after multiplying it by ± 1. This corresponds to a *binary-valued, $2M$-ary CDMA system with random codes* and is akin to IS-95 [8]. However, there are a few significant differences, such as the fact that in IS-95 all users use the same Walsh codes, which are then spread by a low-spreading-factor pseudorandom sequence. This makes multiuser detection very challenging in

IS-95 systems, unlike $2M$-ary CDMA where multiuser detection is readily employed (see Section 2.4).

Denote the $2M$ possible transmitted sequences of a given user by $c_1, c_2, \ldots, c_{2M-1}, c_{2M}$ where $c_{2i} = -c_{2i-1}$ $\forall$ i. Also, denote the probability that sequence c_i is transmitted and sequence c_j is detected by $Pr(c_i \rightarrow c_j)$. Assuming that random codes are being used, the probability of confusing a given sequence with another is approximately the same for all sequences other than the transmitted sequence and its negative. The resulting discrete-time channel model for this system is shown in Figure 2.2, where $\varepsilon_1 = Pr(c_1 \rightarrow c_2)$, $\varepsilon_2 = Pr(c_1 \rightarrow c_j)$, $j \neq 1, 2$, and

Transmitted   Received
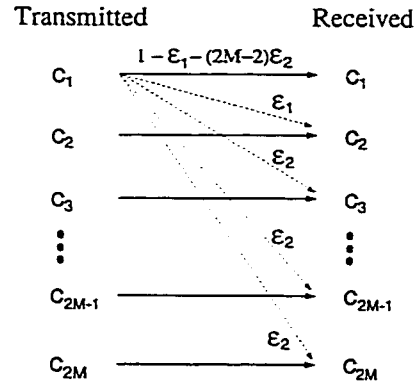
Figure 2.2 : Discrete-time channel model for $\mathcal{M}$-ary CDMA with $m = 1$

$1 - \varepsilon_1 - (2M - 2)\varepsilon_2 = Pr(c_1 \rightarrow c_1)$. It is clear that ε_1 and ε_2 depend on how many sequences each user has and on how many users there are in the system. Therefore, assuming that K users are using this channel, the channel capacity for each user (in bits per channel use per user) is given by

$$C_1(M, K) = \log_2(M) + 1 + H_1(\varepsilon_1, \varepsilon_2, M) \tag{2.2}$$

where

$$H_1(\varepsilon_1, \varepsilon_2, M) =$$

$$(1 - \varepsilon_1 - (2M - 2)\varepsilon_2)\log_2(1 - \varepsilon_1 - (2M - 2)\varepsilon_2)$$

$$+\varepsilon_1 \log_2(\varepsilon_1) + (2M - 2)\varepsilon_2 \log_2(\varepsilon_2)$$

We can thus see that the capacity is equal to the raw data rate plus a correction factor which is a function of the transition probabilities. The total channel throughput in bits per channel use is given by

$$\eta_1(M, K) = K \cdot C_1(M, K) \tag{2.3}$$

The second case that we will explore is $m = M$. In each symbol period each user transmits *all* of his/her available codes, each modulated by ± 1. This corresponds to a *multivalued 2^M-ary CDMA system with random codes* and is akin to conventional CDMA in the sense that each 2^M-ary CDMA user corresponds to M conventional CDMA users. One difference is the fact that the 2^M-ary CDMA user can exploit joint coding and decoding of the M codes being transmitted, something M conventional CDMA users cannot do. Another difference is that all M codes belonging to a 2^M-ary CDMA user will experience the same fading, whereas in conventional CDMA each of the M codes will experience different fading, thus adding diversity to the system.

Denote the 2^M possible transmitted sequences of a given user by $\bar{c}_1, \bar{c}_2, \dots, \bar{c}_{2^M}$, where $\bar{c}_{2i} = -\bar{c}_{2i-1} \forall i$. Each code can be written as $\bar{c}_i = \sum_{j=1}^{M} b_j^i c_j$ where $b_j^i \in \{-1, 1\}$. Assuming that the probability of making an error on b_j^i is independent from the probability of making an error on b_k^i when $k \neq j$, then all the transition probabilities of 2^M-ary CDMA are parameterized by P_e, which is the probability of making a sign error on a sub-code (e.g. c_j). The resulting discrete time channel model for this system is shown in Figure 2.3. It is clear that P_e depends on how many sequences

Transmitted   Received
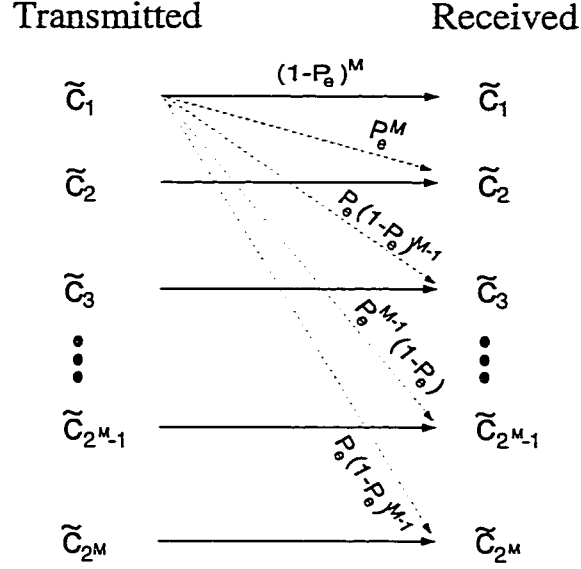
Figure 2.3 : Discrete-time channel model for $\mathcal{M}$-ary CDMA with $m = M$

each user has and on how many users there are in the system. Therefore, assuming that K users are using this channel, the channel capacity for each user (in bits per channel use per user) is given by

$$C_2(M, K) = M + H_2(P_e, M) \tag{2.4}$$

where $H_2(P_e, M) = M P_e \log_2(P_e) + M(1 - P_e) \log_2(1 - P_e)$. As in the case of $m = 1$, the capacity is equal to the raw data rate plus a correction factor which is a function of the transition probabilities. The total channel throughput (in bits per channel use) is given by

$$\eta_2(M, K) = K \cdot C_2(M, K) \tag{2.5}$$

In order to compare $2M$-ary CDMA with 2^M-ary CDMA we will compare

$$\eta_1(M, K) \text{ vs. } \eta_2(M, K) \tag{2.6}$$

It should be noted that each of the K users has a given maximum transmit power constraint. Therefore, the power allocated to each of the M codes of each 2^M-ary CDMA user is equal to $\frac{1}{M}$ of the power allocated to that user.

It should be noted that ε_1, ε_2 and P_e depend not only on M and K, but also on what detection scheme is being used. Therefore, $\eta_1(M, K)$ and $\eta_2(M, K)$ should be compared over various detection schemes.

2.4 DETECTORS

The channel is assumed to be synchronous, single-path flat Rayleigh fading, with AWGN. We also assume that the received amplitudes and phases vary slowly enough to enable their tracking with high precision. The received signal in the 0th symbol period, is therefore given by

$$r(t) = \sum_{j=1}^{K} a_j \tilde{c}_{m_j}^{(j)}(t) + n(t), \qquad t \in [0, T) \tag{2.7}$$

where a_j is the jth user's amplitude and is Rayleigh distributed, $\tilde{c}_{m_j}^{(j)}(t)$ is the $m_j{}^{th}$ code from the jth user's code set, and $n(t)$ is real AWGN with spectral height equal to $\frac{N_o}{2}$.

Assuming that the a_j's are known, the problem of detecting which sequence each user sent is equivalent to $\mathcal{M}^K$-ary hypothesis testing. Unfortunately, this results in prohibitively high complexity. As a result, simpler, suboptimal receivers are needed. The first step is to chip-match filter the received signal.

$$r_i = \frac{1}{T_c} \int_{(i-1)T_c}^{iT_c} r(t) dt \quad i = 1, 2, \ldots, N_c$$

where T_c is the chip period and N_c is the spreading factor. The resulting vector can be written as

$$\mathbf{r} = CAB + \mathbf{n} \tag{2.8}$$

where C contains all the codes of all the users, A contains the user's amplitudes and $\mathbf{B}$ is a vector indicating which m codes each user transmitted, and with what sign. For example, for $K = 4$, $M = 3$, $m = 1$, C and $\mathbf{B}$ will be of the form

$$C = \begin{pmatrix} | & | & | & | & | & | & & | & | & | \\ c_1^{(1)} & c_2^{(1)} & c_3^{(1)} & c_1^{(2)} & c_2^{(2)} & c_3^{(2)} & \cdots & c_1^{(4)} & c_2^{(4)} & c_3^{(4)} \\ | & | & | & | & | & | & & | & | & | \end{pmatrix}$$

$$\mathbf{B} \overset{e.g.}{=} [[0\ 0\ -1]\ [0\ 1\ 0]\ [0\ 0\ 1]\ [-1\ 0\ 0]]^\top$$

The output of the code-matched filter is then expressed as $\mathbf{y} = C^\top \mathbf{r} = C^\top CA\mathbf{B} + C^\top \mathbf{n}$. The *matched-filter detector* is thus given by

$$(\hat{\mathbf{m}}, \hat{\mathbf{b}}) = \max{}^{(m,M)}(\mathbf{y}) \qquad (2.9)$$

where $\max{}^{(m,M)}()$ is a function that finds the m largest absolute values in every "block" of its argument. Each block corresponds to one user and contains M elements corresponding to the M codes each user has. The m block elements with largest absolute values are declared to correspond to the transmitted codes of the given user, and the signs of these elements are declared to be the signs of the transmitted codes. Thus, for the example given above, $\hat{\mathbf{m}} \overset{e.g.}{=} [3\ 2\ 3\ 1]$ and $\hat{\mathbf{b}} \overset{e.g.}{=} [-1\ 1\ 1\ -1]$.

It can be seen that we may "decorrelate" the users by multiplying $\mathbf{y}$ by the inverse of the code correlation matrix. That is, if we define $R = C^\top C$, then

$$R^{-1}\mathbf{y} \overset{e.g.}{=} [[0\ 0\ -a_1]\ [0\ a_2\ 0]\ [0\ 0\ a_3]\ [-a_4\ 0\ 0]]^\top + \bar{\mathbf{n}}$$

Therefore, the *decorrelating detector* is given by

$$(\hat{\mathbf{m}}, \hat{\mathbf{b}}) = \max{}^{(m,M)}(R^{-1}\mathbf{y}) \qquad (2.10)$$

One problem with the decorrelating detector is that R may not have an inverse, or be very badly conditioned. This happens when the total number of codes (KM) is

greater than or equal to the spreading factor (N_c). One way to combat this problem is to use the *MMSE detector*, which is given by

$$(\hat{\mathbf{m}}, \hat{\mathbf{b}}) = \max{}^{(m,M)}((R + \sigma^2 A^{-2})^{-1}\mathbf{y}) \tag{2.11}$$

It is easy to show that $R + \sigma^2 A^{-2}$ always has an inverse, which makes it possible to have a total number of codes that is larger than N_c.

Another possibility is to use a *multistage detector*. The fact is that, at any given time, only $K \cdot m$ codes are actually present in the received signal. Since $m \le M$, this implies that the correlation matrix of the "active" codes is better conditioned than the correlation matrix of all the codes, i.e. R. To explore this, we re-write $\mathbf{r}$ as

$$\mathbf{r} = C_a A \mathbf{b}_a + \mathbf{n} \tag{2.12}$$

where C_a contains the active codes of each user, A contains the user's amplitudes and $\mathbf{b}_a$ is a vector containing the sign of each active code. For example, for $K = 4$, $M = 3$, $m = 1$, C_a and $\mathbf{b}_a$ will be of the form

$$C_a \overset{e.g.}{=} \begin{pmatrix} | & | & | & | \\ c_3^{(1)} & c_2^{(2)} & c_3^{(3)} & c_1^{(4)} \\ | & | & | & | \end{pmatrix}$$

$$\mathbf{b}_a \overset{e.g.}{=} [-1\ 1\ 1\ -1]^\mathsf{T}$$

Starting with an initial estimate of what the active codes are (by using any of the previously mentioned detectors), we can obtain an estimate of $\mathbf{b}_a$ (e.g. using a decorrelator or an MMSE). Thus, we can re-construct the MAI, subtract it from the received signal, re-estimate the active code set and $\mathbf{b}_a$, and iterate until we converge to an active code set and to a $\mathbf{b}_a$. This idea can be expressed as

$$(\hat{\mathbf{m}}_{a(i)}, \hat{\mathbf{b}}_{a(i)}) = \max{}^{(m,M)}(\mathbf{y} - \mathcal{R}(\hat{\mathbf{m}}_{a(i-1)})A\hat{\mathbf{b}}_{a(i-1)})$$

where the subscript i denotes the iteration step, and $\mathcal{R}(\mathbf{m_a})$ is a matrix that contains the correlations of the codes in the active code set with all the users' codes. In practice, only 4 to 5 steps are required for the multistage receiver to converge.

2.5 RESULTS

Unfortunately, for most values of M and m, it is difficult to calculate the transition probabilities for any of the detectors described in Section 2.4, besides the matched-filter detector. Therefore, we obtained estimates using Monte Carlo simulations. These estimates lead to estimates of $\eta_m^{MF}(M,K)$, $\eta_m^{DEC}(M,K)$, $\eta_m^{MMSE}(M,K)$ and $\eta_m^{MS}(M,K)$, where MF denotes the Matched Filter detector, DEC the Decorrelating detector, and MS the Multistage detector.

As mentioned in Section 2.3, the values of m that we explored were $m = 1$ and $m = M$. The throughput of these systems was compared over various combinations of system parameters such as K, M, SNR and detection scheme, and the results are shown in Figures 2.4 through 2.6. We should note that the results for the decorrelator were similar to, or worse than, the MMSE detector, and thus only the latter is included in the plots.

From Figures 2.4(c) and 2.5(a) we see that the behavior of the throughput as a function of M is unchanged when the ratio $\frac{K}{N_c}$ remains constant. Also, from Figure 2.5(b) we see that when the ratio $\frac{K}{N_c}$ increases, the maximum total channel throughput remains approximately the same, and the throughput of multiuser detectors begins to degrade at lower values of M.

From the discussion in Sections 2.2 and 2.3 it is clear that the throughput of a system will equal the raw data rate when the error probability is zero, and will degrade monotonically as the error probability increases. This effect is illustrated in Figure 2.6.
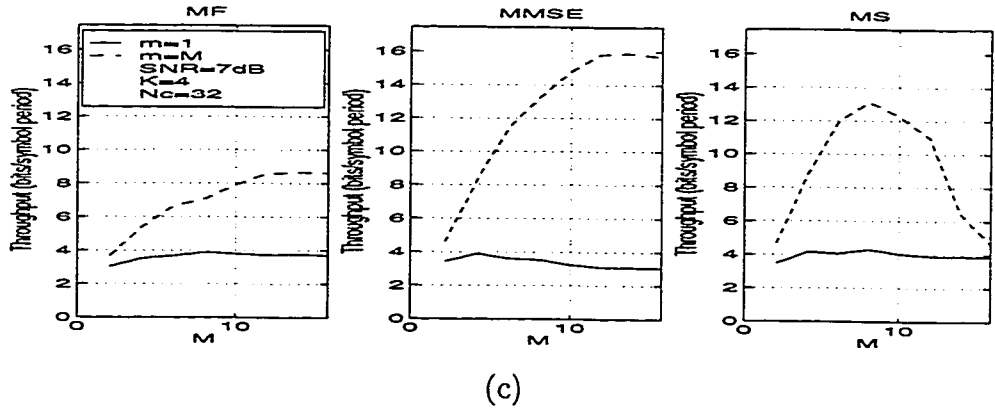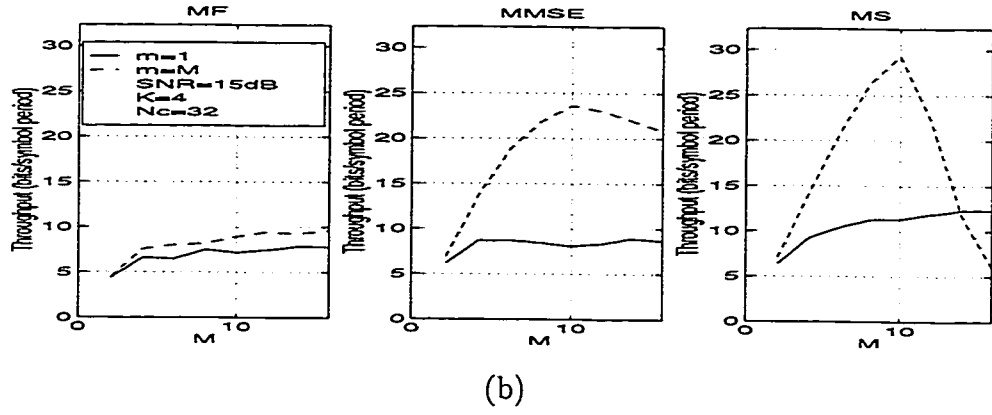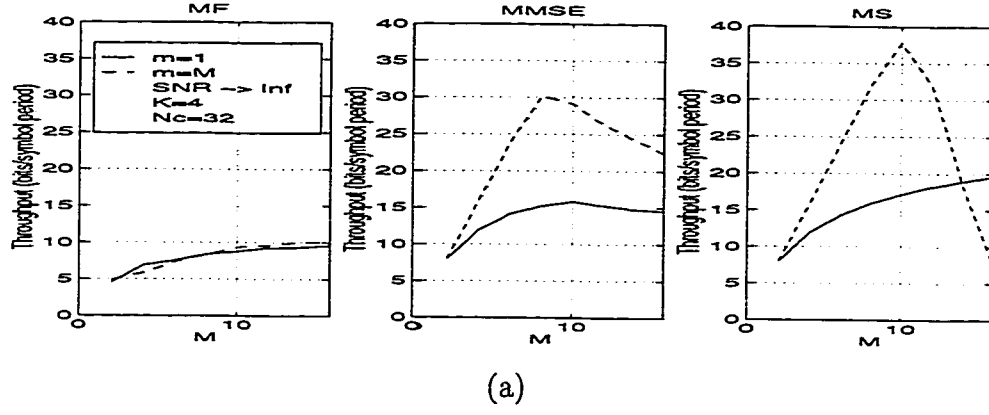
Figure 2.4 : Total channel throughput vs. M when $K = 4$ and $N_c = 32$. The plots in the left column correspond to a Matched Filter detector, the plots in the center column correspond to an MMSE detector and the plots in the right column correspond to a Multistage detector. In (a) the AWGN is essentially non-existent, in (b) the SNR is 15dB and in (c) the SNR is 7dB.
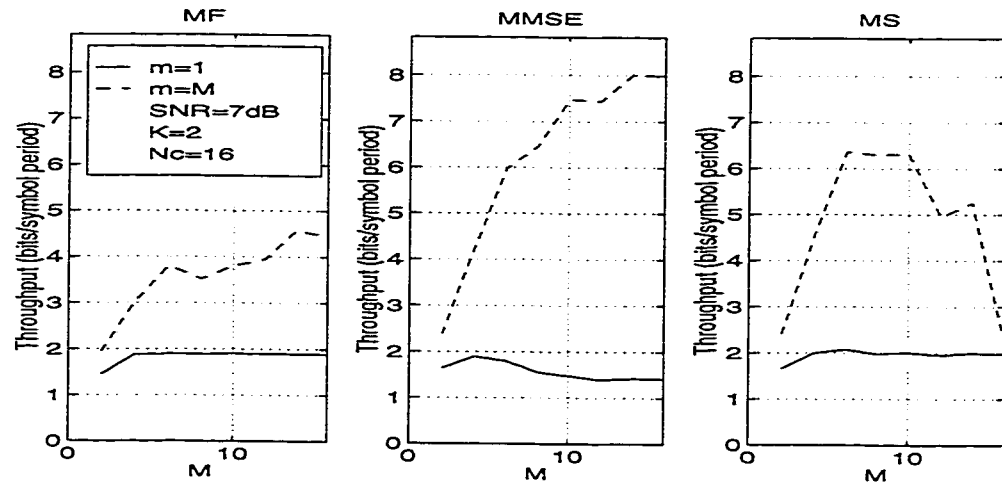
(a)
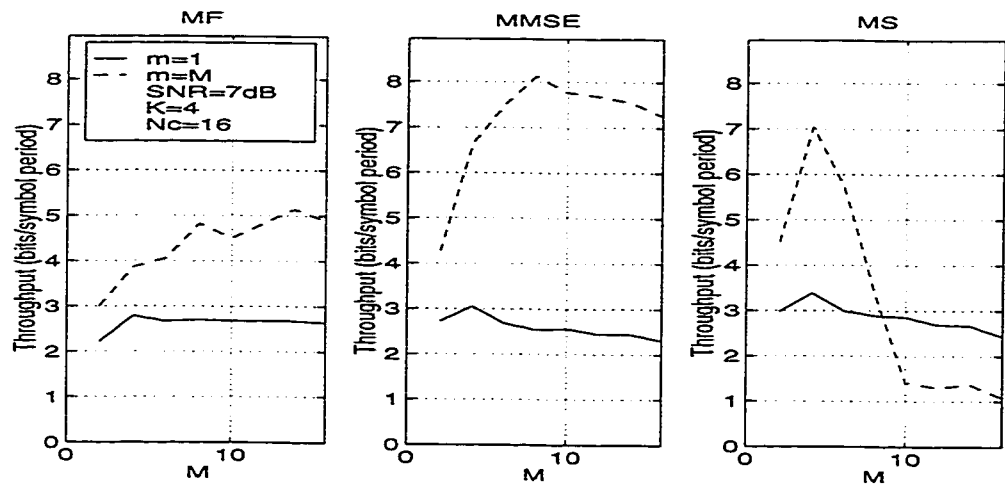
(b)

Figure 2.5 : Total Channel Throughput vs. M when SNR $= 7$dB and $N_c = 16$. In (a) $K = 2$ and in (b) $K = 4$.
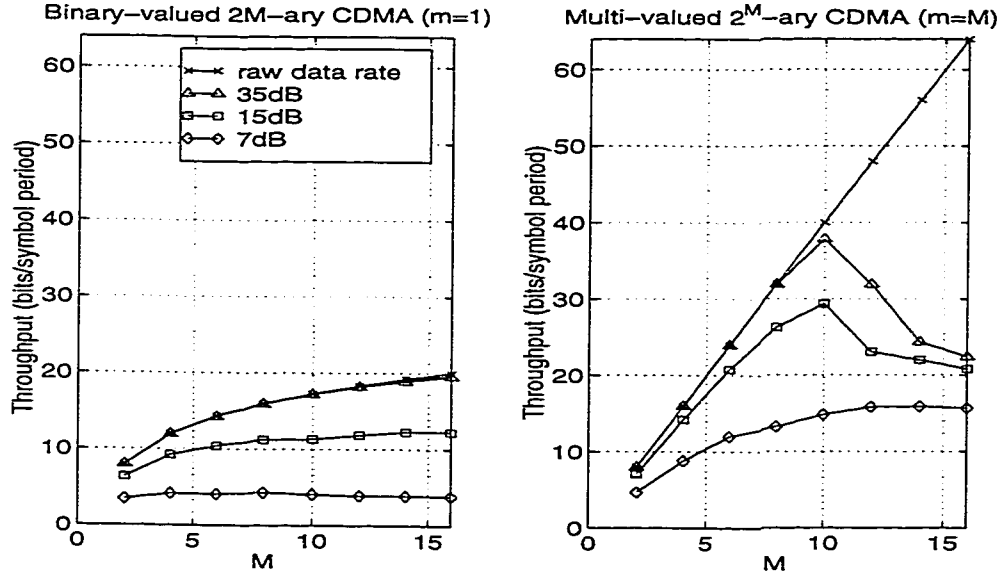
Figure 2.6 : Throughput degradation as SNR → 0. The left graph corresponds to $2M$-ary CDMA and the right graph corresponds to 2^M-ary CDMA. For every value of M, the graphs show the highest throughput achievable by the corresponding system (using any of the detectors being studied).

2.6   CONCLUSIONS/DISCUSSION

There are several conclusions that one can draw from the results in Section 2.5. First, $\mathcal{M}$-ary CDMA can result in high data rates for each user. For example, when Multicarrier Modulation is used, if the multipath delay spread of the channel is approximately $30\mu s$ and if the total bandwidth available is 1.25 MHz (as in IS-95) then for $N_c = 32$, $K = 4$ and SNR $= 7$dB, rough calculations indicate that $\mathcal{M}$-ary CDMA can provide *reliable* transmission at a rate of approximately 125 Kbps for each user.

Second, multivalued 2^M-ary CDMA is superior to binary-valued $2M$-ary CDMA under all the scenarios tested, in the sense that, given the SNR, K and N_c, the maximum throughput achieved is higher. This result was not necessarily expected *a-priori*, even though 2^M-ary CDMA does have a significantly higher raw data rate.

For example, a characteristic of binary-valued $2M$-ary CDMA is the fact that only K codes are present in the channel at any given time. Therefore, the code correlation matrix is always well-conditioned (when $K < N_c$), unlike multivalued 2^M-ary CDMA where, under some scenarios, an ill-conditioned correlation matrix could drastically increase the probability of error, thus severely degrading channel throughput.

Nevertheless, it turns out that, not only does $2M$-ary CDMA have a lower raw data rate than 2^M-ary CDMA, it also suffers from a high probability of error. The fact is that, under low SNR conditions, the probability of making an error in detecting which codes were transmitted increases drastically, thus severely degrading channel throughput. This can be clearly seen in Figure 2.6.

There are still many issues to be studied. First, how does throughput vary as m varies from $m = 1$ to $m = M$? The behavior of the raw data rates shown in Figure 2.1 indicates that throughput may be maximized for a value of m that lies between 1 and M. By being able to use various values of m, as well as various values of M, it is possible to implement a multirate system with a large number of possible rates for each user. Therefore, the second issue is, what is the multirate throughput of $\mathcal{M}$-ary CDMA? Third, how do the results obtained thus far extend to the case when the system is asynchronous? Fourth, what is the effect of employing detectors that are tailored to the $KM > N_c$ case, such as the one described in [9]?

Avenues for future work include the use of non-random Hadamard spreading codes as in [9] which can be designed so that each code of each user is orthogonal to all the codes of all the other users (for certain values of K and M). Also of interest is the throughput of $\mathcal{M}$-ary CDMA when Trellis-Coded Modulation is employed, which has been shown to offer considerable gains in performance [10,11]. Finally, what is needed is a comparison of $\mathcal{M}$-ary CDMA with other high-data-rate and multirate systems, and in particular a test of each system's robustness against inaccuracies

in the estimated amplitudes. It is expected that, for a sufficiently rapidly varying channel, $\mathcal{M}$-ary CDMA will be superior to systems modulating information on the amplitude of the transmitted signals.

Chapter 3

An Optimal One-shot Multiuser Detector for Flat Rayleigh Fading Channels

3.1 INTRODUCTION

With the advent of multiuser detectors [12], CDMA has proven to be a viable technology for the next generation of wireless systems (see, for example, [13]). However, even though the statistics of the channel variations may be known, most multiuser detectors do not incorporate this knowledge into the detection process. Any such knowledge is most often used for tracking the channel variations. The minimum P_e (probability of bit error) receiver, however, is a MAP (Maximum a-posteriori) receiver, that is, a receiver that directly incorporates the density of the channel variations into the bit decisions.

To explore the potential gains of a multiuser MAP receiver, this study focuses on flat fading environments. The attenuation suffered by the transmitted signal is well-modeled as being composed of three components: deterministic path loss, large (time) scale fading, and small (time) scale fading. The latter component is well-modeled as a Rayleigh random variable. Therefore, over a small time scale, since the deterministic and the large time scale components remain approximately constant, the received amplitude may be modeled as a Rayleigh r.v. with a fixed mean. This mean is time-varying, but only over larger time scales, thus making it easier to track by the receiver.

Thus, based on the assumption that the receiver tracks the slowly varying means

of the users' received amplitudes, this work addresses the issue of finding the optimal multiuser one-shot detector, that is, a detector that forms its bit decisions using only the received signal in the corresponding symbol period. Possible reasons for using a one-shot detector may be a channel is that is fading too rapidly, or a desire to reduce the complexity of the receiver. Given the fact that the detector is one-shot, it is necessary to assume that the there is a phase-tracking algorithm in operation [2], due to the phase ambiguity that would otherwise arise.

It should be noted that other work has also dealt with the issue of MAP (i.e. minimum P_e) receivers in Rayleigh fading environments [14–19], but the work focused on single user systems and/or on (computationaly complex) sequence detection.

3.2 PROBLEM SETUP

We assume a synchronous CDMA system that suffers from single-path Rayleigh fading and AWGN. Let N_c denote the spreading factor (number of chips per bit) and assume there are K users in the system. Then, the resulting received $N_c \times 1$ vector, after chip-matched filtering, is given by

$$\mathbf{r} = \mathbf{C}\mathbf{W}\mathbf{b} + \mathbf{n} \tag{3.1}$$

where $\mathbf{C}$ is an $N_c \times K$ matrix whose columns correspond to the spreading codes of the users, $\mathbf{W}$ is a $K \times K$ diagonal matrix whose entries correspond to the (complex) received amplitudes of the various users, $\mathbf{b}$ is a $K \times 1$ vector containing the users' bits, and $\mathbf{n}$ is an $N_c \times 1$ zero-mean complex Gaussian vector with covariance matrix equal to $\sigma^2 I_K$, where I_K is the $K \times K$ identity matrix.

In order to facilitate analysis, $\mathbf{W}$ may be re-written as $\mathbf{W} = \Phi\mathbf{A}$ where Φ and $\mathbf{A}$ are diagonal matrices that contain the phases and the (positive real) amplitudes, respectively, of the various users. Based on the discussion in Section 3.1, Φ is assumed

to be known and can thus be combined with C to form $\bar{C} = C\,\Phi$. As a result, (3.1) may be written as

$$r = \bar{C}\,A\,b + n \tag{3.2}$$

Based on the above system model, the optimal estimator-detector is given by

$$
\begin{aligned}
\hat{A}, \hat{b} &= \arg \max_{\substack{A \in \mathbb{R}_+^{K \times K} \\ b \in \{-1,1\}^K}} p_{A,b|R}(A, b | r) \\
&\equiv \arg \max_{\substack{A \in \mathbb{R}_+^{K \times K} \\ b \in \{-1,1\}^K}} p_{R|A,b}(r | A, b) p_{A,b}(A, b)
\end{aligned}
\tag{3.3}
$$

where $\mathbb{R}_+^{K \times K}$ denotes the set of all $K \times K$ diagonal matrices with positive real entries. The density of r, conditioned on the amplitudes and bits, is

$$
\begin{aligned}
p_{R|A,b}(r | A, b) &= p_N(r - \bar{C}\,A\,b) \\
&= \tfrac{1}{(2\pi\sigma^2)^{N_c/2}} \exp\left(-\tfrac{1}{2\sigma^2}(r - \bar{C}\,A\,b)^H(r - \bar{C}\,A\,b)\right)
\end{aligned}
\tag{3.4}
$$

Also, assuming that the users' bits are equiprobable, that the users' received amplitudes are statistically independent, and that the users' received amplitudes are statistically independent with the users' bits, we have

$$
p_{A,b}(A, b) = \left(\frac{1}{2}\right)^K \prod_{i=1}^K p_{A_{i,i}}(A_{i,i})
\tag{3.5}
$$

where $p_{A_{i,i}}$ denotes the density of the received amplitude of the ith user. Consequently, the optimization problem in (3.3) becomes

$$
\hat{A}, \hat{b} = \arg \min_{\substack{A \in \mathbb{R}_+^{K \times K} \\ b \in \{-1,1\}^K}} \tfrac{1}{2}b^{\top}A^{\top}RAb - b^{\top}A^{\top}y_{MF} - \sigma^2 \sum_{i=1}^K \ln p_{A_{i,i}}(A_{i,i})
\tag{3.6}
$$

where $R = \text{Re}\left[\bar{C}^H\bar{C}\right]$ is the correlation matrix of the users' codes and $y_{MF} = \text{Re}\left[\bar{C}^H r\right]$ is the vector of matched-filter outputs. It appears that the problem in (3.6) is not only analytically intractable, but also prohibitively computationally intensive. This difficulty is alleviated if the problem is re-cast as follows.

Since the elements of $\mathbf{A}$ are positive, $\mathbf{A}$ may be combined with $\mathbf{b}$ to form $\mathbf{x} = \mathbf{A}\mathbf{b} \in \mathbb{R}^K$. No information is lost in doing so since the bits and amplitudes may be extracted from $\mathbf{x}$ according to $b_i = \text{sign}(x_i)$ and $A_{i,i} = |x_i|$. Given the above definition of $\mathbf{x}$, it can be shown that $p_{X_i}(x_i) = \frac{1}{2}p_{A_{i,i}}(|x_i|)$ and that (3.6) becomes

$$\hat{\mathbf{x}} = \arg \min_{\mathbf{x} \in \mathbb{R}^K} \frac{1}{2}\mathbf{x}^\top \mathbf{R}\mathbf{x} - \mathbf{x}^\top \mathbf{y}_{MF} - \sigma^2 \sum_{i=1}^{K} \ln p_{X_i}(x_i) \tag{3.7}$$

with $\hat{b}_i = \text{sign}(\hat{x}_i)$ and $\hat{A}_{i,i} = |\hat{x}_i|$. The first-order conditions for the above problem are given by

$$\mathbf{R}\mathbf{x} - \mathbf{y}_{MF} - \sigma^2 \left[\frac{p'_{X_i}(x_i)}{p_{X_i}(x_i)} \right] = 0 \tag{3.8}$$

Equations (3.7) and (3.8) define the optimal one-shot receiver in a flat fading environment.

3.3   COMPARISON OF AMPLITUDE DENSITY ASSUMPTIONS

The analysis in section 3.2 gives us a class of optimal receivers: each member of this class corresponds to a particular assumption about the statistics of the amplitude variations of the various users. Section 3.4 studies the optimal one-shot multiuser detector in a flat Rayleigh fading channel, that is, when it is assumed that $p_{A_{i,i}}$ is a Rayleigh density. However, for greater insight, this Section investigates three different assumptions about $p_{A_{i,i}}$, all of which lead to well-known multiuser receivers. In fact, due to the fact that these receivers are well-known, we will not elaborate on their properties.

3.3.1 Approach 1: Assume perfect knowledge of amplitudes

Under this approach, $p_{X_i}(x_i)$ consists of two delta functions, one at $-A_i$ and one at $+A_i$. Therefore, the problem in (3.7) reduces to

$$\hat{\mathbf{x}} = \arg \min_{\mathbf{x} \in \{-A_i, +A_i\}^K} \frac{1}{2} \mathbf{x}^T \mathbf{R} \mathbf{x} - \mathbf{x}^T \mathbf{y}_{MF} \qquad (3.9)$$

The above problem has no closed-form solution and thus it is necessary to search over all combinations of $+/-A_i$'s. This results in what is known as the "Maximum Likelihood Detector".

3.3.2 Approach 2: Assume no knowledge of amplitudes

This assumption corresponds to a "uniform" $p_{X_i}(x_i)$, that is, we do not assume that any value of x_i is more likely than any other. As a result, (3.7) reduces to

$$\hat{\mathbf{x}} = \arg \min_{\mathbf{x} \in \mathbb{R}^K} \frac{1}{2} \mathbf{x}^T \mathbf{R} \mathbf{x} - \mathbf{x}^T \mathbf{y}_{MF} \qquad (3.10)$$

whose solution is easily shown to be

$$\mathbf{x} = \mathbf{R}^{-1} \mathbf{y}_{MF} \qquad (3.11)$$

This is of course what is known as the "Decorrelating detector".

3.3.3 Approach 3: Assume amplitude density is a one-sided Gaussian

The reason for this peculiar choice of amplitude density will become apparent shortly. Under this assumption, $p_{X_i}(x_i)$ is a zero-mean Gaussian density with variance σ_i^2. Consequently, the first-order conditions in (3.8) become

$$(\mathbf{R} + \text{diag}(\frac{\sigma^2}{\sigma_i^2}))\mathbf{x} - \mathbf{y}_{MF} = 0 \qquad (3.12)$$

Thus, if we set $\sigma_i = A_{i,i}$ we obtain

$$\mathbf{x} = (\mathbf{R} + \mathrm{diag}(\frac{\sigma^2}{A_{i,i}^2}))^{-1}\mathbf{y}_{MF} \qquad (3.13)$$

which is of course the "MMSE detector". We therefore see that, even though the MMSE is known to be optimal in the minimum mean square error sense, it is also optimal in the minimum P_e sense, given a particular assumption about the density of the users' amplitudes.

3.3.4 Optimality considerations

Even though it is interesting and insightful to see how the previous three well-known receivers may be looked at as optimal receivers under different amplitude density assumptions, the fact is that there are problems with all three of them. First, it is too optimistic to assume perfect amplitude knowledge, and as a result, receiver performance will suffer in the presence of estimation errors. Second, it is too pessimistic to assume no amplitude knowledge, since this degrades receiver performance. Third, the assumption of a one-sided Gaussian density for the amplitudes is ad-hoc, and does not correspond to any practical scenario.

Which density *does* correspond to many practical scenarios is known. Section 3.4 analyzes the receiver that results from the incorporation of this knowledge into (3.7).

3.4 OPTIMAL RECEIVER

As mentioned in Section 3.1, a user's received amplitude is well modeled as a Rayleigh r.v. with a mean that remains approximately constant over small time scales. There-

fore, the model we use for $p_{X_i}(x_i)$ is

$$p_{X_i}(x_i) = \frac{\pi}{4m_i^2}|x_i|e^{-\frac{\pi}{4m_i^2}x_i^2} \qquad (3.14)$$

where m_i is the mean of the amplitude of user i over the time period of interest. Consequently, the first-order conditions in (3.8) become

$$(\mathbf{R} + \operatorname{diag}(\frac{\sigma^2}{\frac{2}{\pi}m_i^2}))\mathbf{x} - \mathbf{y}_{MF} - \sigma^2./\mathbf{x} = 0 \qquad (3.15)$$

where $\sigma^2./\mathbf{x}$ denotes the vector whose i^{th} component equals $\frac{\sigma^2}{x_i}$. The resulting K simultaneous quadratic equations have no closed-form solution. This implies that the solution has to be found numerically. However, as can be seen from Figure 3.1, the objective function is not convex. Thus, even if the solution to (3.15) is found numerically, it will most probably only correspond to a local minimum. Consequently, arriving at the global minimum is best accomplished by numerically minimizing the objective function, rather than solving the F.O.C.'s.

Given the shape of the objective function,

$$f(\mathbf{x}) = \frac{1}{2}\mathbf{x}^{\top}(\mathbf{R} + \operatorname{diag}(\frac{\sigma^2}{\frac{2}{\pi}m_i^2}))\mathbf{x} - \mathbf{x}^{\top}\mathbf{y}_{MF} - \sigma^2\sum_{i=1}^{K}\ln|x_i| \qquad (3.16)$$

that is, the fact that it is non-convex and that it approaches minus infinity as any element of $\mathbf{x}$ approaches 0, any numerical optimization algorithm would fail to find the global minimum, unless the initial guess was in the correct "quadrant". In this study, the above problem has been overcome by a two-step process. First, a smoothed version of the objective function is minimized. The intention is to get inside the quadrant that contains the global minimum. Second, the original objective function is minimized using the above solution as the starting point. Smoothing the objective function is at present achieved via an ad-hoc method. However, as Figure 3.1 and the results in the following section demonstrate, this two-step algorithm is effective. In addition, the computational complexity of this algorithm is manageable.
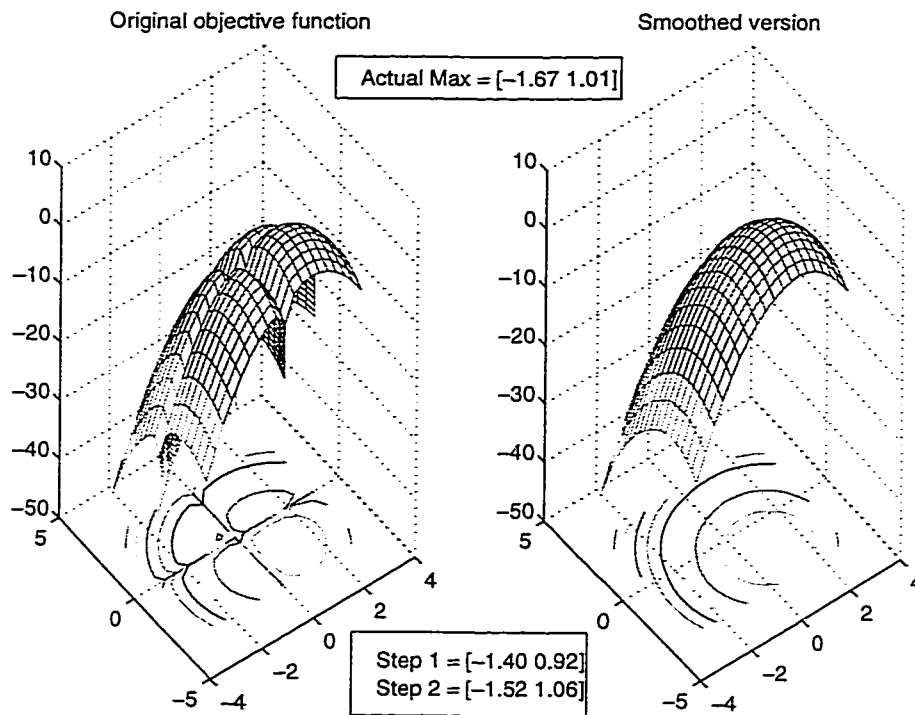
Figure 3.1 : Demonstration of the two-step algorithm for finding the global minimum of the objective function of the optimal receiver in a flat Rayleigh fading environment. (Note: for visual clarity, what is shown is the negative of the objective function)

3.5 RESULTS

Figures 3.2 through 3.4 show the probability of bit error of various receivers, as a function of the signal-to-noise ratio (SNR). The receivers being compared are the conventional matched filter receiver, the decorrelator, the MMSE that has perfect knowledge of users' amplitudes and the optimal receiver that has perfect knowledge of the means of the users' amplitudes. In all figures, the acronym PAK refers to the optimal receiver developed in this study, and is derived from "Partial Amplitude Knowledge" receiver, which is meant to emphasize that the receiver is incorporating partial (statistical) knowledge about the amplitudes into the decision process.
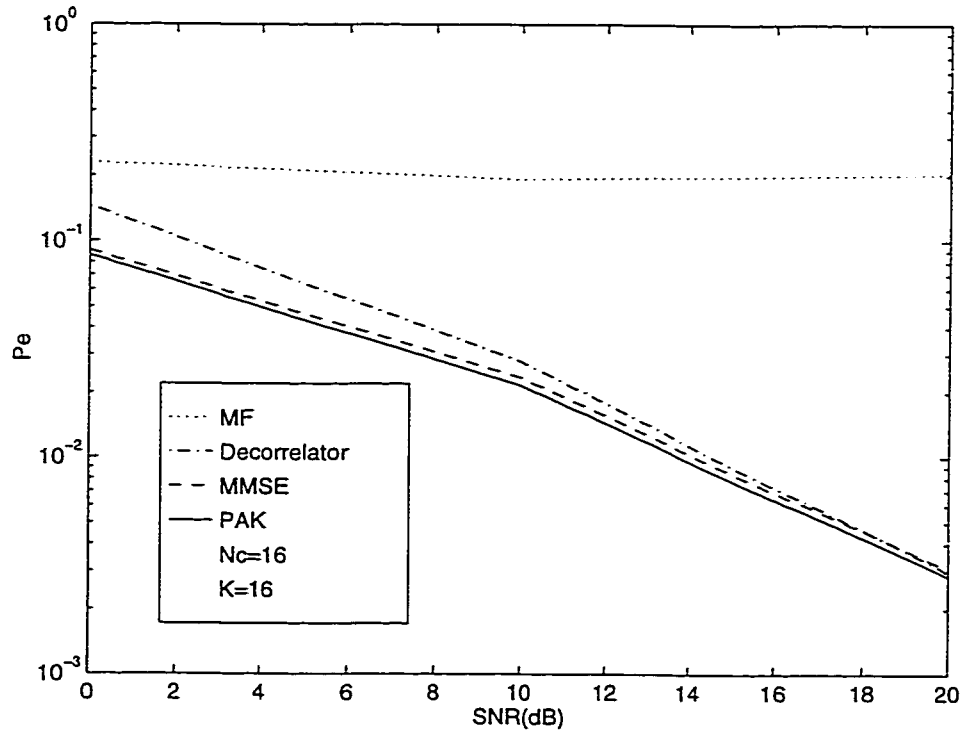
Figure 3.2 : P_e vs. SNR when we have 16 users and a spreading factor equal to 16
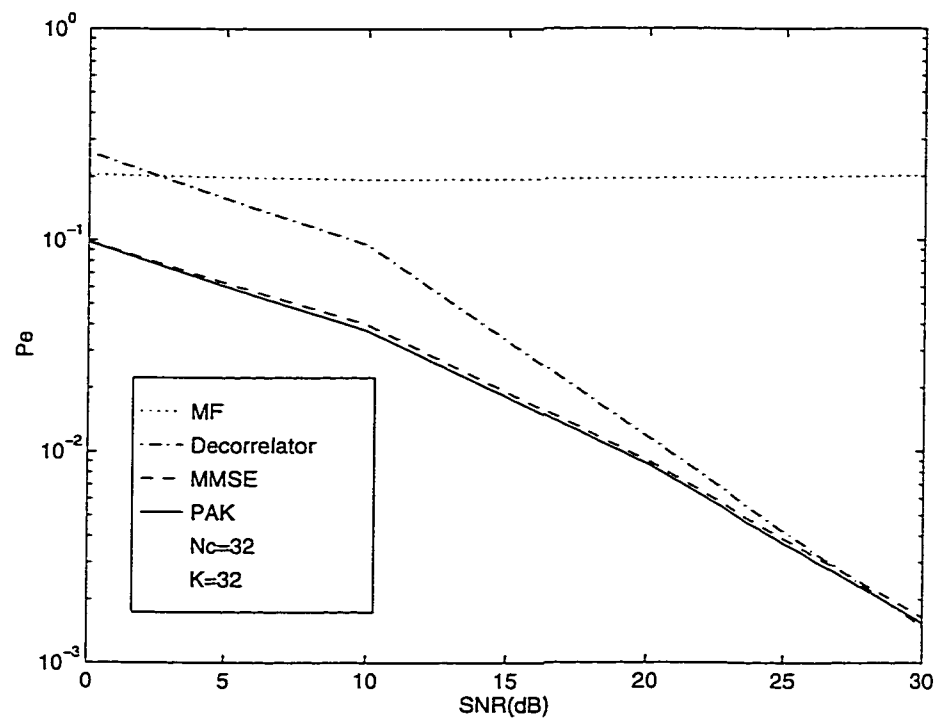
Figure 3.3 : P_e vs. SNR when we have 32 users and a spreading factor equal to 32
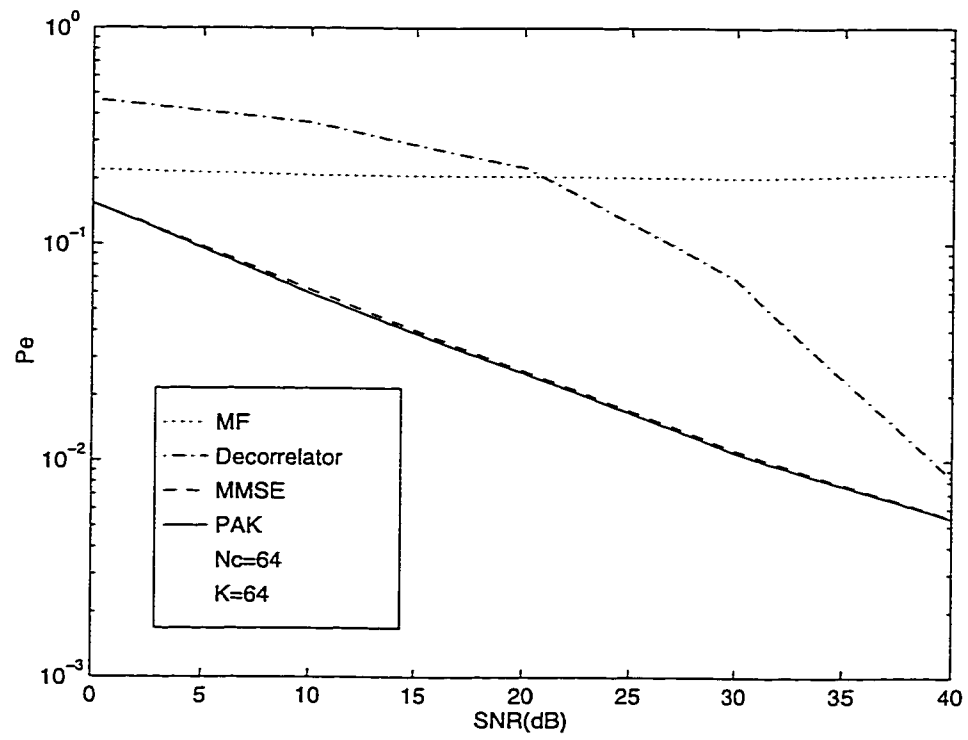
Figure 3.4 : P_e vs. SNR when we have 64 users and a spreading factor equal to 64

3.6 CONCLUSIONS/DISCUSSION

We have derived the optimal one-shot multiuser detector for a flat Rayleigh fading channel. It performs significantly better than the decorrelator and is slightly better than the MMSE which assumes perfect knowledge of amplitudes.

It is important to examine what information is required in order to make the various receivers operational, besides the timing and phases of the users. The matched filter receiver requires knowledge of the desired user's spreading code. The decorrelator, MMSE and PAK receivers, as implemented in this study, require knowledge of all the users' spreading codes. However, the decorrelator requires no more than that, whereas the MMSE requires knowledge of $\frac{\sigma^2}{A_{i,i}^2}$, that is, the *instantaneous* SNR for each user. In contrast, the PAK receiver requires knowledge of m_i and σ^2, that is, the means of the users' amplitudes and the level of the background AWGN, both of which are slowly-varying, and can thus be easily tracked by the receiver. The fact that both the MMSE and the PAK performance, in Figures 3.2 through 3.4, are plotted assuming perfect knowledge of required quantities, is extremely favorable for the MMSE because of the significantly smaller estimation error that would arise from estimating slowly-varying quantities, such as the means of the users' amplitudes, versus more rapidly varying quantities such as the instantaneous SNR for each user. It is expected that when both receivers are run in an adaptive mode, having to estimate their respective required quantities, the difference in performance will increase.

Finally, a note regarding receiver complexity. The fact that the PAK receiver has to track only the means of the users' amplitudes results in significantly lower complexity compared to a receiver that has to track the amplitudes. In addition, the fact that the PAK receiver obtains an automatic amplitude estimate as a result of

the detection process, and thus requires no extra algorithm to track the amplitudes, results in even more complexity reductions compared to a receiver that has separate detection and amplitude estimation algorithms. Also, due to the fact that we were able to transform the mixed-integer optimization problem in (3.3) into the continuous optimization problem in (3.7), the complexity of the optimization algorithm became very manageable.

Avenues for future work include an adaptive implementation of the PAK receiver and an extension of this work to asynchronous systems and to frequency-selective fading environments. Also of interest is optimal multiuser sequence detection, which, unlike one-shot detection, enables the optimal tracking of the users' phases, and which, via the exploitation of the correlation in the fading process, promises significant potential gains. More importantly, this would demonstrate if the loss in performance sustained by the use of a one-shot detector is significant or not.

Chapter 4

Multiuser Detection in Fast Fading Multipath Environments

4.1 Introduction

We propose a new framework for multiuser detection in fast fading channels that are encountered in many mobile communication scenarios. Existing multiuser RAKE receivers, developed to combat multipath fading and multiuser interference in slow fading, suffer substantial degradation in performance under fast fading due to errors in channel state estimation. The detectors proposed in this chapter employ a novel receiver structure based on time-frequency processing that is dictated by a canonical representation of the wide-sense stationary uncorrelated scatterer channel model. The workhorse of the framework is a time-frequency generalization of the RAKE receiver that exploits joint multipath-Doppler diversity. Analytical and simulated results based on realistic fast fading assumptions demonstrate that due to the inherently high level of diversity afforded by multipath-Doppler processing, the proposed multiuser detectors promise substantially improved performance compared to existing systems.

Code division multiple access (CDMA) has emerged as one of the most promising systems for multiuser wireless communication. The need for acommodating the growing number of users, and for communication in diverse environments, has posed unique technological challenges in system design. Two of the most significant factors limiting the performance of existing mobile wireless CDMA systems are multipath

fading and multiaccess interference. Multipath fading is due to the channel dynamics produced by the multiple mobile scatterers encountered in transmission. Multiaccess interference, on the other hand, is caused by the multiple users simultaneously using the channel. The RAKE receiver structure is used in practice to combat fading [20,21], and various multiuser detection schemes have been proposed [22] to overcome multiaccess interference. Recently, multiuser RAKE receivers have been proposed to combat multiaccess interference in fading channels [23,24]. However, such schemes are applicable only in slow fading scenarios in which the channel characteristics change slowly over time.

Fast fading is encountered in many mobile communication scenarios, and it significantly degrades the performance of the RAKE receiver due to less reliable channel estimation [25–27]. In fact, existing systems exhibit a limiting bit-error probability floor that cannot be improved by increasing the transmitted power [25,27]. Recently, a single-user spread-spectrum communication scheme has been proposed for fast fading channels that exploits temporal channel variations to provide another means for diversity — Doppler diversity — to counter such degradation in performance [28–30]. The methodology uses joint time-frequency processing which is a powerful approach to time-varying signal processing [31]. At the heart of the approach is a fundamental time-frequency-based channel decomposition derived from a sampling of the wide-sense stationary uncorrelated scatterer (WSSUS) model. The channel representation naturally leads to a time-frequency generalization of the RAKE receiver that exploits joint multipath-Doppler diversity. The time-frequency (TF) RAKE receiver, by achieving an inherently higher level of diversity, can deliver substantially improved performance compared to existing systems [28–30].

In this chapter, we leverage the time-frequency formulation to propose a new multiuser detection framework in the context of CDMA systems to combat multiac-

cess interference in fast fading multipath channels [32]. Our development is based on the TF RAKE receiver, and includes time-frequency generalizations of the decorrelating [33] and minimum-mean-squared-error (MMSE) [34] multiuser receivers. Analytical and simulation results show that the relatively modest Doppler spreads* (100 − 200Hz) encountered in practical fast fading scenarios can be transformed into significant joint multipath-Doppler diversity gains by the multiuser receivers proposed in this chapter.

In the next section, we develop the relevant time-frequency-based channel and signal models for fast fading CDMA environments. Section 4.3 develops our multiuser detection framework based on the TF RAKE receiver. Analytical and simulated results on the performance of the proposed receivers are provided in Section 4.4. Section 4.5 contains some concluding remarks and directions for future research.

4.2   Time-Frequency-Based Channel and Signal Models

In this section, we provide a brief description of the canonical time-frequency decomposition of the WSSUS [28, 29] in the context of multiuser CDMA systems. The channel representation serves as the backbone of the multiuser detection framework developed in this chapter.

4.2.1   Single-User Channel Representation

As depicted in Figure 4.1, the complex baseband signal $x(t)$ at the output of the channel is related to the transmitted complex baseband signal $s(t)$ by

$$x(t) = \int h(t, \tau) s(t - \tau) d\tau, \tag{4.1}$$

---

*Sufficient to degrade the performance of existing systems due to errors in channel state estimation [25, 27].

where $h(t, \tau)$ is the time-varying impulse response of the channel [20]. An equivalent representation central to our discussion is in terms of the channel *spreading function* $H(\theta, \tau)$:

$$x(t) = \int_0^{T_m} \int_{-B_d}^{B_d} H(\theta, \tau)s(t - \tau)e^{j2\pi\theta t}d\theta d\tau, \quad (4.2)$$

$$H(\theta, \tau) \stackrel{def}{=} \int h(t, \tau)e^{-j2\pi\theta t}dt. \quad (4.3)$$

The channel produces time- and frequency-shifts in the signal, and the output signal $x(t)$ is a linear combination of time-frequency shifted copies of $s(t)$. In (4.2), T_m is the *multipath spread* of the channel, and denotes the maximum delay produced by the channel. Similarly, B_d is the *Doppler spread*, and denotes the maximum (one-sided) Doppler shift introduced by the channel. Fast fading channels encountered in practice exhibit Doppler spreads on the order of $100 - 200$Hz due to relative motions of the users [25, 27].

The dynamics of the channel are best described statistically, and the WSSUS model [20, 35] assumes that $H(\theta, \tau)$ is a two-dimensional uncorrelated Gaussian process

$$E\left[H(\theta, \tau)H^*(\theta', \tau')\right] = \Psi(\theta, \tau)\delta(\theta - \theta')\delta(\tau - \tau'), \quad (4.4)$$

where $\delta(x)$ denotes the Dirac delta function. The function $\Psi(\theta, \tau) \geq 0$ is called the *scattering function*. The multipath spread T_m is the maximum (essential) support of $\Psi(\theta, \tau)$ in the τ direction, and the Doppler spread B_d is its maximum (one-sided) support in the θ direction.

For a spread-spectrum signal $s(t)$ of duration T and chip interval T_c, the WSSUS channel admits the following canonical finite-dimensional decomposition [28–30]:

$$x(t) = \frac{T_c}{T} \sum_{l=0}^{L} \sum_{m=-M}^{M} H^{ml}s(t - lT_c)e^{j\frac{2\pi mt}{T}}, \quad 0 \leq t < T, \quad (4.5)$$

with $L = \lceil T_m/T_c \rceil$, $M = \lceil TB_d \rceil$, and

$$H^{ml} \stackrel{def}{=} \widehat{H}(m/T, lT_c), \tag{4.6}$$

where $\widehat{H}(\theta, \tau)$ is a time-frequency smoothed version of $H(\theta, \tau)$

$$\widehat{H}(\theta, \tau) = \frac{T}{T_c} \int_0^{T_m} \int_{-B_d}^{B_d} H(\theta', \tau') e^{-j\pi(\theta-\theta')T} \text{sinc}((\theta - \theta')T) \text{sinc}((\tau - \tau')/T_c) d\theta' d\tau'. \tag{4.7}$$

The channel samples H^{ml} are approximately uncorrelated

$$\mathrm{E}[H^{ml} H^{*m'l'}] \approx \widehat{\Psi}(m/T, lT_c)\delta_{m-m'}\delta_{l-l'}, \tag{4.8}$$

and the waveforms $u_{ml} \stackrel{def}{=} s(t - lT_c)e^{j2\pi mt/T}$ are approximately orthogonal

$$\int u_{ml}(t) u_{m'l'}^*(t) dt \approx \delta_{l-l'}\delta_{m-m'} \int |s(t)|^2 dt, \tag{4.9}$$

where δ_k denotes the Kronecker delta function.

The representation (4.5) is a Karhunen-Loève-like expansion of the received signal in terms of the uncorrelated random variables H^{ml}'s, and the orthogonal waveforms u_{ml}'s. In (4.5), L denotes the number of multipath components, and M the number of Doppler components that are contributing significant energy to the channel [29]. We note that similar sampled representations for the WSSUS channel have been developed in [35], based on time and bandwidth constraints. However, our formulation and interpretation in terms of diversity signaling is quite different.

The power of the channel representation (4.5) comes from the fact that it facilitates full exploitation of the inherent channel diversity. The $(L + 1)(2M + 1)$ uncorrelated channel samples H^{ml}, corresponding to the time-frequency shifted signal copies $s(t - lT_c)e^{j2\pi mt/T}$, serve as independent fading channels to provide a substantially higher level of diversity compared to conventional systems.[†] In particular,

---

[†]An arbitrarily high level of diversity can be achieved by decreasing T_c (increasing bandwidth;

the utilization of a single ($M = 1$) Doppler component yields $3(L + 1)$-level joint multipath-Doppler diversity, which is three-fold higher than the $(L + 1)$-level multipath diversity attained by existing systems. As we will see, the TF RAKE receiver provides the mechanism for exploiting joint multipath-Doppler diversity by computing the correlator outputs corresponding to the waveforms $s(t - lT_c)e^{j2\pi mt/T}$.

We note that values of $TB_d \approx 0.01 - 0.015$, produced by commonly encountered Doppler spreads, significantly degrade the performance of the RAKE receiver due to errors in channel state estimation [25, 27]. More importantly, at modestly larger $(0.2 - 0.6)$ values of TB_d, significant multipath-Doppler diversity gains can be achieved via appropriate signal processing [29, 36]. There are several approaches for exploiting multipath-Doppler diversity by attaining larger values of TB_d [28–30, 36] (more discussion in Section 4.3.3).

4.2.2 Multiuser Signal Model

For a CDMA system with K users and employing synchronous coherent BPSK signaling, such as may be encountered in the downlink of a mobile communication system [21, 37], the signal at the input of the receiver is given by

$$r(t) = x(t) + n(t) = \sum_{i=-I}^{I} \sum_{k=1}^{K} b_k(i)x_k^i(t) + n(t) \qquad (4.10)$$

where $b_k(i) \in \{-1, 1\}$ is the i-th bit of the k-th user, $x_k^i(t)$ is the unmodulated received baseband signal for the i-th bit of the k-th user, I is the size of the detection window, and $n(t)$ is the complex baseband additive white Gaussian noise (AWGN) with power spectral density $\mathcal{N}_0$. In terms of the representation (4.5), the signal $x_k^i(t)$

---

finer multipath resolution) and/or increasing T (finer Doppler resolution). Exploiting Doppler diversity corresponds to the latter. Note that the two resolutions are not constrained by the uncertainty principle.

can be expressed as

$$x_k^i(t) = \frac{T_c}{T} \sum_{l=0}^{L} \sum_{m=-M}^{M} H_k^{ml}(i) s_k(t - iT - lT_c) e^{j\frac{2\pi mt}{T}}, \qquad (4.11)$$

where $s_k(t)$ is the spreading waveform of the k-th user, and $H_k^{ml}(i)$ are the channel coefficients corresponding to the i-th bit of the k-th user.[‡] Note that we have absorbed the signal powers and the carrier phases for the different users in the channel coefficients $H_k^{ml}(i)$.[§]

For simplicity of exposition, we introduce a vector notation for the signals. Let us start by defining

$$s_k^{ml}(t) \stackrel{def}{=} s_k(t - lT_c) e^{j\frac{2\pi mt}{T}}, \qquad (4.12)$$

and let $s(t)$ denote the $K(L+1)(2M+1) \times 1$ vector

$$s(t) \stackrel{def}{=} \left[s_1^T(t), s_2^T(t), \cdots, s_K^T(t) \right]^T, \qquad (4.13)$$

where the $(L+1)(2M+1) \times 1$ vectors $s_k(t)$ are given by

$$s_k(t) \stackrel{def}{=} \left[s_k^{-M^T}(t), s_k^{-M+1^T}(t), \cdots, s_k^{0^T}(t), \cdots, s_k^{M-1^T}(t), s_k^{M^T}(t) \right]^T, \quad k = 1, 2, \cdots, K, \qquad (4.14)$$

in terms of the $(L+1) \times 1$ vectors

$$s_k^m(t) \stackrel{def}{=} \left[s_k^{m0}(t), s_k^{m1}(t), \cdots, s_k^{mL}(t) \right]^T, \quad m = -M, -M+1, \cdots, 0, \cdots, M-1, M. \qquad (4.15)$$

[‡]For simplicity of notation, we use the same L and M for all the users. However, our discussion can be extended straightforwardly to incorporate different values of L and M for different users.

[§]Note that for the downlink (mobile to user), the receiver sees identical channels for the different users: $H_k^{ml} = H^{ml}$ for all k. However, in the uplink (user to mobile), typically the channels are distinct.

Similarly as $s_k(t)$ and $s_k^m(t)$, define the $(L+1)(2M+1) \times 1$ vectors $h_k(i)$ in terms of the $(L+1) \times 1$ vectors $h_k^m(i)$, which are in turn defined in terms of $H_k^{ml}(i)$. Finally, define the $K(L+1)(2M+1) \times K$ channel matrix for the i-th symbol as

$$H(i) \stackrel{def}{=} \begin{bmatrix} h_1(i) & 0 & \cdots & 0 \\ 0 & h_2(i) & 0 & \cdots \\ \vdots & \vdots & \ddots & \vdots \\ 0 & \cdots & 0 & h_K(i) \end{bmatrix},$$ (4.16)

and the $K \times 1$ vector for the i-th bits as

$$b(i) \stackrel{def}{=} [b_1(i), b_2(i), \cdots, b_K(i)]^T.$$ (4.17)

In terms of the above notation, the received signal $r(t)$ can be expressed as

$$r(t) = \sum_{i=-I}^{I} s^T(t - iT)H(i)b(i) + n(t).$$ (4.18)

Thus, the received signal is a linear combination of the time-frequency shifted signals $s_k^{ml}(t)$, which also define the front-end time-frequency correlators (TF RAKE receiver) for realizing the sufficient statistics for detecting the bits of different users.

For negligible intersymbol interference ($T_m \ll T$), the output of the time-frequency correlators for the p-th bit is given by the $K(L+1)(2M+1) \times 1$ vector

$$z(p) \stackrel{def}{=} \int r(t)s^*(t - pT)dt = RH(p)b(p) + w,$$ (4.19)

where

$$R \stackrel{def}{=} \int s^*(t)s^T(t)dt = \begin{bmatrix} R_{11} & R_{12} & \cdots & R_{1K} \\ R_{21} & R_{22} & \cdots & R_{2K} \\ \vdots & \vdots & \vdots & \vdots \\ R_{K1} & R_{K2} & \cdots & R_{KK} \end{bmatrix},$$ (4.20)

$$R_{kk'} \stackrel{def}{=} \int s_k^*(t) s_{k'}^T(t) dt, \tag{4.21}$$

and

$$w \stackrel{def}{=} \int s^*(t - pT) n(t) dt \tag{4.22}$$

is a zero-mean complex Gaussian noise vector with $\mathrm{E}[ww^H] = \mathcal{N}_0 R$. It follows that in the absence of intersymbol interference, the "one-shot" detector suffices in which the decision about the p-th bit is based on the received waveform for the corresponding bit only. Thus, in subsequent sections, we suppress the bit index p and, without loss of generality, focus on the 0-th bit: $z = RHb + w$.

Recall that the k-th component of $z = [z_1, z_2, \cdots, z_K]^T$ consists of the time-frequency correlator outputs for the k-th user:

$$z_k^{ml} = \int r(t) s_k^{*ml}(t) dt = \int r(t) s_k^*(t - lT_c) e^{-j2\pi mt/T} dt. \tag{4.23}$$

In fact, the front-end time-frequency correlators are a generalization of the RAKE receiver, and can be efficiently implemented via a bank of RAKE receivers [29,28,30]. This is the reason for referring to the proposed receiver structures for joint multipath-Doppler processing as TF RAKE receivers.

4.3 Multiuser Detectors for Fast Fading Channels

In this section, we develop a multiuser detection framework that incorporates the fundamental multipath-Doppler channel model of Section 4.2 to deliver near-far resistant receiver structures for fast fading channels. The TF RAKE receiver plays a central role in our development, and we start our discussion with the computationally intensive optimal multiuser detector, which is an extension of the synchronous receiver derived in [38]. The structure of the optimal detector inspires a unified

formulation of a class of suboptimal, near-far resistant receiver structures that are computationally tractable. The resulting multiuser TF RAKE receivers include generalizations of the decorrelating [33] and MMSE [34] multiuser detectors. Restricted to slow fading scenarios ($M = 0$ in (4.5)), our treatment also serves as a unified formulation of the multiuser RAKE receivers proposed in [23, 24, 39].

4.3.1 Minimum Probability of Error Receiver

Recall the definition of $z = [z_1, z_2, \cdots, z_k]$ in (4.19). In the absence of multiaccess interference, corresponding to the single-user case, the optimal receiver for each user is the TF RAKE receiver with maximal-ratio-combining (MRC) [28, 29]

$$\widehat{b}_k = \text{sign}\left\{\text{Re}\left[h_k^H z_k\right]\right\} = \text{sign}\left\{\text{Re}\left[\sum_{l=0}^{L} \sum_{m=-M}^{M} H_k^{*ml} z_k^{ml}\right]\right\}, \quad k = 1, 2, \cdots, K,$$

(4.24)

which coherently combines the different multipath-Doppler shifted signal components to achieve $(L+1)(2M+1)$-order diversity.[¶] Note that MRC requires the knowledge of the channel coefficients H_k^{ml}, which may be estimated through a pilot transmission, for example. The signal component of z_k in this case is $\mathcal{E}_k h_k b_k$, where $\mathcal{E}_k \stackrel{def}{=} \|s_k\|^2 = \int |s_k(t)|^2 dt$, resulting in $\mathcal{E}_k \|h_k\|^2 b_k$ as the real-valued signal component of the test statistic in (4.24). Of course, in the presence of other users, the detector in (4.24) is not near-far resistant since it ignores multiaccess interference.

It is instructive to study the structure of the optimal multiuser detector which essentially augments the single-user receiver (4.24) by suppressing multiaccess interference. Following the approach in [38], it can be shown that the minimum probability of error reception is achieved by the maximum likelihood (ML) receiver given

---

[¶]The conventional single-user RAKE receiver corresponds to $M = 0$ in (4.24).

by

$$\widehat{b}_{opt} = \arg\max_{b\in\{-1,1\}^K} p(z|b) = \arg\max_b -(z - RHb)^H R^{-1}(z - RHb)$$
$$= \arg\max_b \left[2\mathrm{Re}[b^T H^H z] - b^T H^H RHb\right], \qquad (4.25)$$

where the last equality is equivalent to

$$\widehat{b}_{opt} = \arg\max_b \left[\sum_{k=1}^K 2\mathrm{Re}\left[h_k^H z_k\right] b_k - \sum_{k=1}^K \sum_{k'=1}^K b_k [H_k^H RH_{k'}]b_{k'}\right]. \qquad (4.26)$$

Note that the effects of fast fading are incorporated in the above formulation via the multipath-Doppler channel coefficient matrix H. The first term corresponds to the single-user TF RAKE receiver, and the second term eliminates the multiaccess interference. Given the knowledge of channel coefficients, the optimal decision requires a search over 2^K possibilities for b, which can be efficiently executed with Viterbi sequence decoding [38]. However, due to the exponential computational complexity (in the number of users) of the optimal receiver, lower complexity, suboptimal approaches are sought in practice. Next, we discuss an approach for designing suboptimal near-far resistant TF RAKE receivers that are computationally tractable.

4.3.2 A Class of Suboptimal Near-Far Resistant Receivers

The structure of the suboptimal receivers that we derive is motivated by the optimal single-user MRC detector (4.24). As evident from (4.24), the MRC detector makes the decision by coherently combining the time-frequency correlator outputs z_k corresponding to each user. As mentioned before, in the absence of other users, the signal component of z_k is

$$\int r(t)s_k^*(t)dt\bigg|_{r(t)=x(t)} = h_k b_k. \qquad (4.27)$$

In our suboptimal approach, the basic idea is to obtain an estimate of the noise-free correlator outputs, $h_k b_k$, and then to coherently combine them as in (4.24) to obtain

the bit estimates for each user. The estimation procedure for $h_k b_k$ should be such that the resulting detector is near-far resistant. In terms of the K users, we seek a near-far resistant estimate of

$$y = \int r(t)s^*(t)dt \bigg|_{r(t)=x(t)} = Hb. \tag{4.28}$$

The nature of the estimate of y determines the structure of the receivers. For computational efficiency, both the receiver structures that we propose employ a linear estimate. Generically, the estimate of y takes the form

$$\widehat{y} = Fz = FRHb + Fw = y_s + y_n, \tag{4.29}$$

where $y_n \sim \mathcal{N}(0, Q)$ with

$$
\begin{aligned}
Q &= \mathrm{E}[Fww^H F^H] = \mathcal{N}_0 FRF^H \\
&= \begin{bmatrix}
Q_{11} & Q_{12} & \cdots & Q_{1K} \\
Q_{21} & Q_{22} & \cdots & Q_{2K} \\
\vdots & \vdots & \vdots & \vdots \\
Q_{K1} & Q_{K2} & \cdots & Q_{KK}
\end{bmatrix}.
\end{aligned} \tag{4.30}
$$

The matrix F is chosen to yield a near-far resistant estimate of y. Following the application of F, MRC is applied to the different multipath-Doppler components of each user ($\widehat{y}_k$), analogous to (4.24). However, since the noise in the estimate $\widehat{y}$ is correlated, a prewhitening operation is needed. The general form of the overall multiuser TF RAKE receiver becomes

$$\widehat{b} = \mathrm{sign}\left\{ \mathrm{Re}\left[H^H D\widehat{y} \right] \right\} = \mathrm{sign}\left\{ \mathrm{Re}\left[H^H D F z \right] \right\}, \tag{4.31}$$

where the block-diagonal matrix D

$$D = \begin{bmatrix} Q_{11}^{-1} & 0 & \cdots & 0 \\ 0 & Q_{22}^{-1} & 0 & \cdots \\ \vdots & \vdots & \ddots & \vdots \\ 0 & \cdots & 0 & Q_{KK}^{-1} \end{bmatrix} \tag{4.32}$$

performs the prewhitening, and the matrix H^H performs MRC. A schematic of the overall receiver structure is depicted in Figure 4.2. In the following subsections, we discuss two special cases of the receiver structure (4.31), based on the choice of the estimator matrix F.

ML Estimation: Decorrelating Receiver

If the ML estimate of $y = Hb$ is employed, the resulting receiver is linear, and constitutes a generalization of the decorrelating receiver [23, 33]. The estimator matrix F in this case is

$$F_{ML} = R^{-1} \tag{4.33}$$

since

$$\widehat{y}_{ML} = \arg\max_{y} \left[2\text{Re}[z^H y] - y^H R y \right] = R^{-1} z. \tag{4.34}$$

Note that the correlation matrix of the transformed noise vector is $Q_{ML} = \mathcal{N}_0 R^{-1}$. From (4.31), it follows that the resulting decorrelating TF RAKE receiver takes the form

$$\widehat{b}_{dec} = \text{sign}\left\{ \text{Re}\left[H^H D_{dec}\widehat{y}_{ML} \right] \right\} = \text{sign}\left\{ \text{Re}\left[H^H D_{dec}R^{-1}z \right] \right\}, \tag{4.35}$$

where D_{dec} is defined as in (4.32), with $Q = Q_{ML}$. The decorrelating TF RAKE receiver in (4.35) combats fast multipath fading by exploiting joint multipath-Doppler diversity, and attains near-far resistance via the ML estimate in (4.34).

MMSE Receiver

If a linear MMSE estimate of $y = Hb$ is employed, a generalization of the MMSE detector proposed in [24,34] is obtained. In this case, the estimator matrix F solves

$$F_{mmse} = \arg\min_{F} E\left\|Hb - Fz\right\|^2, \tag{4.36}$$

and, as shown in the Appendix, it takes the form

$$F_{mmse} = (R + \mathcal{N}_0\Psi^{-1})^{-1}, \tag{4.37}$$

where

$$\Psi \overset{def}{=} E[HH^H]. \tag{4.38}$$

The resulting MMSE TF RAKE receiver is given by

$$\widehat{b}_{mmse} = \text{sign}\left\{\text{Re}\left[H^H D_{mmse} F_{mmse} z\right]\right\} \tag{4.39}$$

where D_{mmse} is defined as in (4.32), and the transformed noise correlation matrix is

$$Q_{mmse} = \mathcal{N}_0(R + \mathcal{N}_0\Psi^{-1})^{-1}R(R + \mathcal{N}_0\Psi^{-1})^{-1}. \tag{4.40}$$

Note that Ψ is a function of the powers p_k of different users, and the second-order channel statistics of the corresponding users. Specifically, for the WSSUS channel model, Ψ has the following diagonal structure

$$\Psi \overset{def}{=} E\left[HH^H\right] = \begin{bmatrix} p_1\Psi_1 & 0 & \cdots & 0 \\ 0 & p_2\Psi_2 & \cdots & 0 \\ \vdots & \vdots & \vdots & \vdots \\ 0 & 0 & \cdots & p_K\Psi_K \end{bmatrix}, \tag{4.41}$$

where Ψ_k is a diagonal matrix (due to (4.8)) corresponding to the powers in the different multipath-Doppler channel coefficients H_k^{ml} of the k-th user.[||]

[||]Note that for the downlink the channel statistics are identical for all the users: $\Psi_k = \Psi$. For the uplink, the Ψ_k are distinct, in general.

4.3.3 Discussion

The proposed framework for multiuser detection over fast fading channels promises improved performance on two counts: 1) the underlying TF RAKE receiver is optimally matched to the fast fading WSSUS channel, and 2) the resulting systems achieve an inherently higher level of diversity due to joint multipath-Doppler processing.

As mentioned before, even the relatively small Doppler spreads encountered in practice can be leveraged into significant diversity gains via appropriate signal processing [29,36]. This is due to the fact that a large fraction of the maximum diversity gain due to additional (Doppler) diversity components is attained at relatively small fractions (5% − 10%) of total power in those components [29,36]. Such performance gains are inherited by the multiuser receivers proposed in this chapter, as demonstrated in the next section.

Several system modalities that can be benefit from joint multipath-Doppler diversity are identified in [28–30]. One particularly promising technique is the use of time-selective signaling and reception to achieve sufficiently large (≥ 0.2) values of TB_d [36,30]. The basic idea is to use signaling waveforms that are longer than the intersymbol period, thereby introducing overlap between successive symbol waveforms. For example, $TB_d \approx 0.013$ for a data rate of 10kHz, carrier frequency of 1.8GHz, and maximum vehicle speed of 50mph. Spreading codes that are about 16 times longer than the conventional symbol yield $TB_d \approx 0.2$, facilitating significant joint multipath-Doppler diversity gains (3−6dB) [36]. Clearly, the overlap between successive symbols introduces intersymbol interference (ISI). However, initial studies in the single-user case indicate that the excellent autocorrelation properties of pseudorandom codes result in virtually negligible ISI [36]. Integrating time-selective signaling

into the multiuser formulation developed in this chapter warrants further research. However, we note that the interference-suppression-based formulation adopted in this chapter will automatically account for the additional multiaccess ISI introduced by time-selective signaling.

Finally, we note that the concept of exploiting Doppler diversity in a multiuser CDMA framework based on time-selective signaling is similar in spirit to the ideas proposed in [40, 41]. In fact, the concept of Doppler diversity can be integrated into the formulation in [40, 41] to provide an alternative interpretation of the results. For a more detailed comparison of the two approaches, we refer the reader to [36].

4.4   Performance Analysis

The main objective of this section is to quantify the joint multipath-Doppler diversity gains attainable by the multiuser TF RAKE receivers in practical fast fading scenarios. To provide a reference, we compare the performance of the proposed receivers under realistic fast fading, with that of the conventional multiuser RAKE receiver operating under ideal slow fading conditions. Our results demonstrate that even the relatively small Doppler spreads encountered in practice can yield significant gains via joint multipath-Doppler processing.

Of the two multiuser detectors proposed in the the last section, only the decorrelating receiver lends itself to tractable performance analysis. Proceeding analogous to the standard performance analysis for the decorrelating detector [23, 33], we first derive an expression for the probability of bit error for the decorrelating receiver, and then provide simulated results for both the decorrelating and MMSE TF RAKE receivers.

Recall from (4.35) that the decorrelating receiver is of the form

$$\widehat{b} = \text{sign}\{\text{Re}[g]\},\qquad(4.42)$$

where the test statistic g is given by

$$g = H^H D_{dec} H b + H^H D_{dec} R^{-1} w.\qquad(4.43)$$

It follows that the test statistic g_k corresponding to the k-th user is

$$g_k = h_k^H Q_{kk}^{-1} h_k b_k + h_k^H Q_{kk}^{-1} \tilde{w}_k = g_{s,k} + g_{n,k},\qquad(4.44)$$

where $\tilde{w}_k$ is the component of the vector $R^{-1}w$ corresponding to the k-th user. It can be readily verified that $\text{E}[|g_{n,k}|^2 | h_k] = h_k^H Q_{kk}^{-1} h_k$. Thus, the probability of bit error for the k-th user, conditioned on the knowledge of the channel coefficients h_k, is [20]

$$P_{k|h_k} = Q\left(\sqrt{2 h_k^H Q_{kk}^{-1} h_k}\right),\qquad(4.45)$$

where $Q(x) = \frac{1}{\sqrt{2\pi}} \int_x^\infty e^{-x^2/2} dx$. Note that since h_k consists of independent complex Gaussian random variables,

$$h_k^H Q_{kk}^{-1} h_k = \sum_{l=1}^{(L+1)(2M+1)} \lambda_l \gamma_l,\qquad(4.46)$$

where the λ_l's are the eigenvalues of $p_k Q_{kk}^{-1} \Psi_k$, and the γ_l's are independent χ^2 random variables each with two degrees of freedom, and $\text{E}[|\gamma_l|^2] = 1$. The unconditional probability of bit error can be obtained by averaging $P_{k|h_k}$ with respect to the probability density function of $h_k^H Q_{kk}^{-1} h_k$, and is given by [20, pp. 801–802]

$$P_k = \sum_{l=1}^{(L+1)(2M+1)} \frac{\pi_l}{2}\left[1 - \sqrt{\frac{\lambda_l}{1+\lambda_l}}\right],\qquad(4.47)$$

where

$$\pi_l = \prod_{i=1,i\neq l}^{(L+1)(2M+1)} \frac{\lambda_l}{\lambda_l - \lambda_i} \,. \tag{4.48}$$

Note that the eigenvalues λ_i's include the dependence on the signal powers p_k and $\mathcal{N}_0$.

All the numerical results presented next are based on coherent BPSK signaling with perfect channel knowledge, and employ M-sequences of length $N = T/T_c = 63$ as the spreading codes. Moreover, in slow fading, we assume that 2-level $(L = 1)$ multipath diversity is achievable, with a uniform multipath power profile. For simulating practical fast fading scenarios, we assume that in addition to the multipath components, the $m = \mp 1$ Doppler components contribute about 10% of the total power in the channel, corresponding to 6-level joint multipath-Doppler diversity with a $(0.05, 0.9, 0.05)$ Doppler power profile for $m = -1, 0, 1$. As noted earlier, such a Doppler profile may be achieved in practice by employing appropriate signal processing, such as time-selective signaling and reception [29, 30, 36].

4.4.1 Numerical Results: Decorrelating TF RAKE Receiver

First, we calculate the analytical probability of bit error (P_e) based on (4.47) for the decorrelating TF RAKE receiver and the conventional decorrelating RAKE receiver $(M = 0)$, as a function of signal-to-noise ratio (SNR). Figure 4.3 shows the results for $K = 2$ and 4 users. Evidently, by exploiting joint multipath-Doppler diversity corresponding to only 10% of the total power in the two Doppler components, the multiuser TF RAKE receiver significantly outperforms the conventional multiuser RAKE receiver. For example, for $K = 2$ users, the TF receiver achieves a 5dB SNR gain at $P_e = 10^{-4}$. Moreover, as expected, as the number of users increases, a higher SNR is needed to achieve a prescribed value of P_e, due to increased interference.

However, as illustrated in Figure 4.4, the loss in performance for higher number of users is reduced for longer spreading codes, due to improved correlation properties (and, hence, reduce interference). Moreover, the performance gains of the TF RAKE receiver increase monotonically with increasing SNR (decreasing P_e).

Figure 4.5 shows the performance results based on Monte Carlo simulation. Evidently, analytical and simulated results agree closely; analytical results are slightly optimistic for $K = 4$ users.

4.4.2 Numerical Results: MMSE TF RAKE Receiver

Figure 4.6 compares the simulated performance of the multiuser MMSE receivers. The results are similar to those obtained for the decorrelating receiver, demonstrating superior performance of the TF RAKE receiver due to joint multipath-Doppler diversity.

Figure 4.7 demonstrates the near-far resistance of the proposed MMSE TF RAKE receiver by plotting the P_e for the first (desired) user (at SNR=14dB) as a function of the SNR of the second user relative to that of the first user. Based on similar performance of the two multiuser receivers, we expect similar behavior for the decorrelating receiver.

Finally, Figure 4.8 illustrates the effect of the choice of spreading codes on the performance of the proposed receivers. Comparison is made between M-sequences, which have well-known characteristics, with randomly generated sequences. The results, based on the MMSE receivers, indicate that the choice of spreading codes has no significant effect on performance.

4.5 Conclusions

Multipath fading and multiaccess interference are two of the most significant factors limiting the performance of existing mobile wireless CDMA systems. Receiver structures that combine multiuser detection and multipath diversity processing have been developed recently to address the two problems. However, the performance of existing multiuser RAKE receivers degrades significantly in fast fading encountered in many mobile communication scenarios. In particular, systems based on the conventional RAKE receiver exhibit limiting bit-error rates that cannot be improved by increasing the transmitted power. Additional diversity is needed in practice for improved performance.

In this chapter, we have proposed a novel framework for multiuser detection that achieves an inherently higher level of diversity via joint multipath-Doppler processing. At the heart of our approach is a TF RAKE receiver, derived from a canonical time-frequency decomposition of the fast fading channel that facilitates joint multipath-Doppler diversity. The proposed multiuser TF RAKE receiver structures are near-far resistant, and include generalizations of the conventional decorrelating and MMSE receivers. Analytical and simulated results demonstrate that the relatively modest Doppler spreads encountered in practice can be transformed into significant diversity gains by the proposed multiuser systems.

The multiuser time-frequency RAKE receivers proposed in this chapter espouse the paradigm of removing multiaccess interference first, followed by maximal-ratio-combining of the multipath-Doppler components. However, receiver structures that employ diversity combining first are also possible. According to a study of multiuser RAKE receivers [42], employing diversity combining first yields better performance with perfect knowledge of channel parameters, whereas executing interference sup-

pression first, as in our approach, may be more robust if channel estimates are used. Investigation of the two approaches in the context of fast fading warrants further investigation.

From a diversity viewpoint, we note that an arbitrarily high level of diversity can be achieved in the proposed systems by employing time-selective signaling and reception based on spreading codes that are substantially longer than the intersymbol duration [29,30,36]. For long codes, in addition to improved performance, the system is also less affected by the number of users, as indicated by our analysis. Moreover, such systems effectively transform the fading channel into an AWGN channel (in the limit) [36], thereby facilitating the use of powerful coding techniques developed for the AWGN channel.

Finally, we note that even though we restricted our discussion to the synchronous case for clarity of exposition, the results of this chapter can be readily extended to asynchronous scenarios. Moreover, the multipath-Doppler diversity framework can also be leveraged to develop powerful techniques for noncoherent detection and multiuser timing acquisition [43].
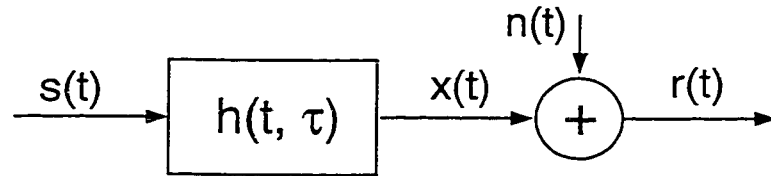
Figure 4.1 : Mobile wireless channel: A linear time-varying system.
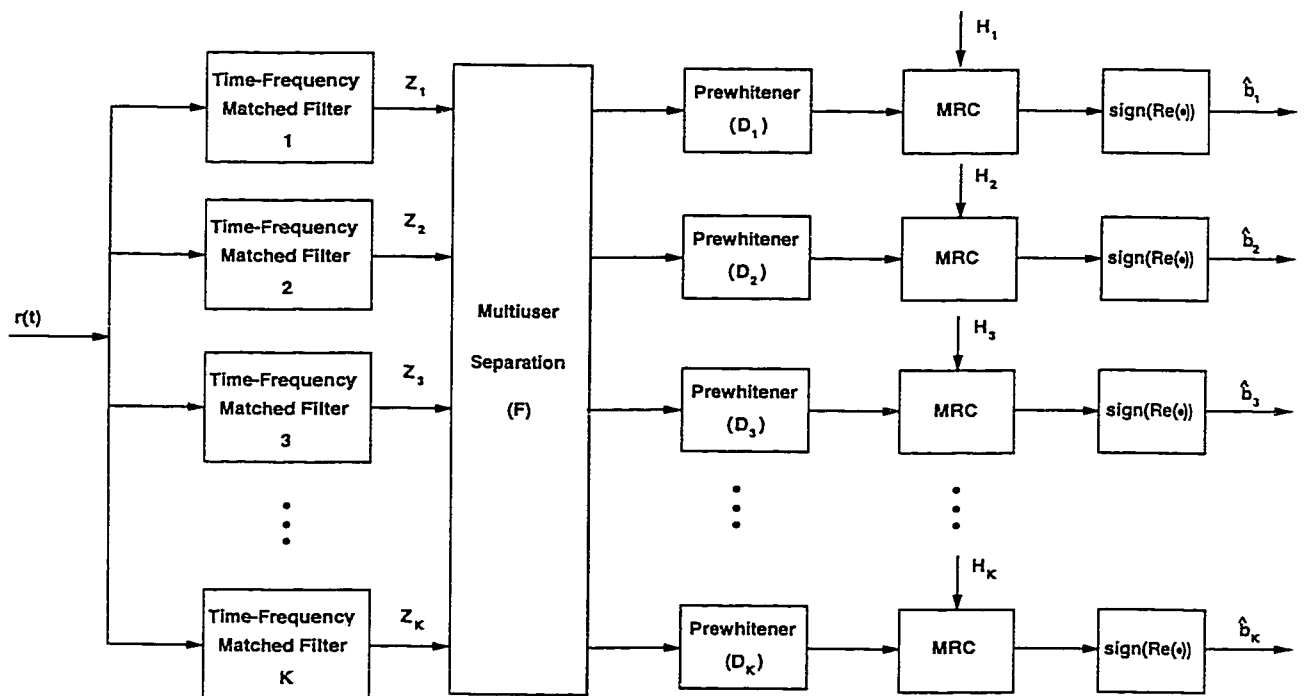
Figure 4.2 : Generic structure of the proposed multiuser time-frequency RAKE receivers.
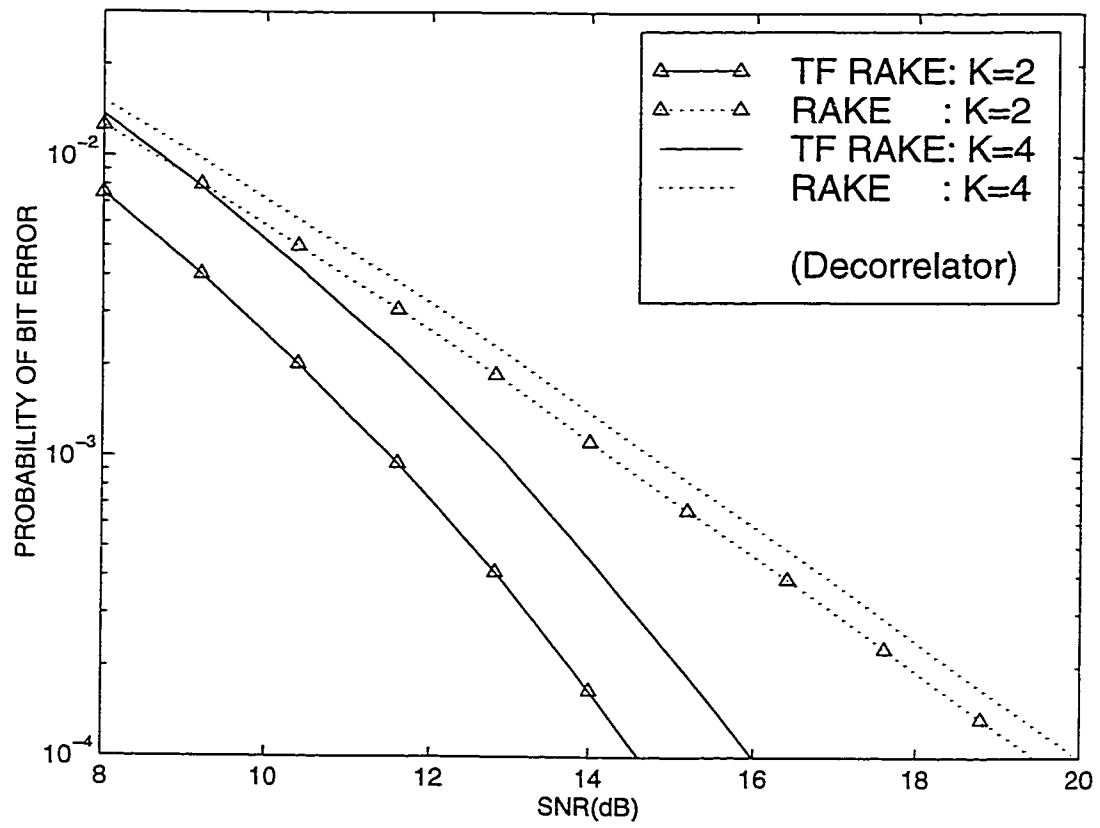
Figure 4.3 : Comparison between the analytical performance of the time-frequency and conventional decorrelating RAKE receivers for 2 and 4 users.
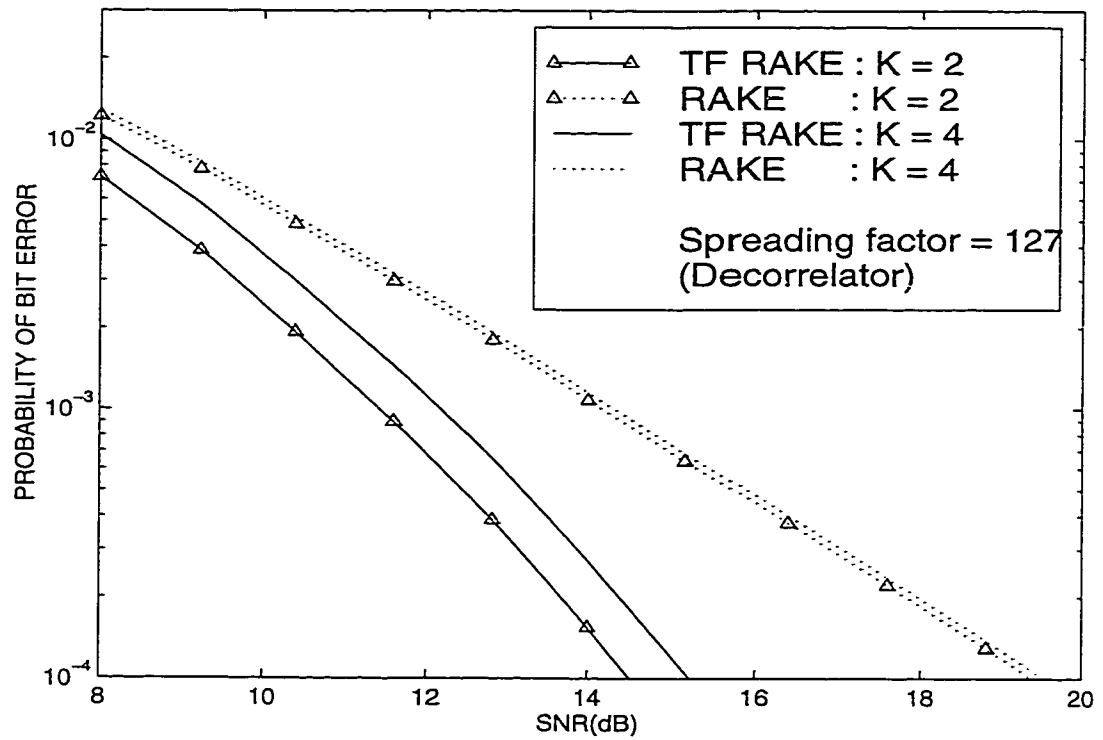
(a)
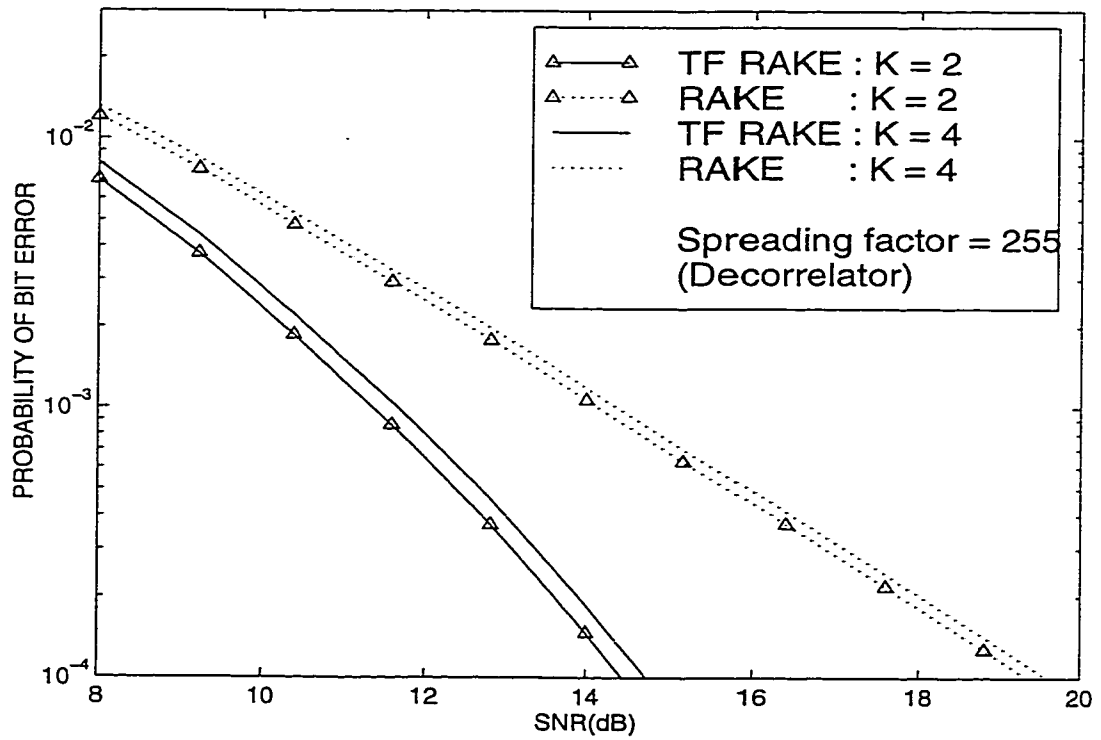
(b)

Figure 4.4 : Analytical performance of the decorrelating RAKE receivers for longer spreading codes: (a) N=127, (b) N=255. The difference in performance for 2 and 4
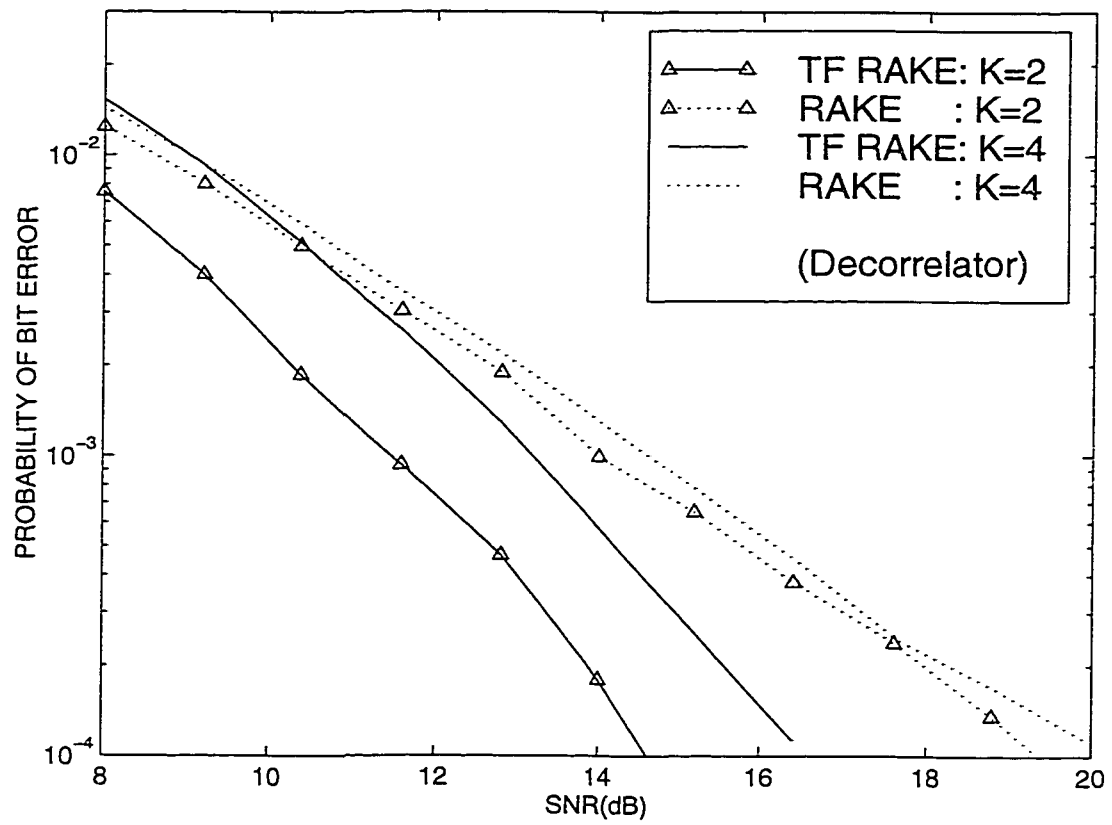
Figure 4.5 : Comparison between the simulated performance of the time-frequency and conventional decorrelating RAKE receivers for 2 and 4 users.
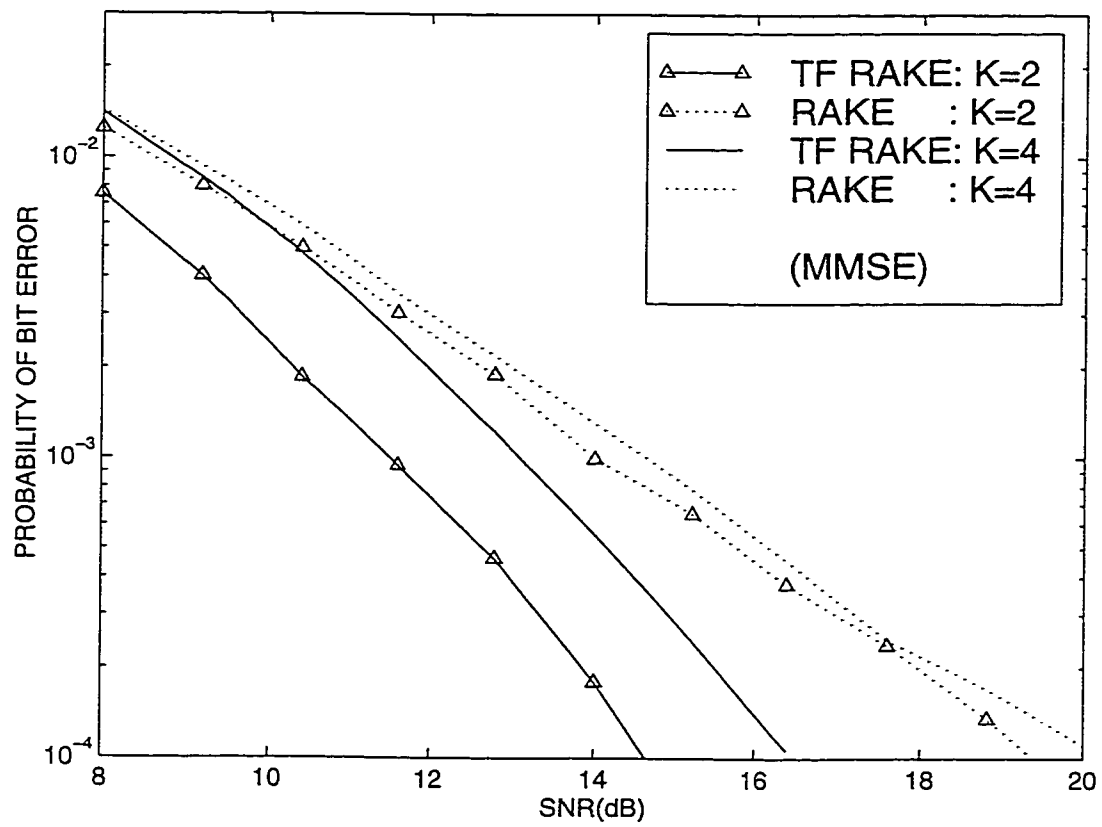
Figure 4.6 : Comparison between the simulated performance of the time-frequency and conventional MMSE RAKE receivers for 2 and 4 users.
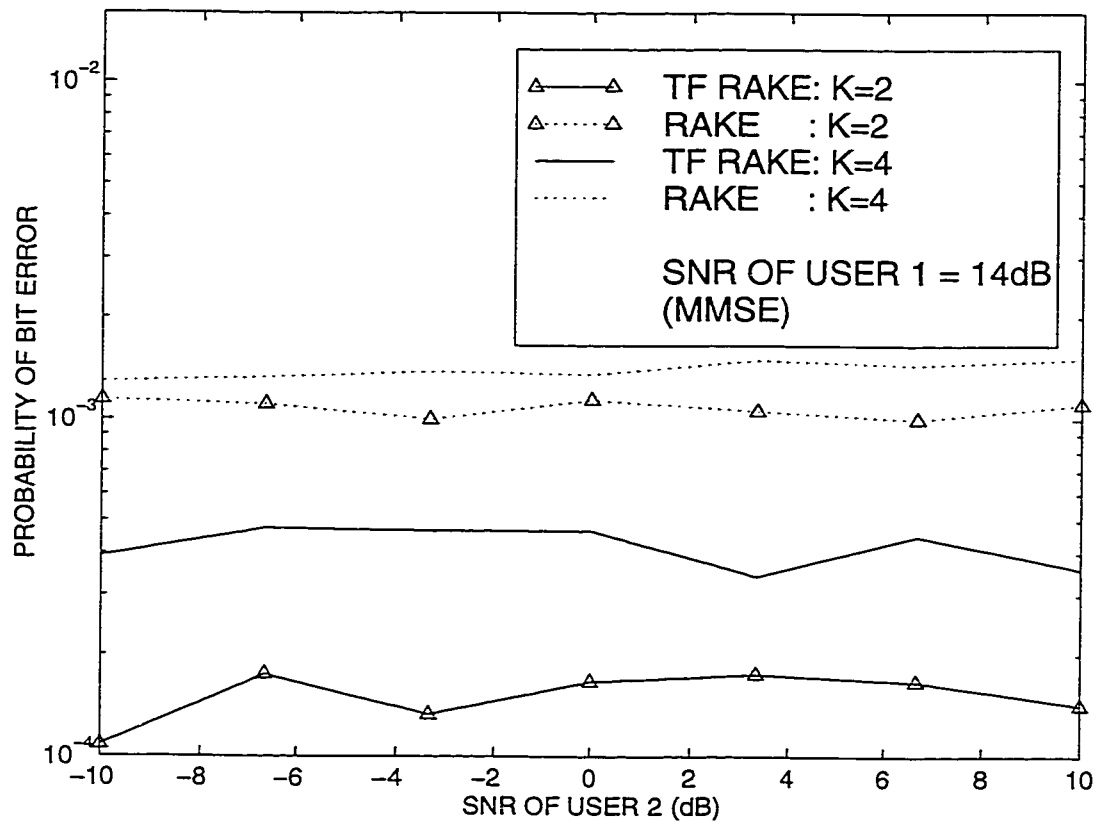
Figure 4.7 : Near-far resistance of the MMSE RAKE receivers (simulation results).
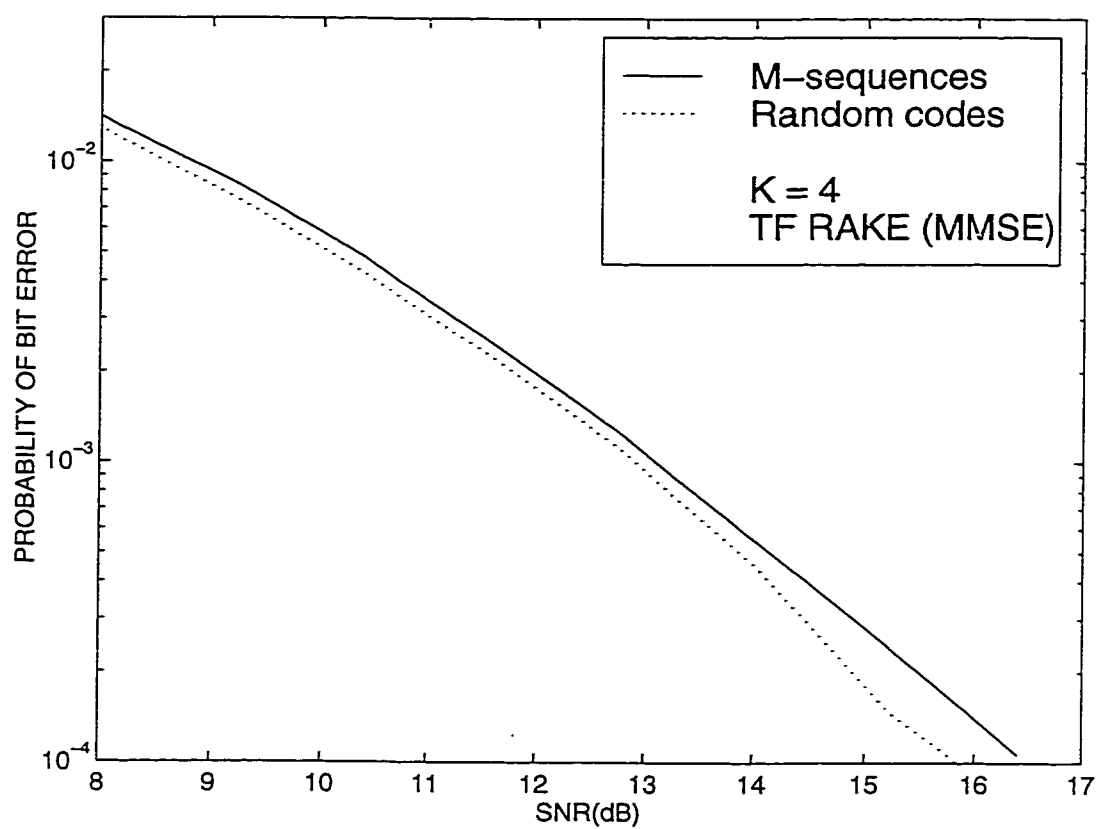
Figure 4.8 : Effect of the choice of spreading codes on performance of MMSE TF RAKE receiver.

Chapter 5

User Cooperation Diversity

5.1 Introduction

The mobile radio channel suffers from multipath fading, implying that, within the duration of any given call, mobile users go through severe variations in signal attenuation. By effectively transmitting or processing (semi)independently-fading copies of the signal, diversity is a method for directly combating the effects of fading. Some well-known forms of diversity are spatial diversity, temporal diversity, and frequency diversity. Spatial diversity relies on the principle that signals transmitted from geographically separated transmitters, and/or to geographically separated receivers, experience fading that is independent.

Therefore, independently of whether other forms of diversity are being employed, having multiple transmit antennas is desirable. Unfortunately, it is infeasible in the uplink of a cellular system, due to the size of the mobile unit. In order to overcome this limitation, yet still emulate transmit antenna diversity, we are proposing a new form of spatial diversity, whereby diversity gains are achieved via the cooperation of in-cell users. That is, in each cell, each user has a "partner". Each of the two partners is responsible for transmitting not only their own information, but also the information of their partner, which they receive and detect. We are, in effect, attempting to achieve spatial diversity through the use of the partner's antenna; however, this is complicated by the fact that the inter-user channel is noisy. It is also complicated by the fact that both partners have information of their own to

send–this is not a simple relay problem.

There is no cost, in terms of transmit power, associated with transmitting to both the base station *and* your partner, since mobile antennas are omnidirectional. However, there are two other factors that affect the required transmit power. First, a user will require more power in order to send both users' information. Second, a user will require less power because of the diversity gains. It is not clear *a priori* which of the above two factors will be dominant.

There are two directions for evaluation of the potential benefits of user cooperation. First, a capacity analysis involving the channel model in Figure 5.1, using information-theoretic concepts. Second, a study involving the calculation of the throughput of a given transmission scheme. Both analyses aid us in evaluating if there are any capacity/transmit power gains associated with user cooperation diversity. Results show that the net effect are higher data rates at the same power level, or alternatively, reduced required transmit power at the same data rate.

This chapter does not address higher protocol level issues that may arise from a potential implementation of user cooperation. We concentrate on physical layer issues, with the anticipation that any higher level overhead will be negligible compared to the gains reported herein.

5.2 Problem Setup

The basic premise in this work is that both users have information of their own to send, denoted by W_i for $i = 1, 2$, and would like to cooperate in order to send this information to the BS at the highest rate possible. The channel model we use is depicted in Figure 5.1. Each mobile receives an attenuated and noisy version of the partner's transmitted signal and uses that, in conjunction with its own data, to construct its transmit signal. The base station, or main receiver, receives a noisy version

of the sum of the attenuated signals of both users. The mathematical formulation of our model is

$$Y_0(t) = K_{10}X_1(t) + K_{20}X_2(t) + Z_0(t) \tag{5.1}$$

$$Y_1(t) = K_{12}X_1(t) + Z_1(t) \tag{5.2}$$

$$Y_2(t) = K_{21}X_2(t) + Z_2(t), \tag{5.3}$$

where $Y_0(t)$, $Y_1(t)$ and $Y_2(t)$ are the baseband models of the received signals at the base station, user 2 and user 1, respectively, during one symbol period. Also, $X_i(t)$ is the signal transmitted by user i, for $i = 1, 2$, and $Z_i(t)$ are the additive channel noise terms at the base station, user 1 and user 2, for $i = 0, 1, 2$, respectively. The fading coefficients, K_{ij}, remain constant over at least one symbol period, and observed over time form independent stationary ergodic stochastic processes, resulting in frequency non-selective fading.

Note that our model assumes there is no contribution from $X_2(t)$ in $Y_1(t)$, even though they are actually present at the same location, that is, user 2. Since $X_2(t)$ does not go through any fading before it reaches the antenna of user 2, as is the case for $Y_1(t)$, it may appear that it will have a detrimental effect on the reception of $Y_1(t)$. However, provided that user 2 knows the relevant antenna gains, canceling the effects of $X_2(t)$ on $Y_1(t)$ is possible, and thus our model gives an accurate representation. A similar argument can be made in the case of user 1, regarding the effects of $X_1(t)$ on the reception of $Y_2(t)$.

Our model further assumes the following: the transmitted signals $X_i(t)$ have an average power constraint of P_i for $i = 1, 2$, the noise terms $Z_i(t)$ are white zero-mean complex Gaussian random processes with spectral height $\frac{N_i}{2}$ for $i = 0, 1, 2$, and the fading coefficients K_{ij} are zero-mean complex Gaussian random variables with variance ξ_{ij}^2 (which corresponds to Rayleigh fading). We also assume that the

base station can track the variations in K_{10} and K_{20}, user 1 can track K_{21} and user 2 can track K_{12}, implying that all the decoding is done with the knowledge of the fading parameters. Due to the reciprocity of the channel, we assume that K_{21} and K_{12} are equal. Finally, for simplicity of analysis and exposition, though with no loss in generality, we assume a synchronous system.

Given the above model, the problem lies in finding the best way for both users to construct their transmit signals, given their own data and the received signal from their partner, so that both users are able to maximize their data rates towards the base station.

It should be pointed out that an important issue impacting the solution to the above problem is the degree of channel state information available at the transmitters. Since the users are assumed to know the inter-user fading coefficient, the question reduces to how much they know about the fading coefficient between them and the base station. Specifically, how much does user i know about K_{i0}? There are three cases: user i knows nothing about K_{i0} besides its statistics, user i knows the phase of K_{i0} but not its amplitude, or user i knows both the phase and amplitude of K_{i0}. The users may obtain information about K_{i0} in two ways. First, there may be feedback from the base station. Second, the system may be operating in TDD (time division duplex) mode, that is, the uplink and downlink share the same bandwidth and are separated via time division. In this case, under certain conditions, the uplink and downlink channel impulse responses are the same, thus giving the mobiles the opportunity to know the uplink fading coefficients (K_{i0}) by tracking the downlink fading coefficients.

If the transmitters know the amplitude of the fading they could theoretically employ some type of waterfilling, that is, allocate their power depending on the different fading states, while still maintaining their average power constraint. However, the

mobile unit has very limited peak power capabilities, thus rendering power allocation into different fading states implausible, if not infeasible. For this reason, as well as trying to keep the mobile units as simple as possible, for the purposes of this study, we will disregard the case of user i exploiting knowledge of the amplitude of K_{i0}.

If the transmitters have knowledge of the phase of the fading parameter between them and the BS, the most they can do to exploit this knowledge it to transmit a signal that offsets this phase. The same holds for the inter-user fading parameter. As a result, the attenuation parameters K_{ij} may, in this case, be treated as real random variables with a Rayleigh distribution.

It should be noted that, while we use a synchronous system model to illustrate in a simple and clear way the potential benefits of user cooperation, in practice the two users will be asynchronous. In a CDMA system, which is the main implementation focus of this chapter, asynchronicity implies that the problem of knowing the phase at the transmitter is not an issue, due to the large time-bandwidth product of CDMA signals and the resulting ability of the BS to track the phases of the users' signals, even when the two mobiles transmit the same signal. Therefore, while the viability of phase feedback or the accuracy of the phase estimate using the TDD method may be questioned, the fact that they are not actually needed in an asynchronous system, justifies assuming them in our synchronous system model.

As a final note, it is clear that all above cases of assumed phase knowledge, either at the transmitters or the BS, involve some residual error. In the synchronous case, the errors arise from imperfect BS phase feedback or, in the TDD case, from the time variations of the channel between uplink and downlink data frames. In the asynchronous case, the errors arise from the effects of MAI (Multiple Access Interference) and the non-ideal correlation of CDMA spreading codes. However, in this study we consider any residual error as negligible and do not take it into account

in our analysis.

In what is the main focus of this chapter, Sections 5.3 through 5.5 explore user cooperation under the assumptions mentioned above. Also, in order to provide a complete treatment of the subject, although not essential due to reasons given above, Section 5.6 discusses user cooperation given that user i knows nothing about K_{i0}.

5.3 Information-Theoretic Analysis

In this chapter, we focus mainly on describing proposed user cooperation schemes and analyzing their throughput and overall performance. However, an analysis of user cooperation based on information-theoretic concepts is important not only for understanding the limits of any proposed user cooperation scheme, but also for providing insight as to how a good user cooperation scheme should be structured. Time and again, we have found that, within a certain transmission framework, the system that most closely emulates the signal structure of the information-theoretic capacity-maximizing system, also has the highest throughput. Therefore, for completeness and for a better grasp of the subject of user cooperation, we present here the most important results from the capacity analysis of user cooperation; for a more extensive treatment of this subject see [44].

5.3.1 An Achievable Rate Region

In this section we present an achievable rate region for the configuration in Figure 5.1, described in Section 5.2. The mathematical model we use is

$$Y_0 = K_{10}X_1 + K_{20}X_2 + Z_0 \tag{5.4}$$

$$Y_1 = K_{12}X_1 + Z_1 \tag{5.5}$$

$$Y_2 = K_{21}X_2 + Z_2, \tag{5.6}$$

with $Z_0 \sim \mathcal{N}(0, N_0)$, $Z_1 \sim \mathcal{N}(0, N_1)$ and $Z_2 \sim \mathcal{N}(0, N_2)$. In general, we assume that $N_1 = N_2$. The system is causal, therefore the signal of user 1 at time i can be expressed as $X_1(W_1(i), Y_2(i-1))$, similarly for user 2 we have $X_2(W_2(i), Y_1(i-1))$ where W_1 and W_2 are the messages that the two users want to transmit to the base station.

The cooperation strategy employed by the two users is based on superposition block Markov encoding [45] and backward decoding [46, 47]. Mobile 1 divides its information W_1 into two parts: W_{10}, to be sent directly to the BS, and W_{12}, to be sent to the BS via mobile 2. Mobile 1 then structures its transmit signal according to

$$X_1 = X_{10} + X_{12} + U_1$$

and divides its total power accordingly

$$P_1 = P_{10} + P_{12} + P_{U1}.$$

Thus X_{10} is allocated power P_{10} and is used for sending W_{10} at rate R_{10} directly to the BS, X_{12} is allocated power P_{12} and is used for sending W_{12} to user 2 at rate R_{12}, and U_1 is allocated power P_{U1} and is used for sending cooperative information to the BS. Mobile 2 structures its transmit signal X_2 and divides its total power P_2 in a similar fashion. The cooperation in block i is achieved by constructing signals U_1 and U_2 based on $(W_{12}(i-1), W_{21}(i-1))$. The transmission is done for B blocks of length n, where both B and n are large. The achievable rate region with user cooperation is obtained by first considering constant attenuation factors and then using [48] to incorporate the randomness.

Theorem 1 *An achievable rate region for the system given in (5.4)-(5.6) is the closure of the set of all rate pairs (R_1, R_2) such that $R_1 = R_{10} + R_{12}$ and $R_2 =$*

$R_{20} + R_{21}$ *with*

$$R_{12} \; < \; E\left\{C\left(\frac{K_{12}^2 P_{12}}{K_{12}^2 P_{10} + N_1}\right)\right\} \tag{5.7}$$

$$R_{21} \; < \; E\left\{C\left(\frac{K_{21}^2 P_{21}}{K_{21}^2 P_{20} + N_2}\right)\right\} \tag{5.8}$$

$$R_{10} \; < \; E\left\{C\left(\frac{K_{10}^2 P_{10}}{N}\right)\right\} \tag{5.9}$$

$$R_{20} \; < \; E\left\{C\left(\frac{K_{20}^2 P_{20}}{N}\right)\right\} \tag{5.10}$$

$$R_{10} + R_{20} \; < \; E\left\{C\left(\frac{K_{10}^2 P_{10} + K_{20}^2 P_{20}}{N}\right)\right\} \tag{5.11}$$

$$R_{10} + R_{20} + R_{12} + R_{21} \; < \; E\left\{C\left(\frac{K_{10}^2 P_1 + K_{20}^2 P_2 + 2K_{10}K_{20}\sqrt{P_{U1}P_{U2}}}{N}\right)\right\} \tag{5.12}$$

for some power assignment satisfying $P_1 = P_{10} + P_{12} + P_{U1}$, $P_2 = P_{20} + P_{21} + P_{U2}$. *The function* $C(x) = \frac{1}{2}\log(1+x)$ *is the capacity of an additive white Gaussian noise channel with signal to noise ratio* x.

5.3.2 Probability of outage

We now consider a slowly fading system with delay requirements and investigate the outage performance of the partner scheme.

We let n (the block length) and B (the number of blocks) be large enough to achieve capacity in the case of constant attenuation factors. If the attenuation factors vary slowly and can be approximated as constants over the B blocks of length n, then over these B blocks we can achieve rates dictated by the current values of K_{10}, K_{20}, K_{12} and K_{21}. However in order to talk about the capacity region in Theorem 1, we need to have even longer block lengths and observe different realizations of our fading amplitudes. When the delay requirements prevent us from having larger coding delays, the rates achieved are random variables rather than real numbers. We observe an *outage* if these random rates fall below a certain level and can consider

the probability of outage as a performance criterion.

In particular, we consider the equal rate point $(R_1 = R_2 = R)$ and calculate the probability of outage versus the cutoff rate r for the cooperation and the no cooperation schemes. The probability of outage, $P_{out} = \Pr(R < r)$, provides us with the probability that the current realization of our slowly fading parameters K_{10}, K_{20}, K_{12} and K_{21} will not be able to support an equal transmission rate of r for the particular scheme under consideration.

5.3.3 Case Studies

The achievable rate region together with the no cooperation and ideal cooperation capacity regions is shown in Figures 5.2 and 5.3. For the no cooperation case, the users ignore the signals Y_1 and Y_2. Ideal cooperation refers to the scenario when $N_1 = N_2 = 0$ and is used mostly as an upper bound for the performance of any cooperation scheme. From Figure 5.2, we observe that when the channels from the users to the base station have similar quality (K_{10} and K_{20} have the same mean) and the channel between the users is better (K_{12} has larger mean) the cooperation scheme greatly improves the achievable rate region. This scenario could occur, for example, if two users are walking on the same street, but neither has a direct line-of-sight link with the BS, thus making the inter-user channel of higher quality than the two user-BS links. As the inter-user channel degrades and the severity of the inter-user fading increases, performance approaches that of no cooperation.

When the user-BS links of the two users experience fading with different means, as would occur for example if the two users were at different distances from the base station, cooperation again improves the achievable rate region as shown in Figure 5.3. In this case, the user with more fading benefits most from the cooperation. The equal rate point $(R_1 = R_2)$ or the maximum rate sum point $(R_1 + R_2)$ is increased
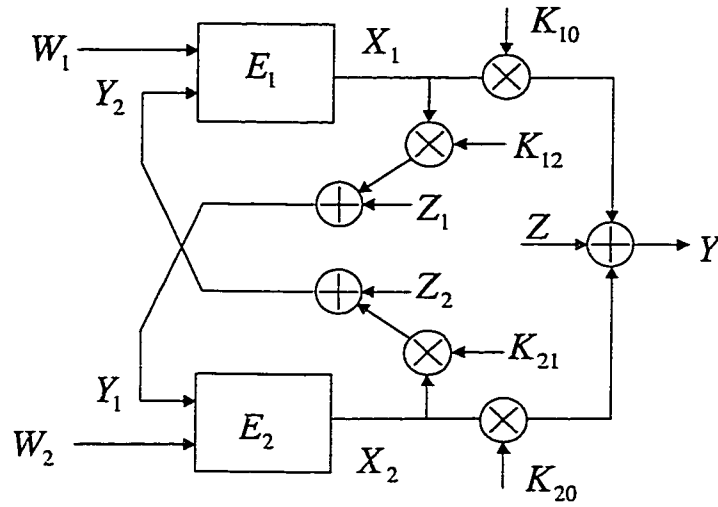
Figure 5.1 : Channel model
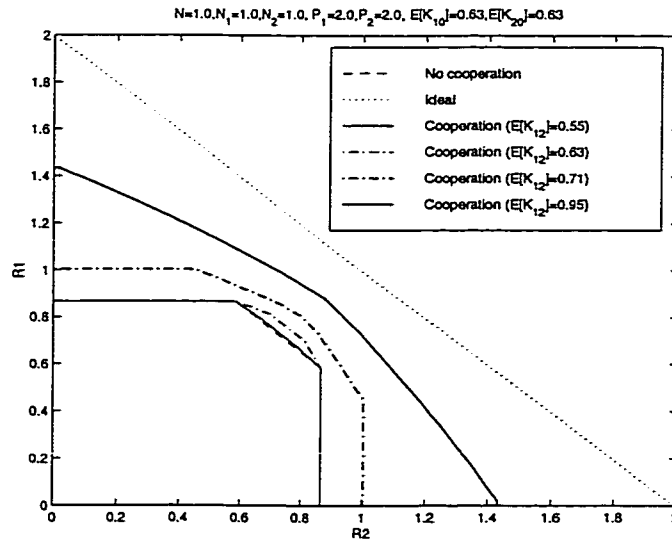
Figure 5.2 : Capacity region when the two users face statistically equivalent channels towards the base station

considerably with cooperation.

It should be pointed out that, in Figures 5.2 and 5.3, the point where any achievable rate curve intersects the Y-axis corresponds to user 2 becoming a relay for user 1, and the point where the curve intersects the X-axis corresponds to user 1 becoming a relay for user 2. This demonstrates that the relay problem is a special, degenerate, case of user cooperation, since the latter corresponds to an entire continuum of possible achievable rate pairs between the two extremes $(R_1^{max}, 0)$ and $(0, R_2^{max})$.

Turning our attention now to outage probability, in Figure 5.4 we consider the equal rate point $(R_1 = R_2 = R)$ and plot the probability of outage versus the cutoff rate r for the cooperation and the no cooperation schemes. We observe that for all cutoff rates, the probability of outage for the cooperation scheme is smaller than the probability of outage under no cooperation. This is true despite the fact that, in the scenario that Figure 5.4 corresponds to, the increase in achievable rate due to cooperation is moderate, as can be seen from Figure 5.2 $(E[K_{12}] = 0.63)$. This demonstrates that even in cases when it does not significantly increase achievable rates, user cooperation is still able to increase robustness against channel variations.

5.4   A CDMA Implementation

Having seen the limits of any cooperation scheme, as presented in the previous section, we now turn our attention to some possible implementations of the user cooperation concept, under some practical wireless system framework such as CDMA (Code-Division Multiple Access). It should be pointed out that, while we focus on CDMA, other frameworks, such as FDMA and TDMA, may be equally suitable–each, of course, with its own unique advantages and challenges.

This section addresses a conventional CDMA system while Section 5.5 addresses a high data rate CDMA system. Given our implementations, our goal is to obtain an
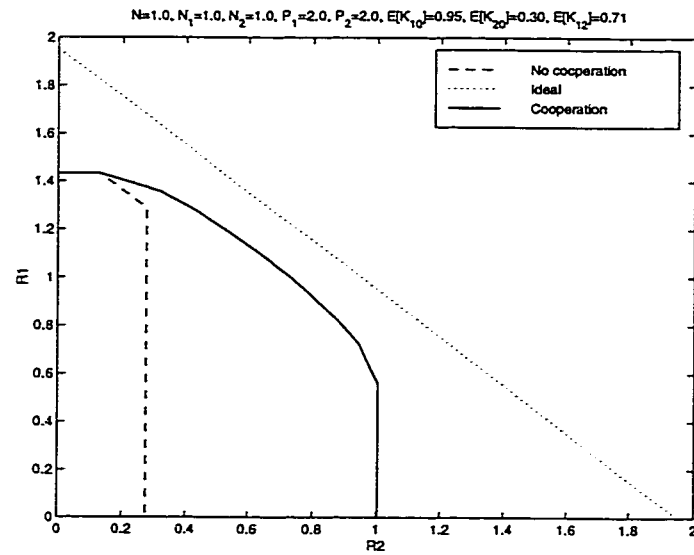
Figure 5.3 : Capacity region when the two users face statistically dissimilar channels towards the base station
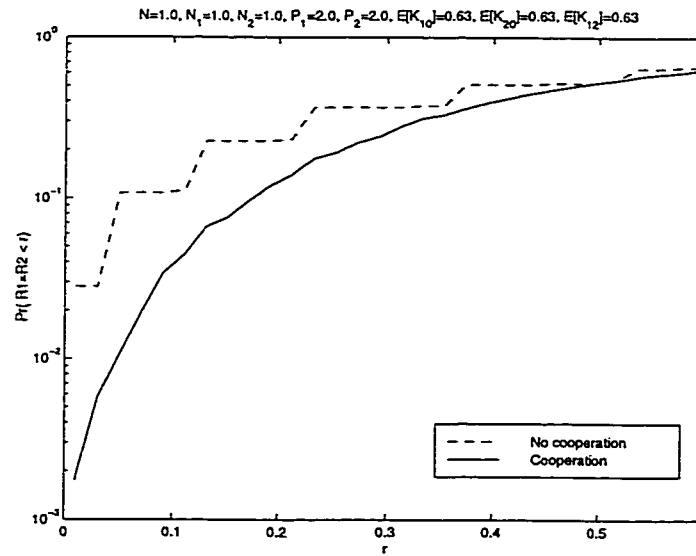
Figure 5.4 : Probability of outage

analytical expression for their *throughput*, that is, the maximum possible data rate that can be transmitted reliably through each of them given sufficiently long error correcting codes. To this end, we first derive the error characteristics of the underlying communication systems, and in Sections 5.4.3 and 5.5.1 use these characteristics in order to find the capacity of the resulting discrete-time channel models.

5.4.1 Problem setup

Consider a CDMA cellular system in which each user has one spreading code, and modulates one bit onto it. Assume that the users' codes are orthogonal and that the coherence time of the channel is L symbol periods. In order to facilitate the presentation, we begin with a simple example ($L = 3$) and then generalize to any L. In the absence of cooperation, during three (L) consecutive symbol periods, the users would transmit

$$
\begin{aligned}
X_1(t) &= a_1 \, b_1^{(1)} \, c_1(t), \quad a_1 \, b_1^{(2)} \, c_1(t), \quad a_1 \, b_1^{(3)} \, c_1(t) \\
X_2(t) &= \underbrace{a_2 \, b_2^{(1)} \, c_2(t)}_{\text{Period 1}}, \quad \underbrace{a_2 \, b_2^{(2)} \, c_2(t)}_{\text{Period 2}}, \quad \underbrace{a_2 \, b_2^{(3)} \, c_2(t)}_{\text{Period 3}}
\end{aligned}
\tag{5.13}
$$

where $b_j^{(i)}$ is user j's i^{th} bit, c_j is user j's code, and $a_j = \sqrt{\frac{P_j}{T_s}}$ where P_j is user j's power and T_s is the symbol period. Now, assume that the two partners decide to cooperate. There are *many* ways for them to do so; one way, which was inspired somewhat by the signal structure in Section 5.3.1, is by transmitting

$$
\begin{aligned}
X_1(t) &= a_{11} \, b_1^{(1)} \, c_1(t), \quad a_{12} \, b_1^{(2)} \, c_1(t), \quad a_{13} \, b_1^{(2)} \, c_1(t) + a_{14} \, \hat{b}_2^{(2)} \, c_2(t) \\
X_2(t) &= \underbrace{a_{21} \, b_2^{(1)} \, c_2(t)}_{\text{Period 1}}, \quad \underbrace{a_{22} \, b_2^{(2)} \, c_2(t)}_{\text{Period 2}}, \quad \underbrace{a_{23} \, \hat{b}_1^{(2)} \, c_1(t) + a_{24} \, b_2^{(2)} \, c_2(t)}_{\text{Period 3}}
\end{aligned}
\tag{5.14}
$$

where $\hat{b}_j^{(i)}$ is the partner's estimate of user j's i^{th} bit. The parameters a_{ji} control how much power is allocated to a user's own bits versus the bits of the partner, while maintaining an average power constraint of P_j for user j.

Period 1 is used to send data to the BS only, akin to the function of the signals X_{j0}, $j = 1, 2$ in Section 5.3.1. On the other hand, period 2 is used to send data not only to the BS, but also to each user's partner, akin to the function of the signals X_{12} and X_{21} in Section 5.3.1. After this data is estimated by each user's partner, it is used to construct a cooperative signal that is sent to the BS during period 3. This is accomplished by each user utilizing both users' codes (c_1 and c_2), and is akin to the function of the signal U in Section 5.3.1. This is done in such a way as to enable the two partners to send a cooperative signal while keeping the total number of codes used by the two users constant.

Also, notice that period 3 is used in order to re-send, in some sense, the information originally sent during period 2. This implies that the users only send *two* new bits per three symbol periods, whereas they would be sending three new bits per three symbol periods if they were not cooperating (see (5.13)). This may seem counter-productive, but, under certain channel conditions, "wasting" a few symbol periods for cooperation may be justified. In order to gain some insight into this subject, we will look at a simple, somewhat related, example where a transmitter voluntarily decides to not transmit during some of its allotted L symbol periods. Since the transmitter has an average power constraint, not transmitting during some of the symbol periods allows it to boost its power during the remaining periods. The throughput of this system, in bits per symbol period, given that the transmitter decides to not transmit during a fraction ν of its L symbol periods, is given by

$$\eta = (1 - \nu)C_{\text{BSC}}\left(Q\left(\sqrt{\frac{SNR_0}{1 - \nu}}\right)\right)$$

where $C_{\text{BSC}}(p)$ is the capacity of a binary-symmetric channel with crossover probability p, $Q(\cdot)$ is complementary cumulative distribution function of a zero-mean unit-variance normal random variable, and SNR_0 is the nominal SNR that would

be in effect if the transmitter were transmitting during all the symbol periods. Some numerical results are given in Figure 5.5. What we notice is that for low SNR the transmitter may waste up to half of its symbol periods and still incur only negligible loss in the overall throughput. As the SNR increases, the fraction of symbol periods that can be left unused while negligibly affecting overall throughput decreases.

Of course, our cooperative scheme is not precisely like the above simple example. When cooperating, the symbol periods given up for cooperation are not unused: they consume some power and also provide some additional throughput for the transmitters. Therefore, the issue is whether the loss incurred by allocating some of the periods for cooperation can be overcome by the additional throughput resulting from the cooperative periods. Nevertheless, when properly considered, our simple example provides some useful insight into the above issue: Figure 5.5 seems to suggest that the fraction of symbol periods allocated for cooperation should be a function of the overall channel conditions. This is precisely the idea that we used in order to arrive at our generalized cooperation scheme, explained below.

Equation (5.14) refers to the special case of $L = 3$. The generalization to arbitrary L is as follows: In each L symbol periods, each of the two partners uses $2L_c$ of the periods for cooperation and the remaining $L - 2L_c$ periods for sending non-cooperative information, where L_c is some integer between 0 and $L/2$. When $L_c = 0$, the two users are not cooperating at all. When $L_c = L/2$, the two users are fully cooperating, that is, cooperating during all symbol periods. For example, in the scenario referred to by (5.14), $L = 3$ and $L_c = 1$, whereas in the scenario referred to by (5.13), $L = 3$ and $L_c = 0$. In general, the value of L_c may be time-varying, a fact which allows time-sharing of different values of L_c, in order to achieve any point on the capacity region. This is discussed in more detail in Section 5.4.3.

The cooperative scheme just described may be expressed, for a given L and L_c,

as

$$X_1(t) = \begin{cases} a_{11} \, b_1^{(i)} \, c_1(t) & \text{periods } i = 1, 2, \ldots, L_n \\ a_{12} \, b_1^{(\frac{L_n+1+i}{2})} \, c_1(t) & \text{periods } i = L_n + 1, L_n + 3, \ldots, L - 1 \\ a_{13} \, b_1^{(\frac{L_n+i}{2})} \, c_1(t) + a_{14} \, \hat{b}_2^{(\frac{L_n+i}{2})} \, c_2(t) & \text{periods } i = L_n + 2, L_n + 4, \ldots, L \end{cases}$$

$$X_2(t) = \begin{cases} a_{21} \, b_2^{(i)} \, c_2(t) & \text{periods } i = 1, 2, \ldots, L_n \\ a_{22} \, b_2^{(\frac{L_n+1+i}{2})} \, c_2(t) & \text{periods } i = L_n + 1, L_n + 3, \ldots, L - 1 \\ a_{23} \, \hat{b}_1^{(\frac{L_n+i}{2})} \, c_1(t) + a_{24} \, b_2^{(\frac{L_n+i}{2})} \, c_2(t) & \text{periods } i = L_n + 2, L_n + 4, \ldots, L \end{cases}$$

$$(5.15)$$

where $L_n = L - 2L_c$, and where the a_{ij} are chosen to satisfy the power constraints given by

$$\frac{1}{L}(L_n a_{11}^2 + L_c(a_{12}^2 + a_{13}^2 + a_{14}^2)) = P_1$$
$$\frac{1}{L}(L_n a_{21}^2 + L_c(a_{22}^2 + a_{23}^2 + a_{24}^2)) = P_2. \tag{5.16}$$

A graphical illustration of this cooperative scheme is depicted in Figure 5.6 for the special case of $L = 6$, $L_c = 2$.

5.4.2 Error Calculations

We now calculate the various probabilities of bit error associated with this scheme, given a particular value for L_c, given a particular power allocation, as defined by the a_{ij}, and given a particular set of fading coefficients, as defined by the K_{ij}. Since we have a CDMA system, we assume that the received signals are chip-matched filtered at the receivers. Therefore, all signals will be written as length-N_c vectors of chip-matched filter outputs, where N_c is the CDMA spreading gain. For a clear exposition, we focus on user 1 and remove all extraneous subscripts and superscripts; user 2's error probabilities follow by symmetry.
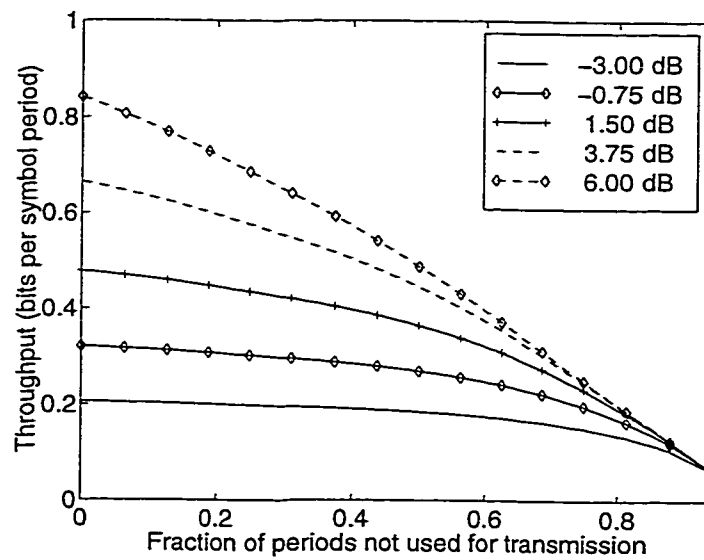
Figure 5.5 : How the throughput varies with ν, the fraction of unused symbol periods
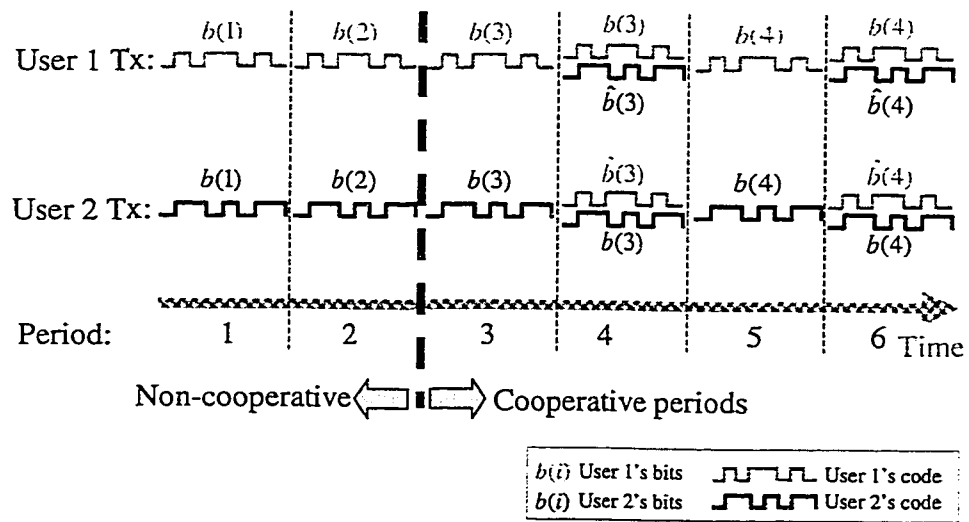
Figure 5.6 : How cooperation is implemented

Non-cooperative periods

During the $L - 2L_c$ non-cooperative periods, each user sends only their own data, which is received and detected by the BS only. The signal transmitted by user 1 is $\mathbf{X}_1 = a_{11}\, b_1\, \mathbf{c}_1$, and is received at the BS according to $\mathbf{Y}_0 = K_{10}\mathbf{X}_1 + K_{20}\mathbf{X}_2 + \mathbf{Z}_0$. Due to the orthogonality of the spreading codes, the estimate of user 1's bit during these periods is given by

$$
\begin{aligned}
\hat{b}_1 &= \operatorname{sign}\left(\tfrac{1}{N_c}\mathbf{c}_1^{\mathsf{T}}\mathbf{Y}_0\right) \\
&= \operatorname{sign}\left(K_{10}a_{11}\, b_1 + n_0\right)
\end{aligned}
\tag{5.17}
$$

where $n_0 \sim \mathcal{N}(0, \sigma_0^2/N_c)$, and where $\sigma_0^2 = \frac{N_0}{2T_c}$, T_c is the chip period and $\frac{N_0}{2}$ is the spectral height of $Z_0(t)$. As a result, the probability of bit error is

$$
P_{e_1} = Q\left(K_{10}a_{11}\frac{\sqrt{N_c}}{\sigma_0}\right).
\tag{5.18}
$$

Cooperative periods

During the $2L_c$ cooperative periods we have a distinction between "odd" and "even" periods. During the "odd" periods, each user sends only their own data, which is received and detected by the partner as well as by the BS. The signal transmitted by user 1 is $\mathbf{X}_1 = a_{12}\, b_1\, \mathbf{c}_1$. It is received by the partner according to $\mathbf{Y}_1 = K_{12}\mathbf{X}_1 + \mathbf{Z}_1$ and by the BS according to $\mathbf{Y}_0^{\mathrm{odd}} = K_{10}\mathbf{X}_1 + K_{20}\mathbf{X}_2 + \mathbf{Z}_0^{\mathrm{odd}}$. The partner uses $\mathbf{Y}_1$ in order to form a hard estimate of b_1, whereas the BS uses its received signal in order to form a soft decision statistic.

The partner's hard estimate of b_1 is given by $\hat{b}_1 = \operatorname{sign}\left(\tfrac{1}{N_c}\mathbf{c}_1^{\mathsf{T}}\mathbf{Y}_1\right)$, resulting in a probability of bit error equal to

$$
P_{e_{12}} = Q\left(K_{12}a_{12}\frac{\sqrt{N_c}}{\sigma_1}\right)
\tag{5.19}
$$

where $\sigma_1^2 = \frac{N_1}{2T_c}$, T_c is the chip period, and $\frac{N_1}{2}$ is the spectral height of $Z_1(t)$. The BS, on the other hand, forms a soft decision statistic by calculating

$$y_{\text{odd}} = \frac{1}{N_c}\mathbf{c}_1^\mathsf{T}\mathbf{Y}_0^{\text{odd}}. \qquad (5.20)$$

This value is used in conjunction with information obtained from the following, "even", period.

During the "even" periods, the two users send a cooperative signal to the BS, based on what each user estimates to be his/her partner's bit from the previous, "odd", period. The transmitted signals of the two partners are

$$\begin{aligned}
\mathbf{X}_1 &= a_{13}\, b_1\, \mathbf{c}_1 + a_{14}\, \hat{b}_2\, \mathbf{c}_2 \\
\mathbf{X}_2 &= a_{23}\, \hat{b}_1\, \mathbf{c}_1 + a_{24}\, b_2\, \mathbf{c}_2
\end{aligned} \qquad (5.21)$$

The BS receives these signals according to $\mathbf{Y}_0^{\text{even}} = K_{10}\mathbf{X}_1 + K_{20}\mathbf{X}_2 + \mathbf{Z}_0^{\text{even}}$ and extracts a soft decision statistic by calculating

$$y_{\text{even}} = \frac{1}{N_c}\mathbf{c}_1^\mathsf{T}\mathbf{Y}_0^{\text{even}}. \qquad (5.22)$$

The BS' combined decision statistics for user 1 are therefore given by

$$\begin{aligned}
y_{\text{odd}} &= K_{10}a_{12}\, b_1 + n_{\text{odd}} \\
y_{\text{even}} &= K_{10}a_{13}\, b_1 + K_{20}a_{23}\, \hat{b}_1 + n_{\text{even}}
\end{aligned} \qquad (5.23)$$

where $\hat{b}_1$ is user 2's estimate of b_1, with an error probability given by (5.19). Also, n_{odd} and n_{even} are statistically independent and both distributed according to $\mathcal{N}(0, \sigma_0^2/N_c)$. Given the above, it can be shown that the optimal detector of b_1 based on y_{odd} and y_{even} is

$$(1 - P_{e_{12}})A^{-1}e^{\mathbf{v}_1^\mathsf{T}\mathbf{y}} + P_{e_{12}}Ae^{\mathbf{v}_2^\mathsf{T}\mathbf{y}} \;\mathop{\gtrless}\limits_{-1}^{1}\; (1 - P_{e_{12}})A^{-1}e^{-\mathbf{v}_1^\mathsf{T}\mathbf{y}} + P_{e_{12}}Ae^{-\mathbf{v}_2^\mathsf{T}\mathbf{y}} \qquad (5.24)$$

where $\mathbf{y} = [y_{\mathrm{odd}} \quad y_{\mathrm{even}}]^{\mathsf{T}}$, $\mathbf{v}_1 = [K_{10}a_{12} \quad (K_{10}a_{13}+K_{20}a_{23})]^{\mathsf{T}}\frac{\sqrt{N_c}}{\sigma_0}$, $\mathbf{v}_2 = [K_{10}a_{12} \quad (K_{10}a_{13} - K_{20}a_{23})]^{\mathsf{T}}\frac{\sqrt{N_c}}{\sigma_0}$, and $A = \exp(K_{10}K_{20}a_{13}a_{23}\frac{N_c}{\sigma_0^2})$. Unfortunately, this detector is not only rather complex, but also does not have a closed form expression for the resulting probability of bit error. This renders an analysis of the proposed system feasible only through computer simulations. Fortunately, there is a way around this predicament–consider the following suboptimum detector

$$\hat{b} = \mathrm{sign}\,([K_{10}a_{12} \quad \lambda(K_{10}a_{13} + K_{20}a_{23})]\mathbf{y}) \tag{5.25}$$

where $\lambda \in [0,1]$ is a measure of the BS' confidence in the bits estimated by the partner. Specifically, it can be shown that when the BS believes that the inter-user channel is "perfect", i.e. $P_{e_{12}} = 0$, then the optimal detector in (5.24) collapses to the detector in (5.25) with $\lambda = 1$, which is to be expected, since this corresponds to Maximal Ratio Combining (MRC). As the inter-user channel becomes more unreliable, i.e. as $P_{e_{12}}$ increases, although there is no equivalence between the optimal and suboptimal detectors, the value of the best λ in (5.25) decreases towards zero. In essence, then, the detector in (5.25) is a modified MRC, where the branch with the partner's uncertain bit estimates is weighed less that the branch with the bits coming directly from the desired user. We will hence refer to this detector as the λ-MRC.

Initially, one may notice a few negative facts about the above detector. First, it can be shown that, for most channel conditions, no $\lambda \in [0,1]$ will result in the same bit estimates as the optimal receiver, thereby implying a loss in performance. Moreover, the best λ (that minimizes the BER) is a function of the current channel conditions, such as the inter-user channel probability of error ($P_{e_{12}}$), a quantity which the BS may or may not have access to. Upon closer inspection, though, we see that the λ-MRC has some very desirable properties.

First, we have found that, under most channel conditions, it has a performance that is very close to that of the optimal detector given in (5.24), if the parameter $\lambda \in [0, 1]$ is chosen appropriately. Therefore, the loss in performance is negligible. Second, the λ-MRC is very simple and computationally undemanding. Third, it has a closed form expression for the resulting BER, thus enabling simulation-free system analysis. Finally, even though the best value for λ is a function of $P_{e_{12}}$ (which, incidentally, is true for the optimal detector also), the λ-MRC may be run in "blind" mode where the optimal λ is found adaptively.

Independently of how the value of λ is set, the probability of bit error for the λ-MRC, given a λ, is given by

$$P_{e_2} = (1 - P_{e_{12}})Q\left(\frac{\mathbf{v}_\lambda^\mathsf{T}\mathbf{v}_1}{\sqrt{\mathbf{v}_\lambda^\mathsf{T}\mathbf{v}_\lambda}}\right) + P_{e_{12}}Q\left(\frac{\mathbf{v}_\lambda^\mathsf{T}\mathbf{v}_2}{\sqrt{\mathbf{v}_\lambda^\mathsf{T}\mathbf{v}_\lambda}}\right) \tag{5.26}$$

where $\mathbf{v}_\lambda = [K_{10}a_{12} \quad \lambda(K_{10}a_{13} + K_{20}a_{23})]^\mathsf{T}$, $\mathbf{v}_1 = [K_{10}a_{12} \quad (K_{10}a_{13} + K_{20}a_{23})]^\mathsf{T}\frac{\sqrt{N_c}}{\sigma_0}$, and $\mathbf{v}_2 = [K_{10}a_{12} \quad (K_{10}a_{13} - K_{20}a_{23})]^\mathsf{T}\frac{\sqrt{N_c}}{\sigma_0}$. Ideally, the BS would like to use the value of λ that minimizes the above probability of error. Practically, though, either due to imperfections in the feedback from the users concerning the value of $P_{e_{12}}$, or due to residual errors in an adaptive method for estimating the optimal λ, the λ being used will most likely not be the optimal. However, by using the optimal value for λ in our calculations henceforth, we are able to find the maximum possible performance of the λ-MRC, thus providing an upper bound for the performance of any actual implementation.

5.4.3 System Throughput

Summarizing the results of the previous section, for every L symbol periods, the BS receives $L - 2L_c$ bits with a probability of bit error equal to P_{e_1}, given in (5.18), and L_c bits with probability of bit error equal to P_{e_2}, given in (5.26). The resulting

throughput for user 1, or maximum data rate at which user 1 can transmit reliably using sufficiently long error correcting codes, is given by

$$\eta_1(L_c, \{a_{ij}\}, \{K_{ij}\}) = \frac{1}{L}[L_n\left(1 - H(P_{e_1})\right) + L_c\left(1 - H(P_{e_2})\right)]$$

where $H(p)$ is the entropy of a Bernoulli random variable with parameter p. This expression, based on the definitions of P_{e_1} and P_{e_2} in Section 5.4.2, holds given a particular value for L_c, given a particular power allocation, as defined by the a_{ij}, and given a particular set of fading coefficients, as defined by the K_{ij}. Since the K_{ij} are randomly time-varying, the throughput for a given value of L_c and a given set of power allocation parameters a_{ij} becomes

$$\eta_1(L_c, \{a_{ij}\}) = \mathrm{E}_{\{K_{ij}\}}\left[\eta_1(\{a_{ij}\}, \{K_{ij}\})\right]. \tag{5.27}$$

The analogous expression holds for user 2's throughput. Therefore, given an L_c and a set of a_{ij} that remain constant over all realizations of the K_{ij}, the two users achieve the rate pair $(\eta_1(L_c, \{a_{ij}\}), \eta_2(L_c, \{a_{ij}\}))$. By time-sharing between different values of L_c and different sets of a_{ij}, while maintaining the power constraints given in (5.16), the two users are able to attain an achievable rate region that is the convex hull of the set of all $(\eta_1(L_c, \{a_{ij}\}), \eta_2(L_c, \{a_{ij}\}))$ pairs.

5.4.4 Case Studies

As in Section 5.3.1, we study the achievable throughput region under two different scenarios, depicted in Figures 5.7 and 5.8. We observe that in both cases, cooperation improves upon the no cooperation result. Due to the fact that the discussion of the results would be similar to that of Section 5.3.3, we do not elaborate further.

In Figure 5.9, we show the same scenario as in Figure 5.8, however, with the achievable throughput regions due to specific values of L_c explicitly shown. This
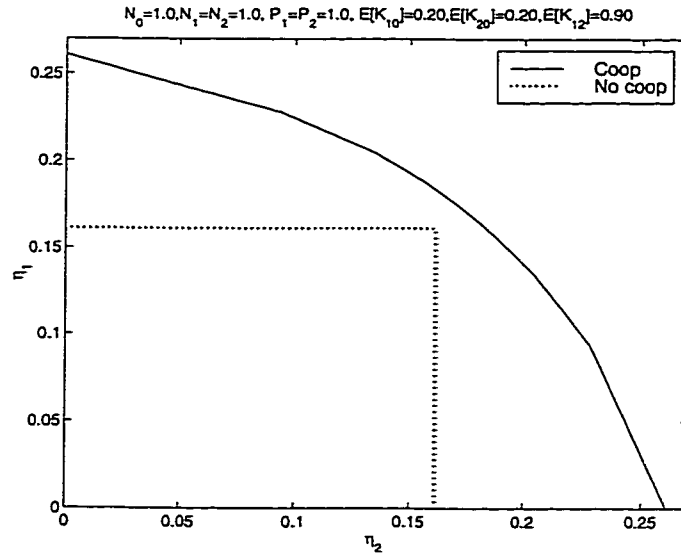
Figure 5.7 : Achievable throughput region when the two users face statistically equivalent channels towards the base station (CDMA implementation).
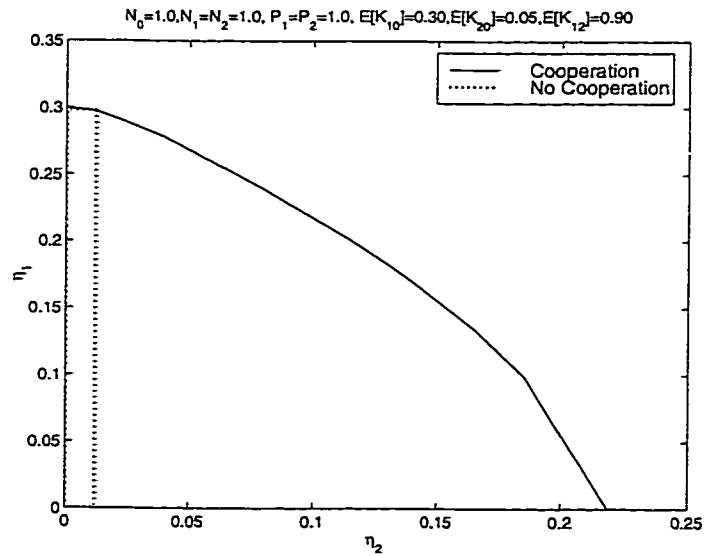

Figure 5.8 : Achievable throughput region when the two users face statistically dissimilar channels towards the base station (CDMA implementation)

enables us to see that various points on the achievable throughput region are achieved using different values for L_c, which shows that our intuition for using a variable number for L_c was correct.

We also study the probability of outage of this system, as defined in Section 5.3.2. Figure 5.10 shows outage probability results for the same scenario as that of Figure 5.7 Again, as in Section 5.3.3, even though the increase in throughput due to cooperation is moderate for this scenario, as seen in Figure 5.7, the resulting system is significantly more robust against channel variations.

The reduced susceptibility to fading due to cooperation is also attested to by a "smoother" data rate as a function of time, which can be measured by calculating the variance of the effective data rate. Specifically, in the example given in Figure 5.10, the non-cooperative strategy results in a data rate whose variance is equal to 0.02, with an average data rate equal to 0.159 bits per symbol period. In contrast, user cooperation results in a data rate with not only a larger average, 0.175, but also a lower variance, 0.01.

5.5 High Data Rate CDMA System

Even though today's CDMA systems assign only one spreading code per user, future generations of CDMA systems, in an attempt to increase their data rate, may assign multiple spreading codes to each user. How, then, do we implement a cooperative scheme under such a system? This question is addressed in the present section. We will see that, with multiple codes per user, there arises a somewhat natural implementation of the cooperative scheme presented in Section 5.3.1.

Consider a high bitrate CDMA cellular system in which users achieve a high data rate by virtue of having more than one spreading code, each code being used to transmit one bit per symbol period. For the purposes of this discussion, we will
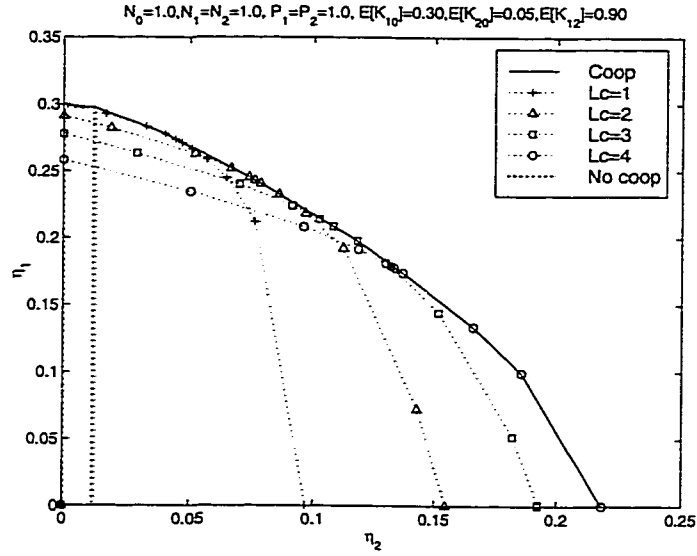
Figure 5.9 : Achievable throughput region when the two users face statistically dissimilar channels towards the base station (CDMA implementation). The effects of using various values of L_c can be clearly seen
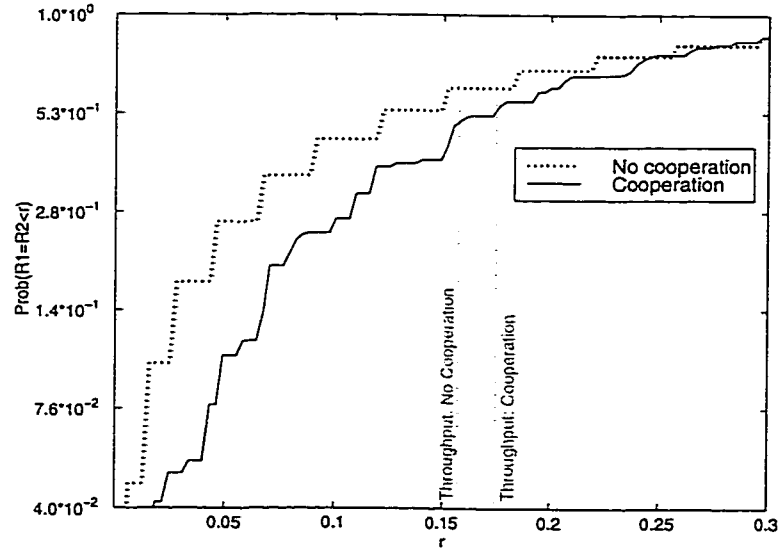

Figure 5.10 : Probability of outage

focus on synchronous systems and on orthogonal spreading codes. Given that the spreading factor of this CDMA system is N_c, the maximum number of orthogonal spreading codes is equal to N_c. Let M_o refer to the number of codes being used by all other users in the system, other than our two desired users. Also, for simplicity, and without loss of generality, assume that the two users under consideration have equal data rate requirements, and are therefore given the same number of spreading codes. Denote that number by M. From the above discussion, it is clear that $1 \leq M \leq (N_c - M_o)/2$.

As in Section 5.4, we begin with a simple example ($M = 3$) and then generalize to any M. Assume that the two users have three spreading codes each. In the absence of cooperation, they would transmit

$$
\begin{aligned}
X_1(t) &= a_{11}\, b_{11}\, c_{11}(t) + a_{12}\, b_{12}\, c_{12}(t) + a_{13}\, b_{13}\, c_{13}(t) \\
X_2(t) &= a_{21}\, b_{21}\, c_{21}(t) + a_{22}\, b_{22}\, c_{22}(t) + a_{23}\, b_{23}\, c_{23}(t)
\end{aligned}
\tag{5.28}
$$

where b_{ji} is user j's i^{th} bit from the current symbol period, and c_{ji} is user j's i^{th} code. The parameters a_{ji} control how much power is allocated to each bit. Now, assume that the two partners decide to cooperate. Then, one way for them to do so is by transmitting:

$$
\begin{aligned}
X_1(t) &= \underbrace{a_{11}\, b_{11}\, c_{11}(t)}_{\substack{\text{akin to } X_{20} \\ \text{from Section 5.3.1}}} + \underbrace{a_{12}\, b_{12}\, c_{12}(t)}_{\substack{\text{akin to } X_{21} \\ \text{from Section 5.3.1}}} + \underbrace{[a_{13}\, b_{12}^{(-1)}\, c_{13}(t) + \tilde{a}_{23}\, \hat{b}_{22}^{(-1)}\, c_{23}(t)]}_{\substack{\text{akin to } U \\ \text{from Section 5.3.1}}} \\
X_2(t) &= a_{21}\, b_{21}\, c_{21}(t) + a_{22}\, b_{22}\, c_{22}(t) + [\tilde{a}_{13}\, \hat{b}_{12}^{(-1)}\, c_{13}(t) + a_{23}\, b_{22}^{(-1)}\, c_{23}(t)]
\end{aligned}
$$

$$\tag{5.29}$$

where $b_{ji}^{(-1)}$ is user j's i^{th} bit from the previous symbol period, and $\hat{b}_{ji}^{(-1)}$ is the partner's estimate of that bit. The parameters a_{ji} control how much power is allocated to a user's own bits versus the bits of the partner.

Codes c_{j1}, $j = 1, 2$, are used to send data to the BS only, akin to the function of the signals X_{j0}, $j = 1, 2$ in Section 5.3.1. On the other hand, codes c_{j2}, $j = 1, 2$ are used to send data not only to the BS, but also to each user's partner, akin to the function of the signals X_{12} and X_{21} in Section 5.3.1. After this data is estimated by each user's partner, it is used to construct a cooperative signal that is sent to the BS. This is accomplished using codes c_{13} and c_{23}, and is akin to the function of the signal U in Section 5.3.1. Notice that user 1 is using one of user 2's codes (i.e. c_{23}), and vice versa. This is done in such a way as to enable the two partners to send a cooperative signal while keeping the total number of codes used by the two users constant.

Also notice that codes c_{13} and c_{23} are used in order to re-send, in some sense, the information originally modulated onto codes c_{12} and c_{22}. This implies that the users only send *two* new bits per symbol period, whereas they would be sending three new bits per symbol period if they were not cooperating (see (5.28)). This is similar to the issue that arose in Section 5.4.1, and the corresponding discussion in that section is applicable here, with appropriate modifications.

Equation (5.29) refers to the special case of $M = 3$. The generalization to arbitrary M is as follows. Each of the two partners uses $2M_c$ codes for cooperation and $M - 2M_c$ codes for sending non-cooperative information, where M_c is some integer between 0 and $M/2$. When $M_c = 0$, the two users are not cooperating at all. When $M_c = M/2$, the two users are fully cooperating, that is, allocating all their available codes for cooperation. For example, in the scenario referred to by (5.29), the value of M_c is 1. In general, the value of M_c may be time-varying, a fact which allows time-sharing of different values of M_c, in order to achieve any point on the capacity region.

The cooperative scheme just described may be expressed, for a given M and M_c,

as

$$X_j(t) = \sum_{i=1}^{M-2M_c} a_{j1}\, b_{ji}\, c_{ji}(t) +$$

$$\sum_{\substack{k=1\to(M-1)\\ i=M-2M_c-1+2k}} \{a_{j2}\, b_{ji}\, c_{ji}(t) + [a_{j3}\, b_{ji}^{(-1)}\, c_{j(i+1)}(t) + \bar{a}_{\bar{\jmath})3}\, \tilde{b}_{\bar{\jmath})i}^{(-1)}\, c_{\bar{\jmath})(i+1)}(t)]\}, \quad j=1,2$$

$$\tag{5.30}$$

where we have used the convention $\bar{\jmath}=1$ if $j=2$, and $\bar{\jmath}=2$ if $j=1$, and where the a_{ij} are chosen to satisfy the power constraints given by

$$
\begin{aligned}
(M-2M_c)a_{11}^2 + M_c(a_{12}^2 + a_{13}^2 + \bar{a}_{23}^2) &= P_1 \\
(M-2M_c)a_{21}^2 + M_c(a_{22}^2 + a_{23}^2 + \bar{a}_{13}^2) &= P_2
\end{aligned}
\tag{5.31}
$$

5.5.1 System Throughput

As a result of this transmission scheme, given a particular value for M_c, given a particular power allocation, as defined by the a_{ij}, and given a particular set of fading coefficients, as defined by the K_{ij}, for every M bits, the BS receives $M-2M_c$ bits with a probability of bit error equal to P_{e_1}, given in (5.32), and M_c bits with probability of bit error equal to P_{e_2}, given in (5.33). Due to the similarity with the contents of Section 5.4.2, we omit the derivation of (5.32) and (5.33).

$$P_{e_1} = Q\left(K_{10}a_{11}\frac{\sqrt{N_c}}{\sigma_0}\right) \tag{5.32}$$

$$P_{e_2} = (1-P_{e12})Q\left(\frac{\mathbf{v}_\lambda^\mathsf{T}\mathbf{v}_1}{\sqrt{\mathbf{v}_\lambda^\mathsf{T}\mathbf{v}_\lambda}}\right) + P_{e12}Q\left(\frac{\mathbf{v}_\lambda^\mathsf{T}\mathbf{v}_2}{\sqrt{\mathbf{v}_\lambda^\mathsf{T}\mathbf{v}_\lambda}}\right) \tag{5.33}$$

where $\mathbf{v}_\lambda = [K_{10}a_{12} \quad \lambda(K_{10}a_{13} + K_{20}\bar{a}_{13})]^\mathsf{T}$, $\mathbf{v}_1 = [K_{10}a_{12} \quad (K_{10}a_{13} + K_{20}\bar{a}_{13})]^\mathsf{T}\frac{\sqrt{N_c}}{\sigma_0}$, $\mathbf{v}_2 = [K_{10}a_{12} \quad (K_{10}a_{13} - K_{20}\bar{a}_{23})]^\mathsf{T}\frac{\sqrt{N_c}}{\sigma_0}$, and $P_{e12} = Q(K_{12}a_{12}\sqrt{N_c}/\sigma_1)$. The resulting throughput for user 1 is given by

$$\eta_1(M_c, \{a_{ij}\}, \{K_{ij}\}) = (M-2M_c)(1 - H(P_{e_1})) + M_c(1 - H(P_{e_2}))$$

Since the K_{ij} are randomly time-varying, the throughput for a given value of M_c and a given set of power allocation parameters a_{ij} becomes

$$\eta_1(M_c, \{a_{ij}\}) = \mathrm{E}_{\{K_{ij}\}} \left[\eta_1(M_c, \{a_{ij}\}, \{K_{ij}\}) \right]. \tag{5.34}$$

The analogous expression holds for user 2's throughput. Therefore, given a value for M_c and given a set of a_{ij}, the two users achieve the rate pair $(\eta_1(M_c, \{a_{ij}\}), \eta_2(M_c, \{a_{ij}\}))$. By time-sharing between different sets of a_{ij}, while maintaining their power constraints, the two users are able to attain an achievable rate region that is the convex hull of the set of all $(\eta_1(M_c, \{a_{ij}\}), \eta_2(M_c, \{a_{ij}\}))$ pairs.

Due to the similarity with Section 5.4, case studies for this system are not presented. We mention only that both the achievable rate region results, as well as the outage probability results, are similar to the ones presented in Sections 5.3.3 and 5.4.4.

5.6 No phase knowledge at the transmitters

The majority of this chapter dealt with the case of known fading phase at the transmitters. This was done mainly for simplicity of exposition of the benefits of cooperation, but was justified by the possibility of having a system in TDD mode and, more importantly, by the fact that in a practical, asynchronous, system this assumption becomes a non-issue, as discussed in Section 5.2.

Nevertheless, for completeness, we present in this section a cooperative transmission scheme that does not require the transmitters to know the phase of the fading coefficient between them and the BS. In essence, this section demonstrates that the known-phase assumption is not critical–cooperation can lead to gains even when this assumption has been removed, even in a synchronous system.

As it turns out, when we remove the known-phase at the transmitters assumption,

it becomes necessary to look at the system in a slightly more general way, in order for cooperation to provide solid gains over a non-cooperative strategy. That is, in Section 5.2, it was assumed that the fading experienced by the various signals was Rayleigh fading. In practice, though, the fading coefficient is actually composed of two parts. For example

$$K_{ij} = K_{ij}^{\lg} K_{ij}^{\rm sm}$$

where $K_{ij}^{\rm sm}$ corresponds to small time-scale variations in signal attenuation, and thus represents Rayleigh fading, and $K_{ij}^{\lg}$ corresponds to large time-scale variations in signal attenuation, and represents what is called long-term or shadow fading. Whereas Rayleigh fading arises from the combination of a large number of multipaths coming in from a large number of directions, adding constructively or destructively on very small time scales, shadow fading arises from the existence of large-scale obstructions between the mobile and the BS, thus providing long-term attenuation of the mobile's transmit and receive signals.

Therefore, while it would have been somewhat impractical for the mobiles to adjust their transmission scheme according to the instantaneous value of the short-term Rayleigh fading, requiring them to do so according to the value of the long-term fading is very much within the limits of what is practical and implementable. As stated in Section 5.2, the mobile unit has very limited peak power capabilities, thus rendering power allocation into different fading states implausible, if not infeasible. Therefore, the only way in which we allow the mobile to dynamically adjust its transmission scheme is by using different sub-signal power allocation strategies (determined by the a_{ij}) according to the value of the long-term fading. In this manner, the average transmit power of each mobile is constant, thus not challenging the peak-power constraints of the mobile, while the power allocation among the sub-signals

of each mobile is a function of the value of the long-term fading, thus enabling the two partners to dynamically choose where on the achievable rate region they want to operate. This benefit is what allows two cooperative mobiles to achieve an overall larger achievable rate region than two non-cooperative mobiles, even when the assumption of known fading phase at the transmitters is discarded.

5.6.1 Cooperative Scheme

We will focus on a system similar to that described in Section 5.4, that is, a CDMA cellular system in which each user has one spreading code, and modulates one bit onto it. However, due to the fact that the mobiles do not know the phase of the fading coefficient between them and the BS, cooperation as in Section 5.4 and in (5.15) is not beneficial, at least not in a synchronous system, since the signals transmitted by the two mobiles in the even cooperative periods would sometimes destructively interfere with each other.

We therefore need to propose a modified method for them to cooperate. Beginning with the simple example of $L = 3$, as in (5.14), the proposed cooperative scheme would be

$$
\begin{aligned}
X_1(t) &= a_{11}\, b_1^{(1)}\, c_1(t)\,, \quad a_{12}\, b_1^{(2)}\, c_1(t)\,, \quad a_{13}\, \hat{b}_2^{(2)}\, c_1(t) \\
X_2(t) &= \underbrace{a_{21}\, b_2^{(1)}\, c_2(t)}_{\text{Period 1}}\,, \quad \underbrace{a_{22}\, b_2^{(2)}\, c_2(t)}_{\text{Period 2}}\,, \quad \underbrace{a_{23}\, \hat{b}_1^{(2)}\, c_2(t)}_{\text{Period 3}}
\end{aligned}
\tag{5.35}
$$

This is akin to the cooperative scheme in (5.14), save for the fact that in period 3 each mobile transmits only the estimated bit of its partner, modulated onto its own

spreading code. The generalization of this scheme, for a given L and L_c, is

$$
X_1(t) = \begin{cases} a_{11}\, b_1^{(i)}\, c_1(t) & \text{periods } i = 1, 2, \ldots, L_n \\ a_{12}\, b_1^{\left(\frac{L_n+1+i}{2}\right)}\, c_1(t) & \text{periods } i = L_n + 1, L_n + 3, \ldots, L - 1 \\ a_{13}\, \hat{b}_2^{\left(\frac{L_n+i}{2}\right)}\, c_1(t) & \text{periods } i = L_n + 2, L_n + 4, \ldots, L \end{cases}
$$

$$\text{(5.36)}$$

$$
X_2(t) = \begin{cases} a_{21}\, b_2^{(i)}\, c_2(t) & \text{periods } i = 1, 2, \ldots, L_n \\ a_{22}\, b_2^{\left(\frac{L_n+1+i}{2}\right)}\, c_2(t) & \text{periods } i = L_n + 1, L_n + 3, \ldots, L - 1 \\ a_{23}\, \hat{b}_1^{\left(\frac{L_n+i}{2}\right)}\, c_2(t) & \text{periods } i = L_n + 2, L_n + 4, \ldots, L \end{cases}
$$

where $L_n = L - 2L_c$, and where the a_{ij} are chosen to satisfy the power constraints given by

$$
\begin{aligned}
\tfrac{1}{L}(L_n a_{11}^2 + L_c(a_{12}^2 + a_{13}^2)) &= P_1 \\
\tfrac{1}{L}(L_n a_{21}^2 + L_c(a_{22}^2 + a_{23}^2)) &= P_2.
\end{aligned}
$$

$$\text{(5.37)}$$

5.6.2 System Throughput

As a result of this transmission scheme, given a particular value for L_c, given a particular power allocation, as defined by the a_{ij}, and given a particular set of fading coefficients, as defined by the K_{ij}, for every L symbol periods, the BS receives $L - 2L_c$ bits with a probability of bit error equal to P_{e1}, given in (5.38), and L_c bits with probability of bit error equal to P_{e2}, given in (5.39). Due to the similarity with the contents of Section 5.4.2, we omit the derivation of (5.38) and (5.39).

$$
P_{e1} = Q\left(\frac{K_{10}\, a_{11}}{\sigma}\right)
$$

$$\text{(5.38)}$$

$$
P_{e2} = (1 - P_{e12})Q\left(\frac{\mathbf{v}_\lambda^\top \mathbf{v}_1}{\sqrt{\mathbf{v}_\lambda^\top \mathbf{v}_\lambda}}\right) + P_{e12}Q\left(\frac{\mathbf{v}_\lambda^\top \mathbf{v}_2}{\sqrt{\mathbf{v}_\lambda^\top \mathbf{v}_\lambda}}\right)
$$

$$\text{(5.39)}$$

where $\mathbf{v}_\lambda = [K_{10}a_{12} \quad \lambda K_{20}a_{23}]^\top$, $\mathbf{v}_1 = [K_{10}a_{12} \quad K_{20}a_{23}]^\top \frac{\sqrt{N_c}}{\sigma_0}$, $\mathbf{v}_2 = [K_{10}a_{12} \quad -K_{20}a_{23}]^\top \frac{\sqrt{N_c}}{\sigma_0}$, and $P_{e12} = Q(K_{12}a_{12}\sqrt{N_c}/\sigma_1)$. The resulting throughput for user 1 is

given by

$$\eta_1(L_c, \{a_{ij}\}, \{K_{ij}\}) = \frac{1}{L}[L_n(1 - H(P_{e_1})) + L_c(1 - H(P_{e_2}))]$$

As mentioned at the beginning of Section 5.6, $K_{ij} = K_{ij}^{lg} K_{ij}^{sm}$, where K_{ij}^{sm} corresponds to small time-scale variations in signal attenuation, and K_{ij}^{lg} corresponds to large time-scale variations. Assuming that K_{ij}^{lg} changes over sufficiently large time scales, we can write the throughput, for a given value of L_c and a given set of power allocation parameters a_{ij}, as

$$\eta_1(L_c, \{a_{ij}\}, \{k_{ij}^{lg}\}) = \mathrm{E}_{\{K_{ij}^{sm}\}}\left[\eta_1(\{a_{ij}\}, \{k_{ij}^{lg} K_{ij}^{sm}\})\right] \qquad (5.40)$$

when the large time-scale fading coefficients equal $\{k_{ij}^{lg}\}$. The analogous expression holds for user 2's throughput. Therefore, given an L_c and a set of a_{ij} that remain fixed while $\{K_{ij}^{lg}\} = \{k_{ij}^{lg}\}$, the two users achieve the rate pair $(\eta_1(L_c, \{a_{ij}\}, \{k_{ij}^{lg}\}), \eta_2(L_c, \{a_{ij}\}, \{k_{ij}^{lg}\}))$.

Even though the mobiles have no knowledge of $\{K_{ij}^{sm}\}$, we assume that the $\{K_{ij}^{lg}\}$ change slowly enough for the BS to provide some feedback about their value to the mobiles. Thus, the mobiles may use a value for L_c and a set of a_{ij} that depend on the current value of $\{K_{ij}^{lg}\}$, in order to achieve some goal, e.g. maximize the equal-rate throughput. In general, the goal will be to maximize $(\alpha \eta_1 + (1 - \alpha) \eta_2)$ where $\alpha \in [0, 1]$. The resulting throughput for user 1, when $\{K_{ij}^{lg}\} = \{k_{ij}^{lg}\}$, becomes

$$\eta_1^\alpha(\{k_{ij}^{lg}\}) = \eta_1(L_c^\alpha(\{k_{ij}^{lg}\}), \{a_{ij}^\alpha(\{k_{ij}^{lg}\})\}, \{k_{ij}^{lg}\}) \qquad (5.41)$$

where L_c^α and a_{ij}^α are chosen to maximize $(\alpha \eta_1 + (1 - \alpha) \eta_2)$ for some $\alpha \in [0, 1]$. The overall throughput for user 1 is thus given by

$$\eta_1^\alpha = \mathrm{E}_{\{K_{ij}^{lg}\}}\left[\eta_1^\alpha(\{K_{ij}^{lg}\})\right] \qquad (5.42)$$

with the analogous expression holding for user 2. Therefore, the achievable rate region is given by the set of all $(\eta_1^\alpha, \eta_2^\alpha)$ pairs, where $\alpha \in [0, 1]$.

Case studies, not included here due to space considerations and due to similarities with results in previous sections, demonstrate that both the achievable rate region results, as well as the outage probability results, are similar to the ones presented in Sections 5.3.3 and 5.4.4.

5.7 Conclusions/Discussion

We have presented a new method of transmit diversity for mobile users: in-cell user cooperation. Results indicate that user cooperation is beneficial and can result in substantial gains over a non-cooperative strategy. These gains are two-pronged: A higher data rate and a decreased sensitivity to channel variations. Furthermore, these results hold both in an unrestricted system model, as well as when the transmission scheme is fixed.

The increased data rate with cooperation can also be translated into reduced power for the users: with cooperation, the users need to use less total power to achieve a certain rate pair than with no cooperation. The partner scheme can thus be used to extend the battery life of the mobiles. Alternatively, the cooperation gains may be used to increase cell coverage in a cellular system.

We should note that since the mobile now has to be able to detect uplink signals, implementation of the proposed system involves an increased-complexity mobile receiver. Complexity is also increased because, for security purposes, users' data now has to be encrypted before transmission, in order for a mobile to be able to detect its partner's transmitted data without being able to understand the information being sent. It can be argued, though, that most future wireless systems will employ some form of encryption anyway, since no modulation technique, even CDMA, can guarantee the security of the information being transmitted. In addition, under certain scenarios, the benefits of an increased and robust data rate, and/or an extended

battery life and/or extended cell coverage will be worth the extra complexity that comes with user cooperation.

In fact, the decreased sensitivity of the data rate to channel variations is a significant enough advantage that it could warrant user cooperation even if there were no other benefits such as increased data rate. This is because of the minimum data rate requirements of some real-time applications, such as voice or video, and the resulting lower probability of outage, and thus better QoS, due to cooperation.

The analysis presented in this chapter represents one possible evaluation of the user-cooperation concept, where one of the main goals was to to achieve a simple and clear exposition. Therefore, some of the assumptions and proposed implementations may be modified in order to achieve greater performance and/or implementability. First, in our CDMA implementations we assumed that the various spreading codes being used were orthogonal. This need not be the case: any codes may be used, along with multiuser detection in order to have optimum performance. Second, in Sections 5.4 and 5.5, the cooperative strategy involved re-sending, in some sense, information using a cooperative signal. Another possibility is for the two users to always transmit new information, even during the cooperative periods, thus necessitating the use of sequence detection due to the intersymbol interference that would result from such a strategy. It is not clear at present if this strategy would result in increased performance or not.

Third, even though we have analyzed only the case of each user having one partner, it is clear that a generalization of this concept would involve multiple partners, thus leading to even better performance, especially more robust data rates. However, the incremental gains from additional partners will diminish as the number of partners grows. Fourth, although this chapter focused on a cellular environment, user cooperation diversity may also be employed in other situations, such as in ad-hoc

networks.

Finally, what we have presented here addresses only physical layer issues, and presents us with what is achievable through partnering. However, there are several higher-layer issues which we did not address but which, nevertheless, are interesting, challenging and difficult to resolve. These involve questions such as who will partner with whom, under what conditions will they partner, at which point on the achievable rate region will they operate and why, and who decides which mobiles partner: the mobiles themselves or the BS?

For example, when the two users face statistically similar channels towards the base station, the issue is easy: both users benefit and therefore would both like to cooperate. However, when the two users face statistically dissimilar channels towards the base station, as would occur if one mobile was near the outskirts of the cell and the other was near the center of the cell, one mobile is giving up some of its data rate in order to help the other user achieve some acceptable level of performance, and thus the question arises as to why one would want to do that. There are two possible answers. First, if we look at long-term performance, i.e. over the duration of an entire call, a user will, on average, benefit from having a "partnering cell-phone". This, of course, assumes that the users are mobile. If they are not, the problem becomes more complex. The second reason for partnering, which addresses the short-term performance of mobile users, as well as the long-term needs of stationary users, can be the possible existence of financial incentives for the higher-quality users, as well as a corresponding fee for the lower-quality users.

If multiple users are allowed to cooperate, the above approach evolves into a very interesting and complex problem involving something akin to market equilibrium theory. That is, the BS will have a group of users willing to pay varying amounts of money for varying degrees of higher QoS, and a group of users willing to receive

varying amounts of monetary compensation for reducing their QoS and assisting other users. The problem, then, faced by the BS is how to use "market forces" and available wireless resources to find an equilibrium that satisfies as many users' monetary and QoS demands as possible. This will be accomplished by finding how to best group the users into cooperation groups, and where on their respective multi-dimensional achievable rate regions these groups should operate. This problem is, of course, an entire research project in itself, as are most higher-layer issues related to user cooperation.

Chapter 6

Concluding Remarks

The subjects presented in this thesis are quite diverse, and thus hard to put under a single umbrella category. Nevertheless, they all involve the use of novel concepts that improve wireless system performance and may aid next-generation wireless systems in achieving their goals, such as multirate support, higher data rates, and more robust data rates.

It should be pointed out that the ideas expressed in Chapters 2 through 5 are neither mutually exclusive, nor require each other in order to provide gains. They should be seen as "orthogonal" concepts, in the sense that any subset of them may be implemented simultaneously. The gains resulting from the implementation of any such subset are, of course, not trivially related to the gains reported herein regarding each individual concept–they need to be determined via additional analysis.

Appendix A

Appendix for MultiUser Doppler Receiver

Recall that

$$\widehat{y}_{mmse} = F_{mmse} z, \tag{A.1}$$

where F_{mmse} solves

$$F_{mmse} = \arg \min_{F} \mathrm{E} \left\| Hb - Fz \right\|^2. \tag{A.2}$$

The MSE functional can be expanded as

$$
\begin{aligned}
\mathrm{E} \left\| Hb - Fz \right\|^2 &= \mathrm{E} \left[z^H F^H F z \right] + \mathrm{E} \left[b^T H^H H b \right] - 2\mathrm{Re} \left\{ \mathrm{E} \left[z^H F^H H b \right] \right\} \\
&= \mathrm{Tr} \left[F \mathrm{E}[zz^H] F^H \right] + \mathrm{Tr} \left[\mathrm{E}[H^H H] \right] - 2\mathrm{Re} \left\{ \mathrm{Tr} \left[F^H \mathrm{E}[Hbz^H] \right] \right\} \\
&= \mathrm{Tr} \left[FQ_1 F^H \right] + \mathrm{Tr} \left[\mathrm{E}[H^H H] \right] - 2\mathrm{Re} \left\{ \mathrm{Tr} \left[F^H Q_2 \right] \right\}, \tag{A.3}
\end{aligned}
$$

where $\mathrm{Tr}[\cdot]$ denotes the trace of a matrix. Using $z = RHb + w$ we get

$$Q_1 \stackrel{def}{=} \mathrm{E}[zz^H] = R\Psi R + \mathcal{N}_0 R, \tag{A.4}$$

where $\Psi = \mathrm{E}[HH^H]$, and we have used the fact that $\mathrm{E}[bb^T] = I$. Similarly,

$$Q_2 \stackrel{def}{=} \mathrm{E}[Hbz^H] = \Psi R. \tag{A.5}$$

Differentiating $\mathrm{E} \left\| Hb - Fz \right\|^2$ in (A.3) with respect to F, we have

$$\frac{\partial \mathrm{E} \left\| Hb - Fz \right\|^2}{\partial F} = 2Q_1 F^H - 2Q_2^H, \tag{A.6}$$

where we have used the following identities

$$\frac{\partial \text{Tr}[\boldsymbol{F}\boldsymbol{Q}\boldsymbol{F}^H]}{\partial \boldsymbol{F}} = 2\boldsymbol{Q}\boldsymbol{F}^H, \tag{A.7}$$

$$\frac{\partial \text{Re}\left\{\text{Tr}[\boldsymbol{F}^H\boldsymbol{Q}]\right\}}{\partial \boldsymbol{F}} = \boldsymbol{Q}^H. \tag{A.8}$$

Setting the gradient in (A.6) equal to zero yields the optimal $\boldsymbol{F}$

$$\boldsymbol{F}_{mmse} = \boldsymbol{Q}_2\boldsymbol{Q}_1^{-1} = (\boldsymbol{R} + \mathcal{N}_0\boldsymbol{\Psi}^{-1})^{-1}, \tag{A.9}$$

where we have used (A.4) and (A.5).

Bibliography

[1] TIA/EIA/IS-95, "Mobile station — base station compatibility standard for dual-mode wideband spread spectrum cellular systems," tech. rep., Telecommunications Industry Association, July 1993.

[2] J. G. Proakis, *Digital Communications*. New York: McGraw-Hill, 2nd ed., 1989.

[3] J. Salz and S. Weinstein, "Data transmission by frequency-division multiplexing using the discrete fourier transform," *IEEE Transactions on Communications Technology*, vol. COM-19, pp. 628–634, Oct. 1971.

[4] D. L. Goeckel and W. E. Stark, "Throughput optimization in faded multicarrier systems," in *33rd Annual Allerton Conference on Communication, Control and Computing*, Oct. 1995.

[5] E. A. Sourour and M. Nakagawa, "Performance of orthogonal multicarrier CDMA in a multipath fading channel," *IEEE Transactions on Communications*, vol. 44, pp. 356–366, Mar. 1996.

[6] T. M. Cover and J. A. Thomas, *Elements of Information Theory*. New York: John Wiley, 1991.

[7] J. Zhu and G. Marubayashi, "Properties and application of parallel combinatory SS communication system," in *IEEE Second International Symposium on Spread Spectrum Techniques and Applications*, pp. 227–230, Nov. 1992.

[8] T. S. Rappaport, *Wireless Communications: Principles and Practice.* Prentice Hall, 1996.

[9] A. Elmilady and S. G. Wilson, "Interference cancellation in high-density S-CDMA systems using power control and decision feedback detectors," in *Thirty First Annual Conference on Information Sciences and Systems*, Mar. 1997.

[10] B. D. Woerner and W. E. Stark, "Trellis-coded direct sequence spread-spectrum communications," *IEEE Trans. Commun.*, 1994.

[11] U. Fawer and B. Aazhang, "Multiuser receivers for code-division multiple-access systems with trellis-based modulation," *IEEE Journal on Selected Areas in Communications*, vol. 14, Oct. 1996.

[12] S. Verdu, "Multiuser detection," in *Advances in Detection and Estimation*, JAI Press, 1993.

[13] F. Project, "FMA2 - a wideband-CDMA proposal for IMT-2000," tech. rep., CSEM/Pro Telecom, Ericsson, France Telecom-CNET, Nokia, Siemens, 1997.

[14] W. Dam and D. Taylor, "An adaptive maximum likelihood receiver for correlated rayleigh-fading channels," *IEEE Transactions on Communications*, 1994.

[15] D. Matolak and S. Wilson, "Detection for a statistically known, time-varying dispersive channel," *IEEE Transactions on Communications*, 1996.

[16] G. Lee, S. Gelfand, and M. Fitz, "Bayesian techniques for blind deconvolution," *IEEE Transactions on Communications*, 1996.

[17] S. Vasudevan and M. Varanasi, "Achieving near-optimum asymptotic efficiency and fading resistance over the time-varying rayleigh-faded cdma channel," *IEEE Transactions on Communications*, 1996.
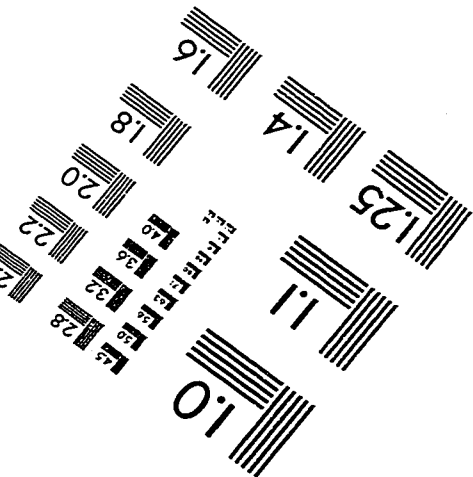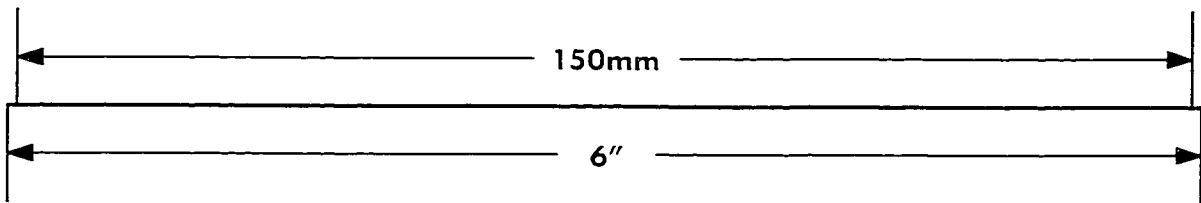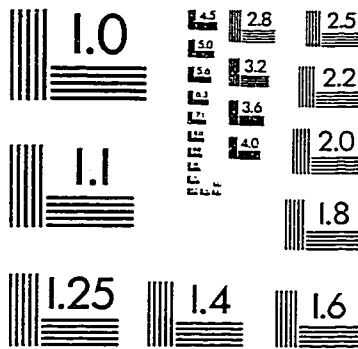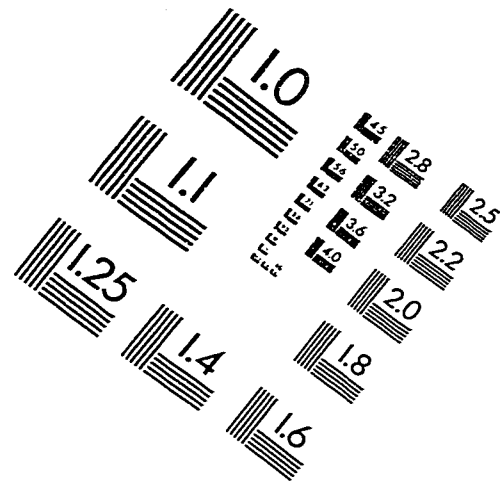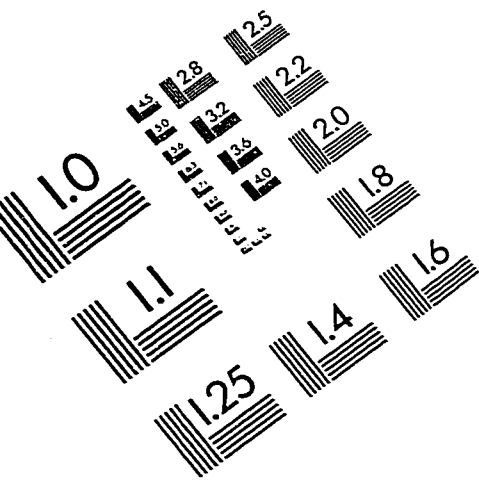
[18] G. Castellini, F. Conti, E. Re, and L. Pierucci, "A continuously adaptive MLSE receiver for mobile communications: Algorithm and performance," *IEEE Transactions on Communications*, 1997.

[19] C. Georgiades and J. Han, "Sequence estimation in the presence of random parameters via the EM algorithm," *IEEE Transactions on Communications*, 1997.

[20] J. Proakis, *Digitial Communications 3rd ed.* New York: McGraw Hill, 1995.

[21] T. Rappaport, *Wireless Communications*. Upper Saddle River, NJ: Prentice Hall, 1996.

[22] S. Moshavi, "Multi-user detection for DS-CDMA communications," *IEEE Communications Magazine*, pp. 124–136, Oct 1996.

[23] Z. Zvonar and D. Brady, "Linear multipath-decorrelating receivers for CDMA frequency-selective fading channels," *IEEE Trans. Commun.*, vol. 44, pp. 650–653, Jun 1996.

[24] M. Latva-aho and M. Juntti, "Modified adaptive LMMSE receiver for DS-CDMA systems in fading channels," in *Proc. PIMRC '97*, pp. 554–558, 1997.

[25] J. Cavers, "An analysis of pilot symbol assisted modulation for Rayleigh fading channels," *IEEE Trans. Vehic. Tech*, pp. 689–693, Nov 1991.

[26] M. S. H. Andoh and F. Adachi, "Channel estimation using time multiplexed pilot symbols for coherent Rake combining for DS-CDMA mobile radio," in *Proc. PIMRC '97*, pp. 954–958, 1997.

[27] B. Sklar, "Rayleigh fading channels in mobile digital communication system Part II: Mitigation," *IEEE Communications Magazine*, pp. 103–109, Jul 1997.

[28] A. M. Sayeed and B. Aazhang, "Exploiting Doppler diversity in mobile wireless communications," in *Proc. 1997 Conf. Inf. Sci. Syst. (CISS'97)*, 1997.

[29] A. M. Sayeed and B. Aazhang, "Joint multipath-Doppler diversity in mobile wireless communications," *to appear in the IEEE Trans. Commun.*

[30] A. M. Sayeed and B. Aazhang, "Communication over multipath fading channels: A time-frequency perspective," in *Wireless Communications: TDMA versus CDMA* (S. Glisic and P. Lippänen, eds.), pp. 73–98, Kluwer Academic Publishers, 1997.

[31] F. Hlawatsch and G. F. Boudreaux-Bartels, "Linear and quadratic time-frequency signal representations," *IEEE Signal Processing Magazine*, Apr 1992.

[32] A. S. A. M. Sayeed and B. Aazhang, "Multiuser detectors for fast-fading multipath channels," in *Proc. 31st Asilomar Conf. Signals, Syst., and Computers*, 1997.

[33] R. Lupas and S. Verdu, "Near-far resistance of multiuser detectors in asynchronous channels," *IEEE Trans. Commun.*, vol. 38, pp. 496–508, Apr 1990.

[34] U. Madhow and M. L. Honig, "MMSE interference suppression for direct-sequence spread-spectrum CDMA," *IEEE Trans. Commun.*, vol. 42, pp. 3178–3188, Dec 1994.

[35] P. Bello, "Characterization of randomly time-variant linear channels," *IEEE Trans. Commun. Syst.*, pp. 360–393, 1963.

[36] A. S. S. Bhasyam and B. Aazhang, "Time-selective signaling and reception in for fading channels," in *submitted to 1998 IEEE Intl. Symp. Inform. Th.*

[37] A. Viterbi, *CDMA: Principles of Spread Spectrum Communications*. Addison Wesley, 1995.

[38] S. Verdu, "Minimum probability of error for asynchronous Gaussian multiple-access channels," *IEEE Trans. Inform. Theory*, pp. 85–96, Jan 1986.

[39] Z. Zvonar, "Combined multiuser detection and diversity reception for wireless CDMA systems," *IEEE Trans. Veh. Technol.*, vol. 45, pp. 205–211, Feb 1996.

[40] G. Wornell, "Spread-signature CDMA: Efficient multiuser communications in the presence of fading," *IEEE Trans. Inform. Theory*, pp. 1418–1438, Sep 1995.

[41] G. Wornell, "Spread-response precoding for communication over fading channels," *IEEE Trans. Inform. Theory*, pp. 488–501, Mar 1996.

[42] S. S. H.C. Huang and S. Verdu, "Combined multipath and spatial resolution for multiuser detection: Potentials and problems," in *Proc. 1995 Intl. Symp. Inform. Th.*, p. 380, 1995.

[43] A. Sayeed and B. Aazhang, "Multiuser timing acquisition over multipath fading channels," in *Proc. 1998 Conf. Inf. Sci. Syst. (CISS'98)*, 1998.

[44] E. Erkip, A. Sendonaris, and B. Aazhang, "An achievable rate region for systems employing user cooperation diversity," *To be submitted to IEEE Transactions on Information Theory*.

[45] T. Cover and C. Leung, "An achievable rate region for the multiple-access channel with feedback," *IEEE Transactions on Information Theory*, vol. IT-27, pp. 292–298, May 1981.

[46] F. Willems and E. V. D. Meulen, "The discrete memoryless multiple-access channel with cribbing encoders," *IEEE Transactions on Information Theory*, vol. IT–31, pp. 313–327, May 1985.

[47] C. Zeng, F. Kuhlmann, and A. Buzo, "Achievability proof of some multiuser channel coding theorems using backward decoding," *IEEE Transactions on Information Theory*, vol. IT–35, pp. 1160–1165, November 1989.

[48] R. Gallager, "An inequality on the capacity region of multiaccess fading channels," in *Communications and Cryptography–Two Sides of One Tapestry*, pp. 129–139, Kluwer, 1994.

IMAGE EVALUATION
TEST TARGET (QA-3)

150mm

6"